Hutton Symposium V, Field Guidebook
Geological Survey of Japan, Interim-Report no.28, p.81－102, 2003

Trip B1

Crustal section and anatexis of lower crust due to mantle flux in the Hidaka metamorphic belt, Hokkaido, Japan

Masaaki OWADA[1], Yasuhito OSANAI[2], Toshiaki SHIMURA[3], Tsuyoshi TOYOSHIMA[4] and Yoshio KATSUI[5]

Abstract: This field trip focuses primarily on a crustal section and anatexis of lower crust due to mantle flux. The Hidaka metamorphic belt situated in south-central Hokkaido consists of steeply eastward dipping thrust sheets composed of pelitic-psammitic and mafic metamorphic rocks and various intrusive rocks of Eocene to early Miocene age. The intrusive rocks are composed mainly of layered gabbros, gabbros-diorites, and S- and I-type tonalites-granodiorites. Metamorphic grade in the Hidaka metamorphic belt increases from the prehnite-pumpellyite grade in the east through the greenschist and amphibolite facies to the granulite facies in the west. It is stressed that the Hidaka metamorphic belt represents almost the whole section of an island-arc crust. We can observe the layered olivine gabbro complex, probably the heat source of Hidaka metamorphism, the anatectic rocks in the lowest structural level and S- and I-type granitic rocks in the middle level of the Hidaka metamorphic belt. Fresh mantle peridotite (plagioclase lherzolites and harzburgites) complex situated in the lowest structural level of the belt will be also visited. Another highlight is an active volcano, which represents the subduction-related magmatism situated on the arc-arc junction.

Keywords: Hutton Symposium, field excursion, Hidaka metamorphic belt, partial melting, Hokkaido, Tertiary

1. Introduction

Two arc-trench systems, the Eurasian margin subduction zone (Northeast Japan arc) in the west and the Kuril arc in the east, juxtaposed during Late Cretaceous to Early Tertiary in Hokkaido, and then collided each other during Eocene to form central Hokkido. It means that the pre-Neogene geology of Hokkaido is divided into three major provinces; Western, Central and Eastern Hokkaido (Fig. 1). The trend of each geological unit is oblique to the present active arc-trench systems.

Recent studies of vivroseismic analysis have revealed the subsurface geological structures. It is stressed that the lower part of lower crust along with lithospheric mantle of the eastern part of Hokkaido (Kuril arc) have descended and delaminated (Tsumura *et al.*, 1999). On the other hand, the upper part of the crust upthrust on the western part of Hokkaido (Northeast Japan arc), and is exposed in the Hidaka Mountains (Arita *et al.*, 1998; Ito *et al.*, 1999; Fig. 2). This zone is, therefore, named Hidaka Collision Zone (Arita *et al.*, 1998).

In this field trip, we will observe the Tertiary crustal section, from lower to upper crustal sequence, of the Hidaka metamorphic belt, and then visit an active volcano, Tokachi-dake, in central Hokkaido. An approximate route of the field trip B1 is shown in Fig. 3.

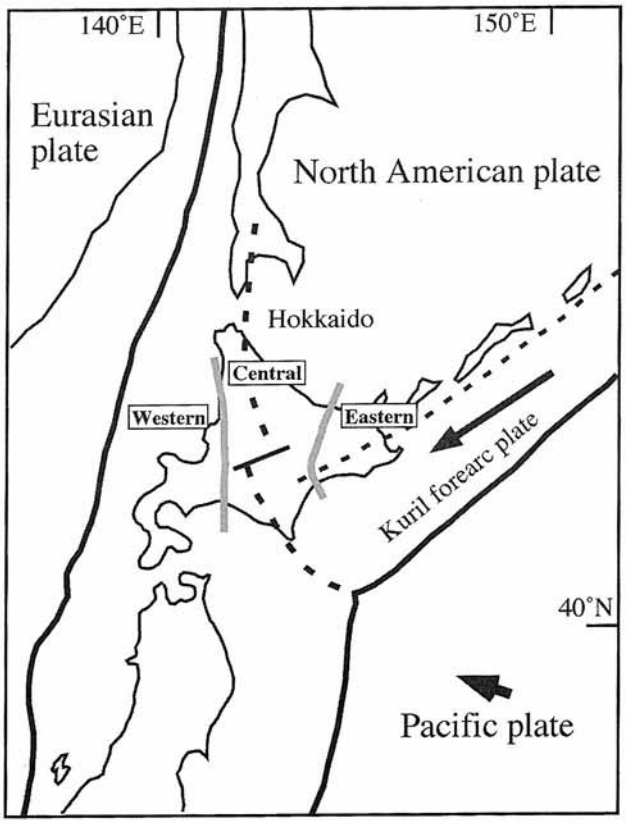

Fig. 1. Geotectonic framework of Hokkaido Island.

[1] Department of Earth Sciences, Yamaguchi University, Yoshida 1677-1, Yamaguchi 753-8512, Japan. E-mail: owada@mail.sci.yamaguchi-u.ac.jp
[2] Department of Earth Sciences, Okayama University, Tsushima-naka 3-1-1, Okayama 700-8530, Japan. E-mail: osanai@cc.okayama-u.ac.jp
[3] Department of Geology, Faculty of Science, Niigata University, Ikarashi 2-8050, Niigata 950-2181, Japan. E-mail: smr@gs.niigata-u.ac.jp
[4] Graduate School of Science and Technology, Niigata University, Ikarashi 2-8050, Niigata 950-2181, Japan. E-mail: ttoyo@geo.sc.niigata-u.ac.jp
[5] Kita-ku Kita 24, Nishi-14, Sapporo 001-0024, Japan.

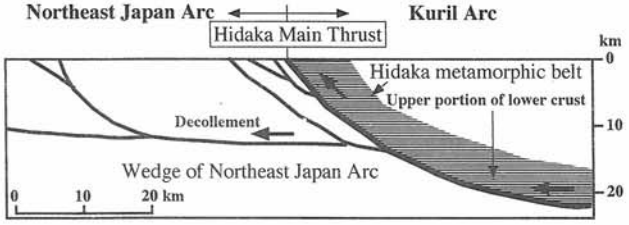

Fig. 2. Schematic structural cross-section of south-central Hokkaido (modified after Ito *et al.*, 1999).

2. Geological outline of the Hidaka metamorphic belt

The Hidaka Mountains situated in the south-central part of Hokkaido, northern Japan, consists of two major metamorphic terranes with the Hidaka metamorphic belt in the east and the Poroshiri Ophiolite Belt in the west (Fig. 4). The boundary between them is the Hidaka Main Thrust (HMT) with a large dextral shear, along which the Hidaka metamorphic belt overthrusts on the Poroshiri Ophiolite Belt as a duplex (Komatsu *et al.*, 1982, 1983; Arita *et al.*, 1986).

The Hidaka metamorphic belt extends over a distance of *ca.* 140 km along the north-south trending mountain ridge of the Hidaka Mountains and has a width of 10-20 km as a southern half of the Hidaka Magmatic Zone of Tertiary age (Maeda *et al.*, 1986; Maeda, 1990). This metamorphic belt is displaying a steeply eastward-tilted metamorphic sequence and consists of various metamorphic rocks with felsic to mafic intrusive rocks (Fig. 5), which is considered to be a series of exposed crustal slab from deeper part in the west to shallower level in the east, derived from an immature island-arc (Komatsu *et al.*, 1989; Osanai *et al.*, 1991).

The metamorphic rocks of the Hidaka metamorphic belt can be divided into two lithological sequences; the Lower metamorphic sequence in the western half is predominant in mafic metamorphic rocks, and the Upper metamorphic sequence in the eastern half consists mainly of pelitic to psammitic metamorphic rocks without mafic rocks. The Lower metamorphic sequence can be subdivided lithologically into granulite, brown-Hbl amphibolite, and Hbl-Bt gneiss units from lower to higher structural level, *i.e.* from the west to the east. The Upper metamorphic sequence can also be subdivided into Bt-Ms gneiss/schist and Chl-Ms metasediment units from the west to the east (Osanai, 1985). The boundary between the two sequences seems to be a tectonic discontinuity, where S-type and I-type granitic large masses are exposed. Gabbro-diorite is exposed in both of the sequences.

The felsic to mafic intrusive rocks are emplaced at various structural levels of the metamorphic rock sequence. The S- and I-type granitic rocks can be classified into four types in terms of the differences in emplacement horizon, mineral assemblages, and enclaves; such as 1) basal, 2) lower and 3) middle tonalite to granodiorite and 4) upper granite (Komatsu *et al.*, 1986; Table 1). The mafic to intermediate intrusive rocks are also subdivided into lower Ol gabbro (tholeiitic), lower gabbro-diorite (calc-alkaline) and upper gabbro-diorite (calc-alkaline). Part of the lower gabbros was

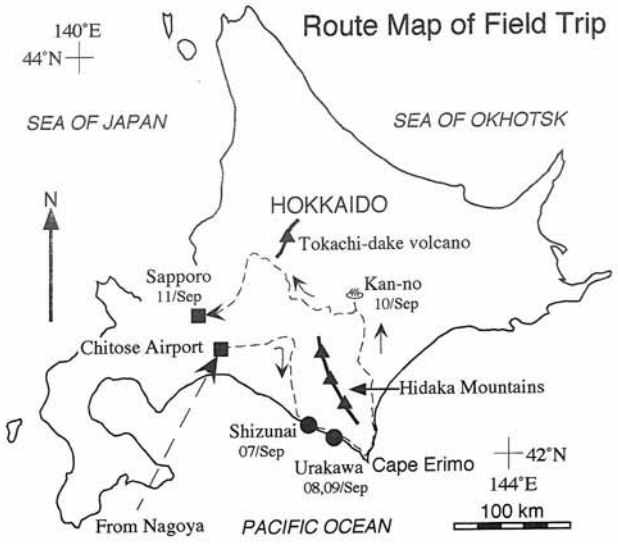

Fig. 3. Route map of the Field trip B1.

metamorphosed under the amphibolite- and granulite-facies conditions depending on their intrusive level in the crust. Schematic succession of metamorphic and intrusive rocks of the Hidaka metamorphic belt is shown in Figure 6.

Regional subdivision of the Hidaka metamorphic belt is also possible due to their lithological constitutions and geological structures, such as northern, central and southern areas (Osanai and Owada, 1994; Fig. 4). The northern area is a northern part from Niikappu - Satunai River districts that is characterized by the predominance of gabbro-diorite and granitic rocks with minor exposures of metamorphic rocks. In the central area, the metamorphic rock sequence from basal (west) to the upper most part (east) is well preserved, where the most wilderness part in the Hidaka Mountains around Mts. Kamui-ekuuchikaushi, Petegari, and Kamui. The southern area is a southern part from Menashun'betsu River-Rakko River districts, which are characterized by a large amount of ultramafic, mafic and felsic intrusive rocks and the gentle geological structure with many nappes.

3. Geological structures

The tectonic evolution of the Hidaka metamorphic belt is divided into three stages based on the nature and sequence of deformation, metamorphism and igneous activity during the early Paleocene to Miocene time; I: formation of magmatic arc (D0 and D1), II: exhumation of the crust (D2 and D3), and III: post-kinematic brittle deformation (Toyoshima *et al.*, 1994, 1997; Fig. 7). Pre-metamorphic and -igneous stage (D0) involving tectonic thickening of the Late Cretaceous and Early Tertiary accretionary complex. D1 is the prograde metamorphic stage, accompanying surfacial extension (flattening) and vertical uplifting of metamorphic rocks caused by mafic magmatic underplating. The D1-mafic magma is also possible heat source for the high-temperature type metamorphism.

Subsequent to the D1 stage, top-to-the south subhorizontal

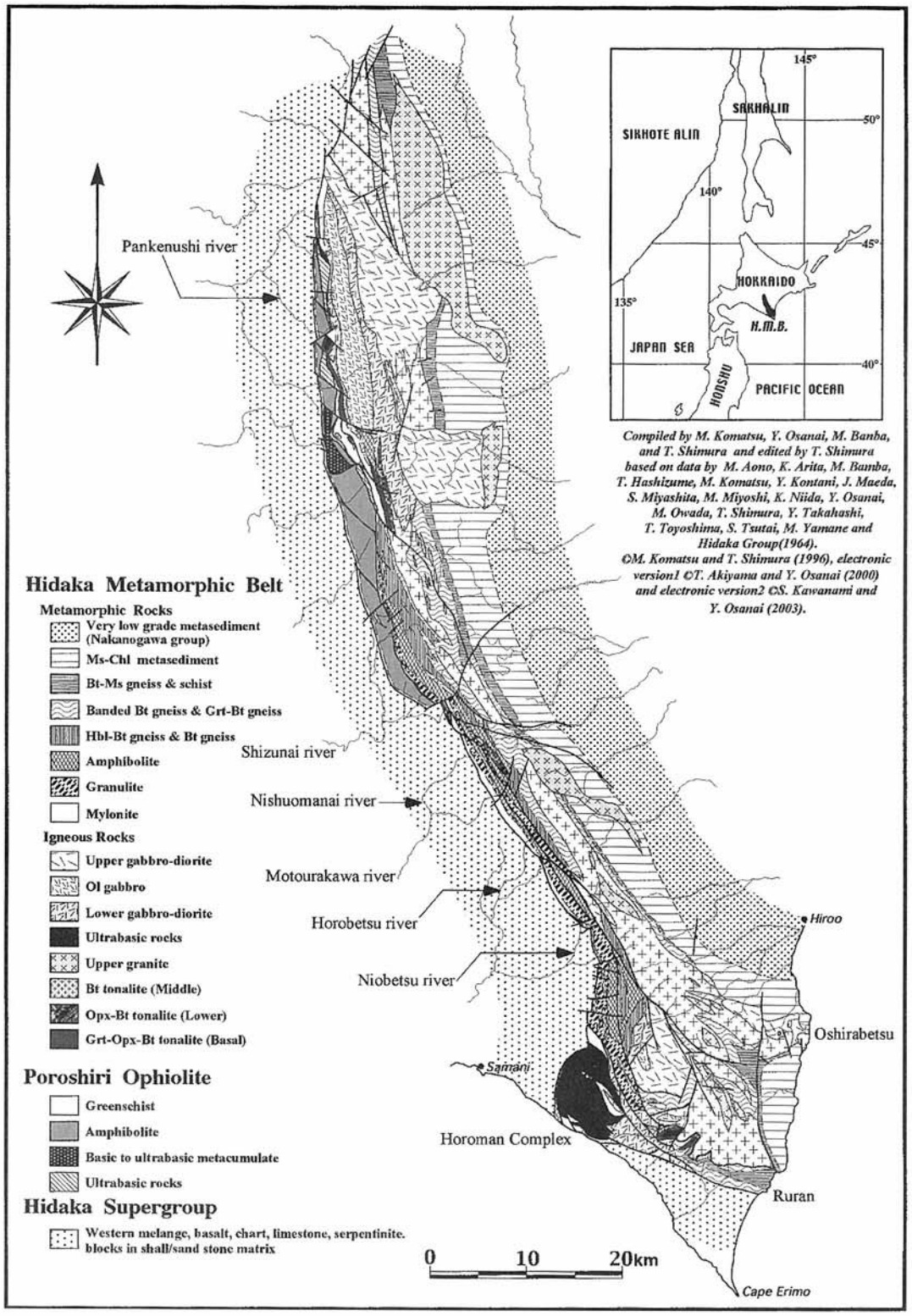

Fig. 4. Geological map of the Hidaka metamorphic belt.

displacement of detached lower to upper crustal rocks occurred under an N-S compression, associated with the formation of duplex structure, high-temperature mylonitization, and the S-type granitic intrusion (D2). The S-type magmas penetrated along a basal detachment (decollement) of the duplex. The decollement was formed along the transitional zone from the amphibolite to the granulite facies, where partial melting incipiently took place and was likely intensified in the deeper part. The depth of the intra-crustal decollement was possibly defined by relative amounts of partial melt fraction and fluid flux. The D2-event occurred as a result of transcurrent tectonics in a flat-lying structural state. The crustal decollement during the early D2 stage might have extended to the crust-mantle boundary and/or to

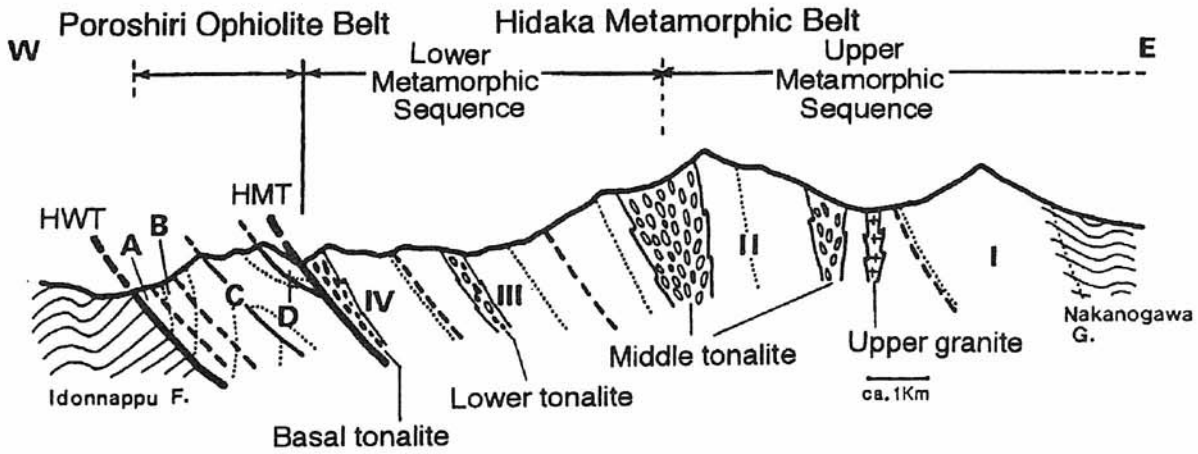

Fig. 5. Cross-section of the central area of the Hidaka metamorphic belt (after Osanai *et al.*, 1986).

Table 1. Characteristic mineral assemblages of the granitic rocks from the Hidaka metamorphic belt classified in terms of the intrusive levels and peraluminous and metaluminous types (after Shimura *et al.*, 1992).

Depth type	Rock type	Intrusive level	Characteristic mineral assemblage	
			Metaluminous (I-type)	Peraluminous (S-type)
Upper	granite granodiorite	Chl-Ms metasediment unit	Bt+Hbl+Pl+Qtz±Kfs	Bt+Pl+Qtz±Kfs
Middle	granodiorite tonalite	Bt-Ms gneiss and schist unit	Bt±Hbl+Pl+Qtz	Bt±Ms±Crd+Pl+Qtz±Kfs
Lower	tonalite	amphibolite unit	Bt+Hbl+Opx±Cpx±Cum+Pl+Qtz	Bt+Opx±Crd+Pl+Qtz±Kfs Bt+Grt±Crd+Pl+Qtz±Kfs
Basal	tonalite	granulite unit		Bt+Opx+Grt±Crd+Pl+Qtz±Kfs

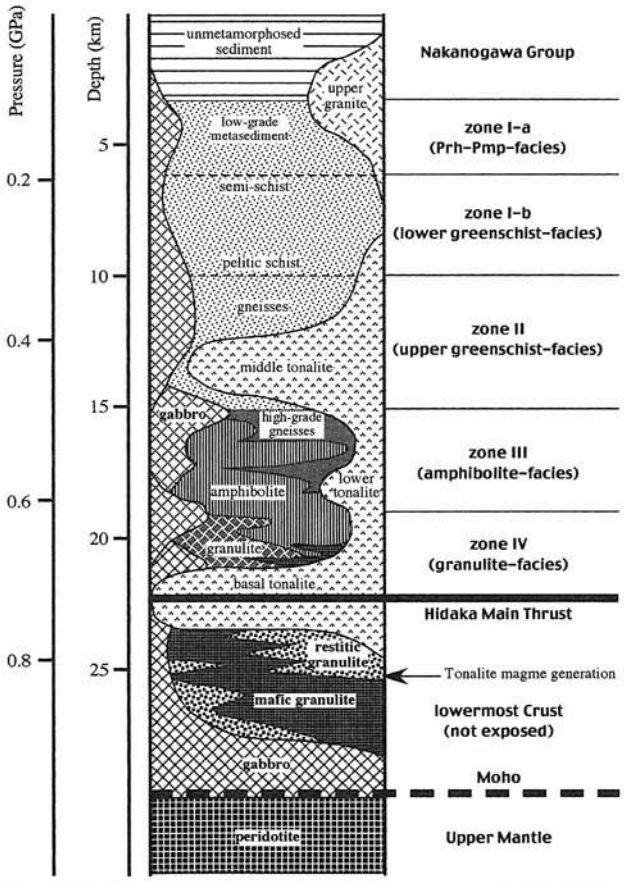

Fig. 6. Idealized succession of the Hidaka metamorphic belt (after Komatsu et al., 1986).

the lithosphere and asthenosphere boundary (Toyoshima *et al.*, 1994, 1997).

The D3-dextral transpressional movement accompanied by retrograde mylonitization resulted in eastward tilting (steepening) on N-S axis and exhumation of the belt. The granitic intrusion enhanced the crustal deformation and exhumation in the D2- and D3 stages.

The exhumed crustal rocks were partly modified by brittle deformations of later stages, especially by sinistral shearing to form asymmetric kink folds, and then by conjugate faulting associated with the formation of pseudotachylytes. The conjugate fault set was formed under the ENE-WSW compressional event during the latest Miocene, cutting the general trend of the belt nearly at right angles.

4. Metamorphism

4.1 Metamorphic zones (progressive change in mineral assemblages)

The metamorphic rocks of the Hidaka metamorphic belt can be divided into four metamorphic zones (Zone I to IV) from top (east) to base (west) on the basis of the mineral parageneses of pelitic and psammitic rocks (Osanai, 1985; Osanai *et al.*, 1986, 1991). In the Lower sequence, mafic rocks also show changes in mineral parageneses, which are consistent with the paragenetic changes in pelitic rocks. The critical mineral parageneses of different rock compositions

	Deformation stage	Tectonics	Deformation & structure	Igneous activity	Metamorphism	Relative temperature	Structural state of shear plane
I	D_0	Tectonic thickening of sedimentary precursors	?	?	Low-grade metamorphism	?	?
	D_1	Magmatic underplating & extensional doming	Flattening & shearing Bedding foliation (S_1) & non-rotated boudinage Locally preserved fold with axial foliation (S_1')	Gabbro-diorite intrusion	Prograde metamorphism & anatexis Metamorphic peak up to granulite facies		Flat-lying
II	D_2	Initiation of décollement Subhorizontal top-to-the south displacement	Shearing, folding & mylonitization Mylonitic foliation & fold with axial foliation (S_2) Duplex	Tonalite-quartz diorite intrusion into décollement & ramp-roof thrust of duplex	Initiation of retrograde metamorphism	Time	Flat-lying
	D_3	Eastward tilting & dextral-slip movement	Shearing, folding & retrograde mylonitization Mylonitic foliation & fold with axial foliation (S_3) Duplex	Minor intrusion of olivine gabbro & diorite	Retrograde metamorphism lower part: granulite to greenschist facies upper part: amphibolite to greenschist facies		
III		?	?	Minor intrusion of leucocratic granite			
	D_k	Sinistral movement	Shearing & kinking Kink fold or kink band with kink plane (S_k) Monoclinic or conjugate type		Retrograde metamorphism greemschist facies		Steeply inclined
			Faulting with cataclasite I				
			Fracturing with prehnite-quartz vein				
	D_{pt}	ENE-WSW compression	Seismic faulting & frictional heating Conjugate fault with pseudotachylyte & cataclasite II		Retrograde metamorphism zeolite facies		
			Fracturing with zeolite vein		Retrograde metamorphism zeolite facies		

Fig. 7. Tectonic and metamorphic history of the lower sequence of the Hidaka metamorphic belt. Relative temperature is metamorphic conditions of the granulite unit (after Toyoshima *et al.*, 1997).

are as follows (Osanai *et al.*, 1986, 1991; Komatsu *et al.*, 1989).

For pelitic/psammitic rocks,

Zone I: Chl, Phe

Zone II: Bt, Ms, (And, Grt or Crd)

Zone III: Bt, Grt, Sil, (Crd or Kfs)

Zone IV: Grt, Crd, Kfs, (Sil or Bt)/ Grt, Crd, Opx, Bt.

For mafic rocks,

Zone II: green brown Hbl, Bt, Ep

Zone III: brown Hbl, Cum, (Bt, Grt)

Zone IV: brown Hbl, Opx, (Cpx).

The regional distribution of these zones in the Hidaka metamorphic belt is shown in Figures 5 and 8 (Osanai *et al.*, 1986, 1991, 1997; Osanai and Owada, 1994). Owing to the mineral assemblages, Zone I corresponds to the Prh-Pmp facies. Zones II, III, and IV are also equivalent to the greenschist/Ep-amphibolite facies, amphibolite facies, and granulite facies, respectively. This progressive changes in metamorphic grade through each crustal level shows the metamorphic field gradient to be 33-40°C/km (Osanai *et al.*, 1986, 1991; Komatsu *et al.*, 1989). This gradient may correspond to those of active island-arcs (Komatsu *et al.*, 1983).

4.2 *P-T-X*$_{H_2O}$ conditions

4.2.1 Upper Sequence

According to Miyoshi (1986) and Tsuchiya *et al.* (1991), d(002) and Lc(002) values of carbonaceous material change drastically between Zones I and II. In Zone III, however, the graphite is fully ordered. In comparison with the experimental data of Landis (1971) and Tagiri and Oba (1983), the metamorphic temperatures of the transitions between Zones I and II, and Zones II and III are estimated to be *ca.* 400°C and *ca.* 500°C, respectively.

The Bt-Ms-Chl-Qtz geobarometer of Powell and Evans (1983) is employed for the pressure estimation of Zone II, which gives a value of 260-350 MPa. An accurate meaurement of porosity for the unmetamorphosed sediment from the basal part of Nakanogawa Group indicates the pressure condition of 180-220 MPa (Osanai *et al.*, 1989).

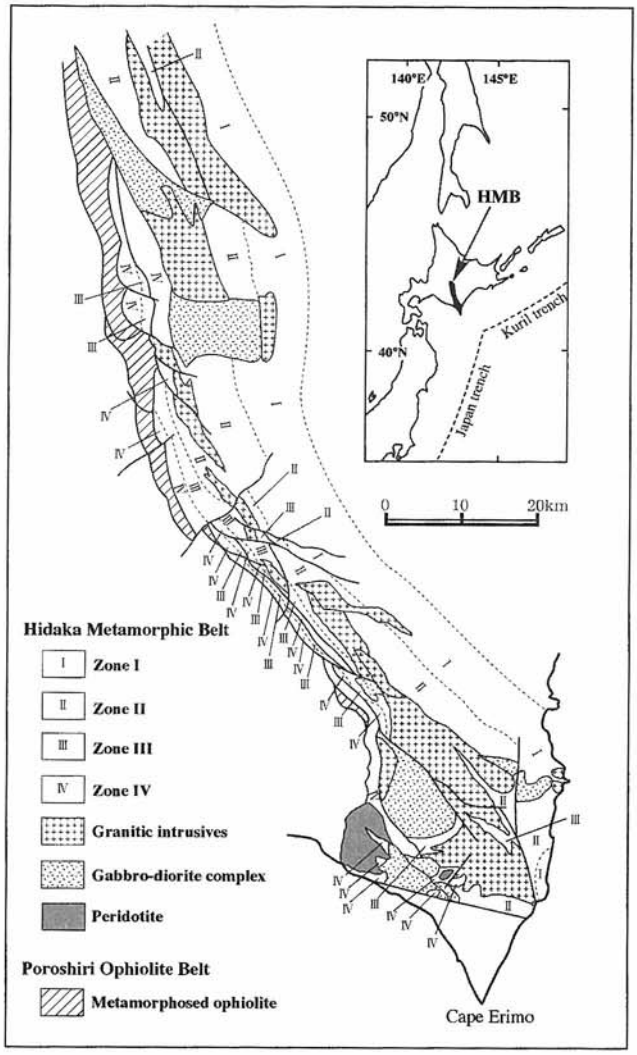

Fig. 8. Metamorphic zonation of the whole area of the Hidaka metamorphic belt (after Osanai *et al.*, 1997).

4.2.2 Lower Sequence

In the structurally upper to middle part (amphibolite unit) of the lower sequence, the metamorphic temperatures were estimated using Fe-Mg exchange geothermometers of Grt-Bt (Thompson, 1976; Perchuk, 1991; Holdaway *et al.*, 1997) for pelitic rocks and Grt-Hbl (Graham and Powell, 1984; Himmelberg *et al.*, 1994) for mafic rocks. The obtained values are 530-580°C for the upper part and 630-700°C for the middle part.

To estimate pressures, the following two geobarometers were employed for intercalated metapelites: (i) GASP (Newton and Haselton, 1981; Ganguly and Saxena, 1984; Powell and Holland, 1988), (ii) Grt-Crd-Al_2SiO_5-Qtz (Wells, 1979; Martignole and Sisi, 1981; Perchuk, 1991). The calculated values for the middle part of the lower sequence are 510-560 MPa.

At the basal part of the lower sequence (granulite unit), metamorphic temperatures were estimated for undeformed rocks using Fe-Mg exchange geothermometers between Grt-Bt for pelitic and psammitic rocks, Grt-Crd (Perchuk and Lavrent'eva, 1983; Perchuk *et al.*, 1985; Perchuk, 1991) and Grt-Opx (Harley, 1984; Lee and Ganguly, 1988; Perchuk, 1991; Lal, 1993), and between Opx-Cpx for mafic rocks (Wood and Banno, 1973; Wells, 1977; Brey and Köhler, 1990). Metamorphic pressures were estimated using GASP and Grt-Opx-Pl-Qtz equilibria (Newton and Perkins, 1982; Perkins and Chipera, 1985; Lal, 1993) for pelitic and psammitic rocks. The peak metamorphic *P-T* conditions of Zone IV vary from 740 to 870°C and from 570 to 730 MPa (Fig. 9). Further information on the *P-T* estimates for the granulites is given by Osanai *et al.* (1991). These *P-T* conditins are estimated using granulite-facies rocks from the central area of the Hidaka metamorphic belt (Shizunai River and Motourakawa River areas). However, an estimated *P-T* values of Zone IV in the south-centarl area (Horobetsu River and Menashun'betsu River areas) are 450-590 MPa and 750-790°C (Komatsu *et al.*, 1994).

Under the highest *P-T* conditions for the granulite unit, it is likely that vapor-present partial melting took place in the pelitic rocks (*e.g.* Vielzeuf and Holloway, 1988). The values of X_{H_2O} estimated by the methods of Ferry (1981) and Bhattacharya and Sen (1985) are lower in the Grt-Opx-Crd gneiss (0.11-0.21) compared to the Grt-Crd-Bt gneiss (0.40-0.44) (Osanai *et al.*, 1991). These mineralogical and petrological features suggest that the Grt-Opx-Crd gneiss is a possible restite remaining after partial melting of the Grt-Crd-Bt gneiss (Osanai *et al.*, 1992, 1997).

4.3 *P-T-t* path

The metamorphic evolution of the Hidaka metamorphic belt includes five stages, from M0 to M4, in terms of geological and petrological studies. The multi-stage evolutional path of the Hidaka metamorphic belt is illustrated in Figure 9. The near isobaric prograde metamorphic path (M0 to M1) caused by the older gabbro intrusion before the peak metamorphism can be evaluated only in the pelitic granulite of Zone IV. Osanai and Owada (1990) reported the presence of staurolites in the pelitic granulite of Zone IV. In Qtz-bearing domains the Mg-rich St shows two modes of occurrence; as corroded crystals included in Grt porphyroblasts coexisting with Sil and Mg-rich Crd (X_{Mg}=0.75-0.80) (type-1) and as small anhedral crystals included in Pl coexisting with Bt (type-2). Sometimes Ky and Qtz are also found as inclusion in Grt as well as type-1 St. In contrast, in Qtz-free domains Mg-poor St occurs as euhedral crystals (type-3) coexisting with a symplectic intergrowth of Hc-Sil and of Mg-poor Crd (X_{Mg}=0.60-0.67)-Hc-Sil. These staurolites (types 1-3) can be observed within the same thin section and have different chemical compositions. Both the St breakdown-and producing- reactions are sensitive to a temperature change because they have high-dP/dT slopes, Mg-rich St being more stable in high *P-T* conditions than Mg-poor St (Richardson, 1968; Dutrow and Holdaway, 1989).

The metamorphic reactions during prograde metamorphism in the St-bearing pelitic granulites can be shown as follows (Osanai *et al.*, 1991; Komatsu *et al.*, 1994);

Ms + Chl = Mg-rich St + Bt + Qtz + Vapor (1)

Mg-rich St + Qtz = Grt + Mg-rich Crd + Sil + Vapor (2)

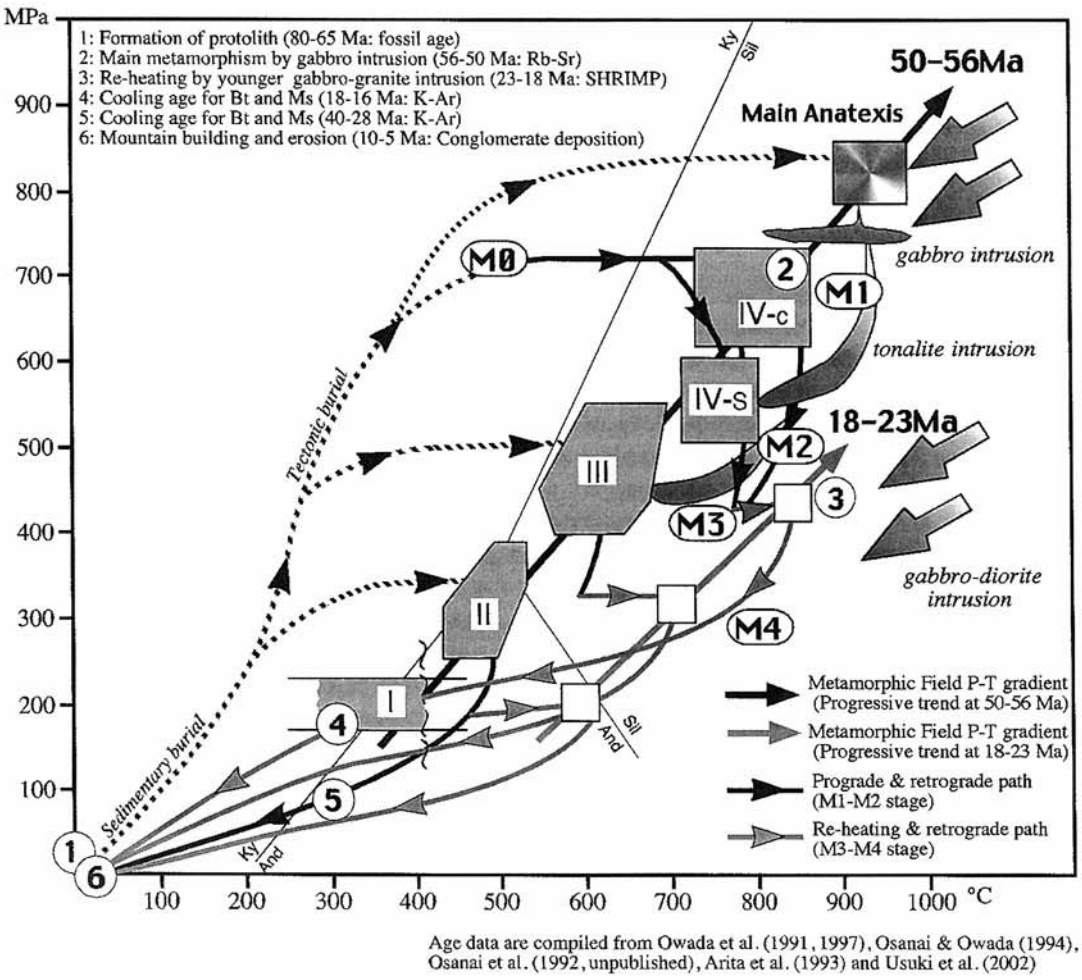

Fig. 9. Pressure-temperature-time path of the Hidaka metamorphic belt.

Mg-rich St = Grt + Mg-rich Hc + Sil + Vapor (3)

The metamorphic rocks, especially those in Zones III and IV, underwent varying degrees of retrograde metamorphism, caused by shearing during the early deformation involving subhorizontal displacement (D2) and later strike-slip related movement (Komatsu *et al.*, 1989, Toyoshima *et al.*, 1997). The early retrograde stage is characterized by near isothermal decompression (M2). The retrograde metamorphism of M2 stage after Ml event is shown by the following reactions;

Grt + Sil + Vapor = Mg-poor Crd + Mg-poor Hc (4)

Mg-poor Crd + Mg-poor Hc + Sil +Vapor = Mg-poor St (5)

Immediately after M2 decompression stage, reheating took place due to the younger gabbro-diorite intrusion (*ca.* 20 Ma) under the low-pressure condition (M3). At this stage, degree of temperature increase is more effective in the low-grade part (structurally upper level). The latest stage that decreases both of pressure and temperature (M4) would have been led by exhumation of the Hidaka metamorphic belt. The metamorphic evolution of the Hidaka metamorphic belt can therefore be explained by a clockwise *P-T-t* trajectory.

5. Magmatism

5.1 Distribution and characterization of the intrusive suites

Tertiary magmatism (56 to 17 Ma) took place in the meridian zone extending over *ca.* 550 km long from the SW part of Sakhalin to the southern end of central Hokkaido. The intrusive rocks in the Hidaka metamorphic belt correlate with the southern part of this magmatic zone. The mafic to intermediate intrusive rocks are mainly exposed on the northern and southern areas of the Hidaka metamorphic belt, *e.g.* Pankenushi River to Memurodake River and Tottabetsu River areas (northern area of the belt), and Niobetsu River area, Horoman River to Nikanbetsu River area and Oshirabetsu area (southern area of the belt). On the other hand, felsic intrusive rocks are exposed throughout the Hidaka metamorphic belt (Fig. 4).

The intrusive rocks are classified petrographically into four groups, namely Ol-bearing Px gabbro, Hbl gabbro to diorite, and Crd-bearing tonalite and Hbl-bearing tonalite to granodiorite. These four groups geochemically correspond to tholeiite, calc-alkaline series, S-type and I-type granitic rocks, respectively. In addition to these rocks, faylite- and

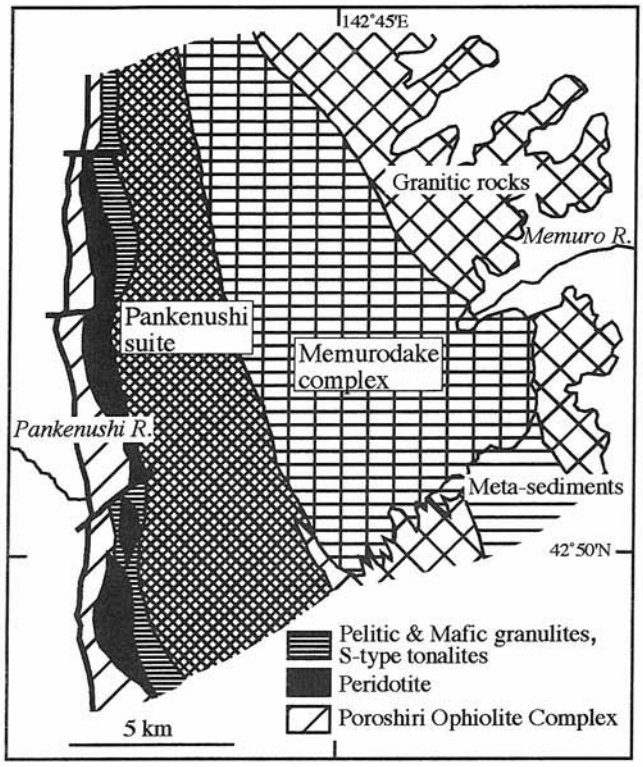

Fig. 10. Simplified geologic map of the Pankenushi-Memurodake area (after Maeda and Saito, 1997).

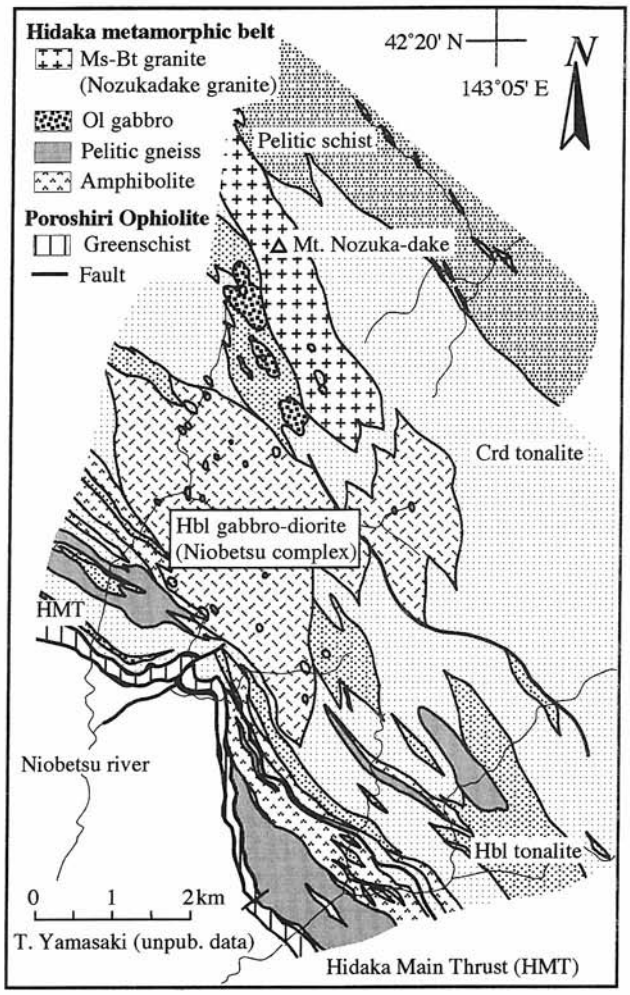

Fig. 11. Geological map of the Niobetsu river area.

almandine-bearing Bt-Qtz norite with peraluminous affinity is also reported (Maeda *et al.*, 1985; Maeda *et al.*, 1991). We describe several mafic to intermediate suites, which we will visit during our field trip, and the felsic rocks.

5.2 Pankenushi River to Memuro River area

Pankenushi gabbroic suite (Pankenushi suite) and Memurodake dioritic complex (Menurodake complex) are the typical examples of the tholeiitic Ol-bearing Px gabbro group and calc-alkaline Hbl gabbro to diorite group, respectively (Fig. 10).

The Pankenushi suite is a tholeiitic layered intrusion *ca.* 30 km long in N-S direction and 4 km wide in E-W. Layered structures of NNW-SSE striking and steeply eastward dipping are commonly observed. Major rock types are, from W to E, troctolite, Ol-gabbro, and ferrogabbro. Anorthosite is commonly intercalated within the layered gabbros. These rocks locally show recrystallized-granoblastic texture overprinted by the mylonitic foliation, and have undergone granulite-facies metamorphism during the cooling and deformation stages. The Pankenushi suite would be emplaced under the lower part of the Hidaka metamorphic rocks, and give the thermal effect to the host rocks (Maeda and Saito, 1997). In other words, the Pankenushi suite is one of the candidates for heat source of the low *dP/dT* Hidaka metamorphism.

Dikes and veins of fine-grained metagabbro of picritic composition, Chiroro dikes, discordantly intrude the Pankenushi layered gabbros (Maeda and Kagami, 1994). The Chiroro dikes are characterized by high MgO, Ni, and Cr contents and able to coexist with mantle Ol (*Fo*>90). Therefore, it is likely that the Chiroro dikes represent a composition of primitive magma generated at upper mantle beneath the Hidaka metamorphic belt. The K_2O/Na_2O ratios, chondrite-normalized patterns of REE and Sr and Nd isotope ratios of the Chiroro dikes are similar to those of MORB (Maeda and Kagami, 1994).

The Memurodake complex is located on the east of the Pankenushi suite. The Px-bearing Hbl gabbro, Hbl gabbro, Hbl-Bt diorite, and Bt tonalite are observed in the complex. Although complicated occurrences consisting of fine-grained mafic facies and coarse-grained felsic ones are commonly observed in outcrop scale, the complex lithologically becomes more felsic toward east. The complicated occurrences suggest mingling and/or mixing processes of mafic and felsic magmas. The isotope ratios vary significantly within the Chiroro dikes, the Pankenushi suite and the Memurodake complex, indicating that intracrustal evolution of normal MORB was accompanied by assimilation of the host rocks (Maeda and Kagami, 1996).

5.3 Niobetsu River area

The mafic to felsic intrusive rocks with small amounts of

the metamorphic rocks occur in the Niobetsu River area (Fig. 11). In this area, the field relationship among the intrusive rocks is recognized clearly.

The igneous activities in this area are divided into three stages. In the first stage, the igneous rocks underwent mylonitic deformation along the HMT. The rocks of the second and third stages intruded after the time of mylonitic deformation (Owada *et al.*, 2002).

The Crd tonalite, the Hbl tonalite and the Ol-bearing Px gabbro belong to the first stage. In the second stage, the Hbl gabbro to diorite complex (Niobetsu complex) and the Ms-Bt granite (Nozuka-dake granite) were emplacement after elevation of the Hidaka metamorphic belt. In addition to these igneous suites, dolerite dikes intruded in this area as the third stage.

The Ol-bearing Px gabbro is exposed as a small stock or a dike at the upper stream of the Niobetsu River, where the Crd tonalite intimately intruded, and the heterogeneous Hbl-bearing Bt-Opx quartzdiorite occurs along the contact between the Ol-bearing Px gabbro and the Crd tonalite. Complicated occurrence of the Hbl-bearing Bt-Opx quartzdiorite can be explained by results of magma mingling and/or mixing between the Ol-bearing Px gabbro and the Crd tonalite.

The Niobetsu complex occurs as a stock cutting the mylonitic foliation of the host Crd tonalite, and consists of Hbl-bearing Px gabbro, Hbl diorite and faylite- and almandine-bearing Bt-Qtz norite. The layered structure of N-S striking and steeply dipping is commonly observed along marginal part of the body. Various size (few cm to several m in diameter) of xenoliths derived from the host Crd tonalite are included in the Niobetsu complex (Fig. 11). The host Crd tonalite and the xenoliths have undergone contact metamorphism caused by thermal effect from the Niobetsu complex. Especially in the xenoliths, following reactions can be considered.

Bt + Pl + Qtz = Opx + Grt + Kfs + melt

Bt + Pl + Qtz = Opx + Spl + Kfs + melt

Opx + Spl + melt = Crd + Bt

These reactions indicate that partial melting took place under the condition of low-pressure granulite facies, probably Spl+Qtz stable field. According to Vielzeuf and Montle (1994), these reactions occur around 300-500 MPa and 800 - 900°C, as revealed by experimental investigation.

The Ms-Bt granite (Nozukadake granite) is exposed as a stock along the mountain ridge of this area, and occurs as a synchronous intrusion with the Niobetsu complex (Yamasaki *et al.*, 2000). The granite has high concentration in SiO_2, Na_2O and K_2O, and low in FeO, MgO and CaO compared to the Crd tonalite. The chemical relationship among the Nozuka-dake granite, the Crd tonalite and the xenoliths corresponds to melt, source rock and restite, respectively, if we adapted the restite-unmixing model (Yamasaki *et al.*, 2000; Owada *et al.*, 2002).

The dolerite dikes with several cm to m in width are representative igneous activities in the third stage. Intrusive direction of these dikes strikes N-S with steeply dipping.

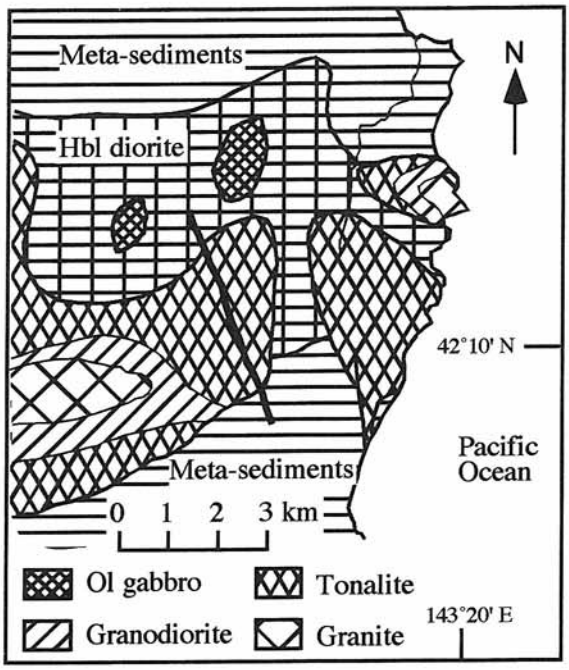

Fig. 12. Geological map of the Oshirabetsu area.

5.4 Oshirabetsu area

In this area, Oshirabetsu gabboic complex (Oshirabetsu complex) and Hbl tonalite to Bt granite are exposed as stocks intruding weakly metamorphosed Nakanogawa group, which is regarded as the Late Cretaceous to Early Tertiary accretionary complex. The Hbl tonalite to the Bt granite occurring as a zoned pluton intrudes the Oshirabetsu complex (Fig. 12).

The Oshirabetsu complex crops out 10 km long in E-W and 2 km wide in N-S, and consists mainly of Ol gabbro, troctolite, coarse-grained gabbro, norite and Hbl diorite (Takahashi, 1983). In addition to these rocks, Phl- and Ol-bearing Px gabbro is present as inclusions in the Bt granite. The Oshirabetsu complex represents a calc-alkaline chemical signature (Takahashi, 1983).

The Ol gabbro and troctolite have a cumulate texture, but show no sings of any layering and magmatic flow structures. The Oshirabetsu complex, excluding the Ol gabbro to troctolite, plots a monotonous calc-alkaline differention trend in the variation diagrams, suggesting that the complex have been derived from a single parental magma (Takahashi, 1983).

The Oshirabetsu complex used to yield economically nickel and graphite deposits until 1960's. The mineralization of nickel-sulfide deposit in the complex was regarded as an orthomagmatic deposit. Sulfur isotope study, however, revealed that at least a half amount of sulfur included in the sulfide-deposits was originally taken from the host sedimentary rocks (Takahashi and Sasaki, 1983).

The graphite deposits occur as spherules with 0.5 to 6 cm in diameter included in the Hbl diorite. The carbon isotope ratios of the graphite deposits are similar to those of the carbon materials from the host Nakanogawa group (Tsuchiya *et al.*, 1991). The graphite deposits in the Oshirabetu complex

would, therefore, be made from sediment-hosted carbon materials through the mechanism of assimilation and graphitization during the magma ascending and emplacement (Tsuchiya *et al.*, 1991).

5.5 Felsic magmatism

The felsic intrusive rocks (granitic rocks) lithologically correspond to tonalite, granodiorite and granite, and occur as laccoliths, lenses, sheets, dikes and stocks with various sizes from meter to several kilometer orders. In many outcrops, the tonalite and granodiorite commonly show heterogeneous lithology because of including the metamorphic inclusions, and locally occur as migmatites. On the other hand, the granite commonly shows homogeneity.

The basal tonalite intrudes the granulite unit with the S-type features containing aluminous-Opx, Grt, Crd and Bt. The basal tonalite often shows agmatitic or migmatitic structures including many kinds of granulites. The lower tonalite found in the brown Hbl amphibolite unit are geochemically S-type Grt-Crd tonalite with subordinate I-type Px-Hbl tonalite. They include many amphibolite blocks and show migmatitic structures. The middle tonalite, mainly aluminous Crd-Bt (-Ms) tonalite (S-type), is exposed along the main ridge of the Hidaka Mountains and situated in the boundary zone between lower and upper metamorphic sequences. The Hbl-Bt tonalite (I-type) associated with the Crd-Bt tonalite is also exposed. The upper granite exposed in the upper most part of the metamorphic sequence and further eastern unmetamorphosed sediments is homogeneously leucocratic Bt granite.

6. Age of metamorphic and igneous rocks

The well defined Rb-Sr whole-rock isochron using the restite (Grt-Opx-Crd gniss), the leucosome and the S-type tonalite (Grt-Opx tonalite: anatexite) gives the age of anatexis of *ca.* 55 Ma (Owada *et al.*, 1991, 1992). In the southern area of the Hidaka metamorphic belt the Hbl-bearing tonalite (I-type tonalite) is intruded into the metamorphic rocks that have already undergone the low *dP/dT* metamorphism. The Rb-Sr whole-rock and Bt-bearing internal isochrons give ages of 51.2 ± 3.6 Ma and 40.5 ± 0.3 Ma, respectively (Owada *et al.*, 1997). The peak metamorphic event, therefore, should be older than *ca.* 50 Ma.

Recently, zircon U-Pb SHRIMP dating was conducted on the granulite facies metamorphic rocks collected from the central part of the Hidka metamorphic belt (Usuki *et al.*, 2002). These ages mostly show *ca.* 23-18 Ma. They implied

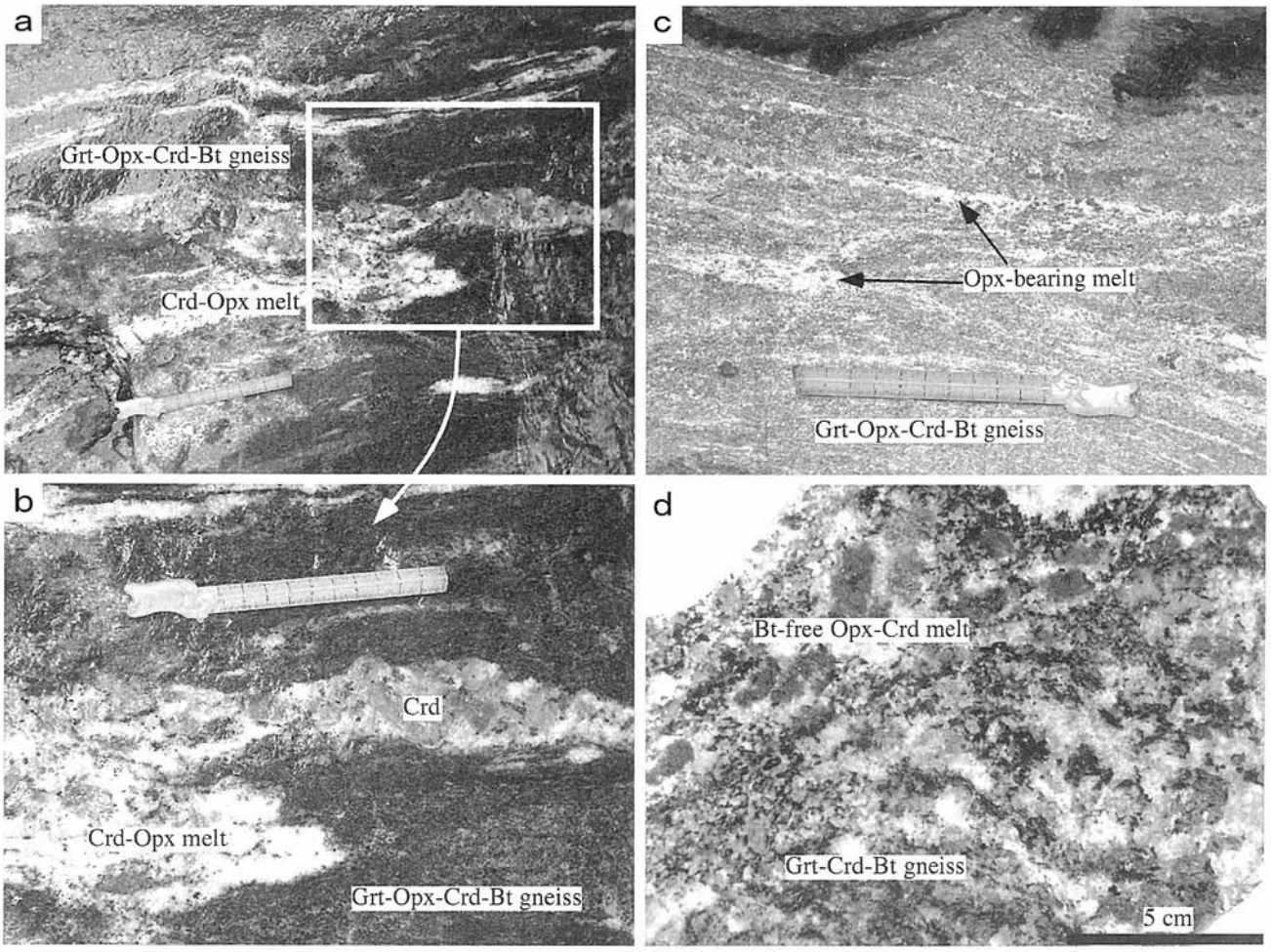

Fig. 13. Mode of occurrence of the anatexites having pelitic compositions.

that the high-grade metamorphic event attaining up to the granulite facies took place at *ca.* 23-18 Ma in the Hidaka metamorphic belt. As mentioned above, igneous activity in the Hidaka metamorphic belt is divided into at least three stages. Especially in the Niobetsu River area, the igneous activity of the second stage clearly cut the mylonitic foliations, which were formed by dextral movement during the elevation (D3 event) of the Hidaka metamorphic belt.

The Niobetsu complex (mainly Hbl diorite) belonging to the second stage includes a large amount of the xenoliths derived from the host rock. These xenoliths underwent thermal effects by the Niobetsu complex, and their metamorphic *P-T* conditions reached to the granulite facies. The intrusive and/or solidified age of the complex would be *ca.* 18 Ma, as revealed by Sm-Nd internal isochron involving magmatic garnet (Owada *et al.*, 2002). The SHRIMP ages are identical with the age of the second stage igneous activity, and would represent the time of thermal effects of the second stage magmatism. Therefore, we imply that the tectonothermal activities in the Hidaka metamorphic belt mainly occurred at 56-50 Ma and 23-18 Ma.

Most of K-Ar and Rb-Sr mineral ages of the metamorphic and igneous rocks reported from the Hidaka metamorphic belt cluster at 40-28 Ma (Late Eocene to Early Oligocene) and 20-15 Ma (Early Miocene) (Arita *et al.*, 1993; Saeki *et al.*, 1995). The metamorphic and igneous rocks with older ages occur only in the southern part of the Hidaka metamorphic belt, whereas the younger age group is widespread throughout the belt. Although the mineral ages are considered to be the cooling ages passing through the blocking temperature of Bt in the K-Ar and Rb-Sr systems, they can correspond to the above-mentioned tectonothermal events.

7. Relationship between metamorphism and magmatism

7.1 Field occurrences of in situ partial melting in Zone IV

A most suitable and acceptable model for the origin of granitic magmas is a "partial melting" of lower crustal metamorphic rocks (*e.g.* White and Chappell, 1977). The basal granulite unit of the Hidaka metamorphic belt locally includes leucosomes (leucocratic patches, lenses and veinlets) which consist mainly of Opx, Pl and Qtz with or without minor amounts of Grt, Bt and Kfs and are assumed to be derived from partial melting of pelitic and mafic granulites.

The Grt-Bt (-Sil) gneiss in Zone IV often contains Bt-free, euhedral Opx- and Crd-bearing leucocratic patches and veins (leucosomes) derived from in-situ partial melting (Fig. 13). The leucosome lacks any foliations and cuts obliquely the foliations of the host pelitic gneisses, in which the leucosome would have formed during syn- and a bit after-deformation. Partial molten mafic granulites are also found in Zone IV. The melt phase sometimes still remains as pods at the in-situ

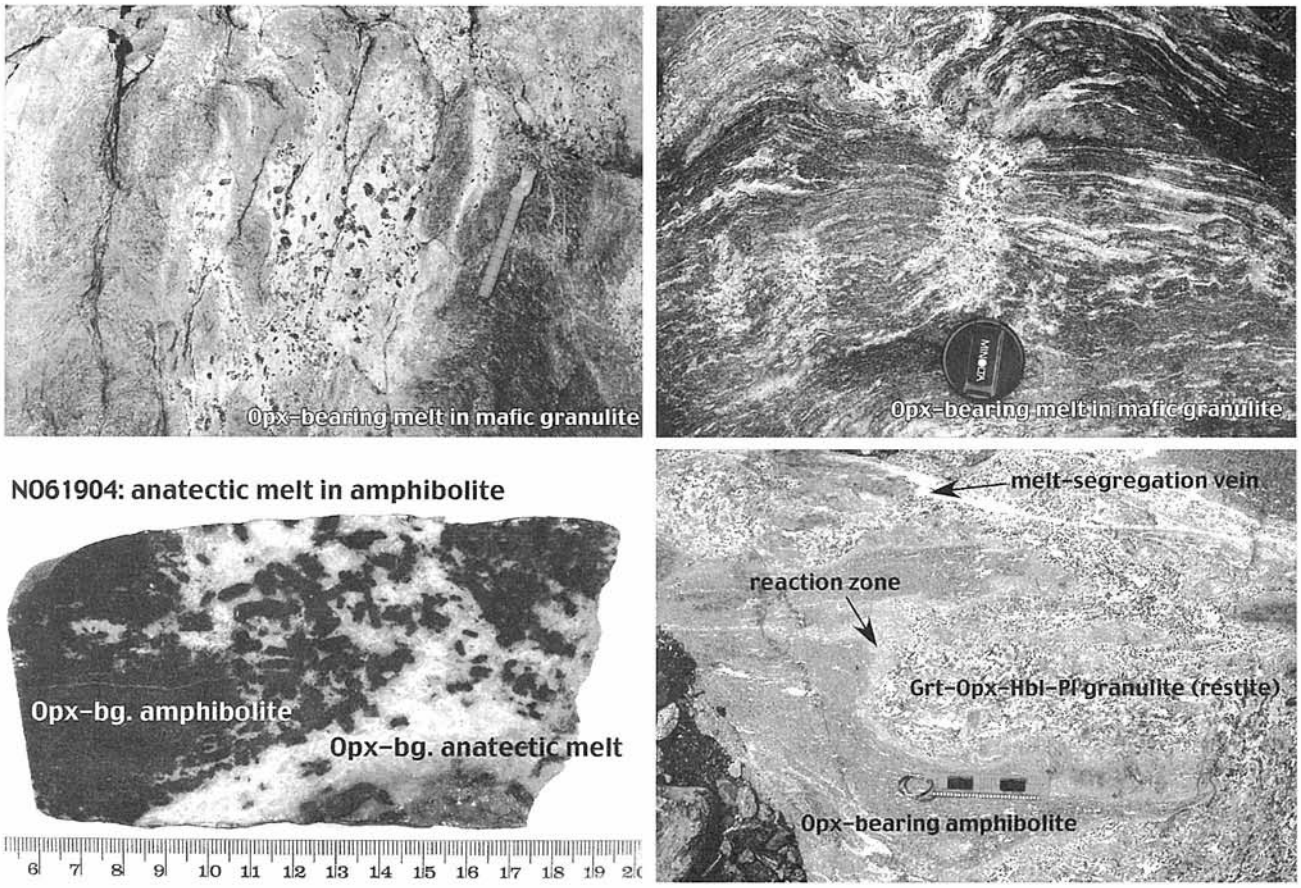

Fig. 14. Mode of occurrence of the anatexites having basaltic compositions.

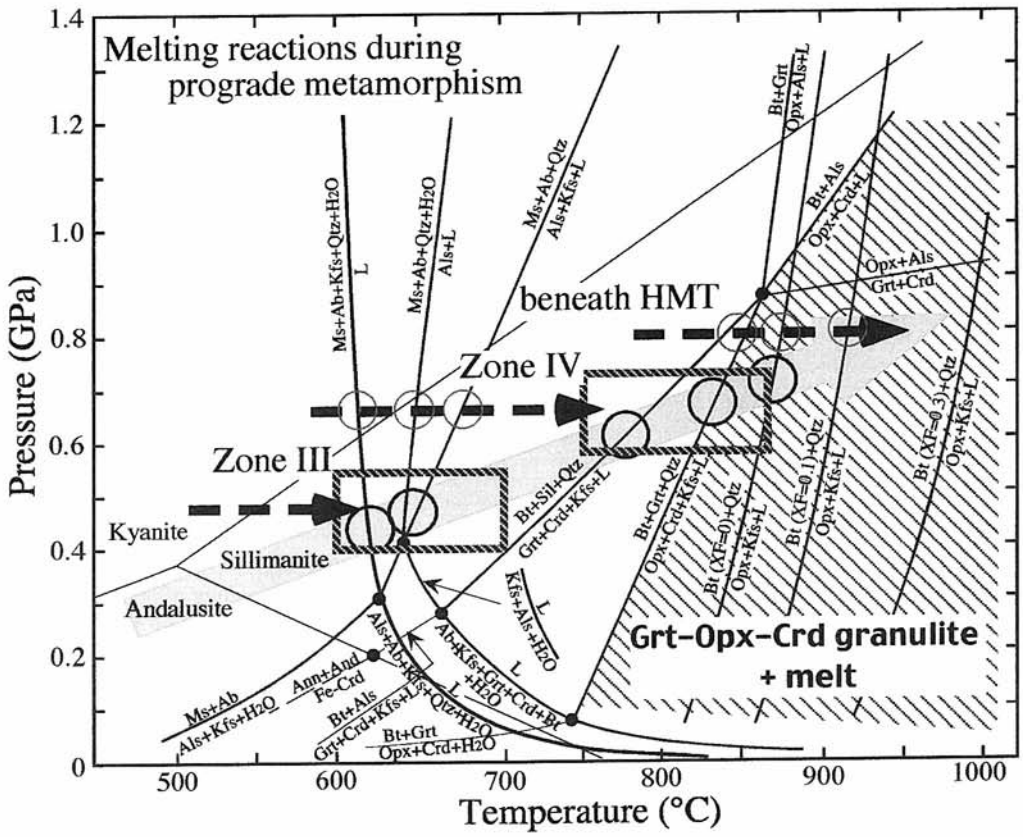

Fig. 15. Pressure-temperature conditions of the metamorphic rocks from Zones III and IV and of the mafic granulite xenoliths included in the basal tonalite.

melting position, and segregated and assembled to form an agmatitic structures and boudin necks (Fig. 14). These leucosomes related to mafic granulites usually contain euhedral orthopyroxene and calsic-Pl as products of the incongruent melting (Fig. 14).

7.2 Melting experiments using natural pelitic granulites of Zone IV

Biotite from pelitic granulite (Grt-Crd-Sil-Bt gneiss) and Hbl from mafic granulite contain little fluorine (X_F= F/F+Cl+OH: 0.02-0.04 in Bt and <0.01 in Hbl) that suggests a partial melting would take place under the *P-T* condition of Zone IV (up to 730 MPa, 870°C as described above) (Hensen and Osanai, 1994; Osanai *et al.*, 1997). As a preliminary test that H_2O-saturated anatexis may have occurred in the pelitic granulite from Zone IV, a simple melting experiment of the pelitic metamorphic rocks was carried out at 850°C and 700 MPa, which are close to the highest *P-T* conditions for the Main Zone (Osanai *et al.*, 1992, 1997).

The Grt-Bt metapelites (80901 and 81106A: Grt-Bt-Pl-Qtz-Ilm-Po-Gr), which were collected from near the leucosome-bearing pelitic granulite, were selected as the starting material of the experiment using the Boyd-England type of piston cylinder high-pressure apparatus. The run products are melt (33-38%, depending on adding water content) + Opx (21-24%) + Pl (37-43%) for 80901 and melt (37%) + Opx (24%) + Crd (3%) + Pl (36%) for 81106, which are equivalent to mineral (+melt) associations in natural leucosomes derived by in-situ partial melting in Zone IV. Assumed melting reactions are as follows (Osanai *et al.*, 1992; Komatsu *et al.*, 1994);

$Bt + Qtz + H_2O = Opx + melt$,

$Bt + Grt + Qtz + H_2O = Opx + melt$,

$Bt + Grt + An\text{-}poor\ Pl + Qtz \pm H_2O = Opx + An\text{-}rich\ Pl + melt$,

$Bt + Grt + An\text{-}poor\ Pl + Qtz \pm H_2O = Opx + Crd + An\text{-}rich\ Pl + melt$,

$Bt + Grt + Rt\ (in\ Grt) + Qtz \pm H_2O = Opx + Crd + Ilm + melt$.

7.3 Timing and place of granite magma genesis in lower crustal part of the Hidaka metamorphic belt

As described above, the highest-grade metamorphic rocks of the Hidaka metamorphic belt are exposed in Zone IV of the western margin of the belt where deeper part of the metamorphic sequence is cut by the HMT. The natural occurrences and the results of melting experiment (*ca.* 30-40 vol.% of melt) indicate that only incipient partial melting of granulites would have taken place in Zone IV, even though the S-type granitic rocks occur widespread and in large quantities.

The maximum *P-T* condition of Zone IV is up to 730 MPa and 870°C, but mafic granulite enclaves in the basal tonalite in Zone IV indicates higher temperature up to 950°C (Osanai

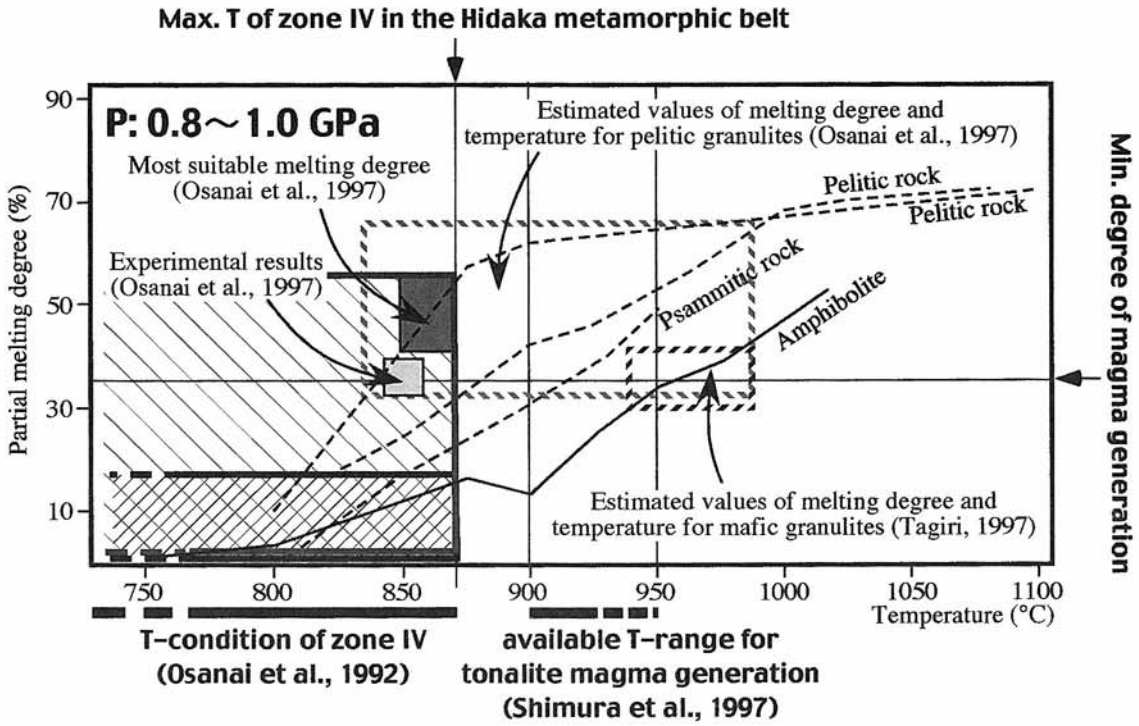

Fig. 16. Partial melting degree (%) vs. temperature diagram estimated from the petrological investigations of the anatexites from the Hidaka metamorphic belt compared to published experimental results.

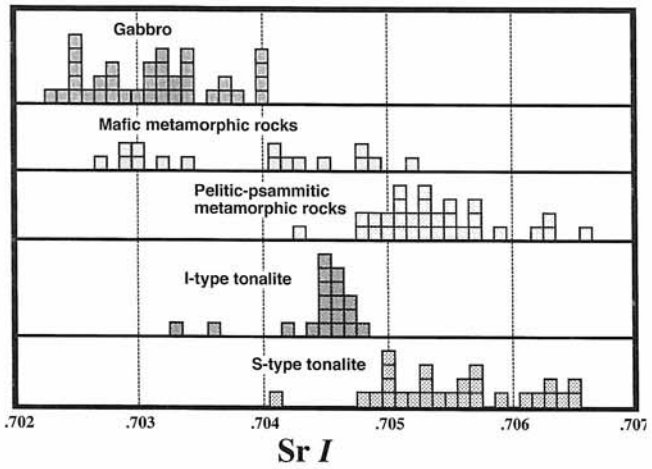

Fig. 17. Histogram of Sr isotopic ratios corrected with 55 Ma of the metamorphic and igneous rocks from the Hidaka metamorphic belt (Shimura, 1999 and the compiled data therein).

et al., 1991; Shimura *et al.*, 1992) (Fig. 15). Shimura *et al.* (1992) carried out the melting experiments using the natural S-type tonalites to determine the melting and emplacement positions of those magma in the Hidaka metamorphic belt. The result of their experiment suggests the place of magma genesis would be at around 800 MPa and more than 900°C among the missing part of the metamorphic sequence during the duplex-forming thrust-up movement. That position is assumed to be a few km deeper part (*ca.* 25-27 km in depth) compared to the basal part of Zone IV (*ca.* 23 km in depth) along the HMT, where supposed melting degree of pelitic granulite is up to 65% (Vielzeuf and Holloway, 1988) (Fig. 16). This value is close to estimated maximum values of melt volume through the experiment as described above and then it would be easy to make a melt segregation and intrusive mass. The continuous intrusion of the S-type tonalite from deeper to middle horizon into the metamorphic sequence at the Niikappu river district in the central area is evident occurrence of magma movement (*e.g.* Shimura *et al.*, 1997). The Sr isotope initial rations (Sr*I*) normalized at 55 Ma for the S-type tonalites and the pelitic granulites taken from a whole area of the Hidaka metamorphic belt show quite similar values ranging from 0.7041 to 0.7066, which indicates the strong consanguinity between them (Fig. 17).

The origin of the I-type tonalites (metaluminous Opx-Hbl-Bt tonalite and Hbl-Bt tonalite) was considered as (1) fractionation-assimilation product from mantle derived gabbro-diorite magma (Ishihara and Terashima, 1985) or (2) anatexite derived from mafic granulites (Ikeda, 1984; Tagiri *et al.*, 1989; Owada and Osanai, 1989; Tagiri, 1997; Osanai *et al.*, 1997; Shimura, 1999). The Sr*I* for the I-type tonalites normalized at 55 Ma show the same values to mafic granulite of Zone IV ranging from 0.7027 to 0.7052, while gabbro and diorite from the Hidaka metamorphic belt have different Sr initial ratios (Fig. 17; 0.7023-0.7040: Maeda and Kagami, 1994; Shimura, 1999). These isotopic characteristics indicate the strong relationship between the I-type tonalites and the mafic granulites on their origin. Commonly the degree of partial melting of mafic granulites and/or amphibolites is smaller than that of pelitic metamorphic rocks (*e.g.* Beard and Lofgren, 1991; Wolf and Wyllie, 1994). A melting

degree of the mafic granulite (pyroxene-bearing amphibolite) in Zone IV (*ca.* 850°C) is assumed to be less than 20% through the melting experiment of Wolf and Wyllie (1994), which value is not suitable to behave the melt as a magma. Based on model calculation using major, trace and rare-earth elements, the generation of I-type tonalite can be explained by partial melting of the mafic granulite with 20-30 % degree of melting (Owada and Osanai, 1989; Shimura, 1999). The melting degree of the mafic granulite will be supposed to be up to 35% at the place of the S-type magma generation (800 MPa and 900 - 950°C) as described above, where the melt derived from the mafic granulites would be segregated and play as a magma.

8. Field Trip

The geological map of the whole area of the Hidaka metamorphic belt and the area visited on this excursion is shown in Figure 4 and Figure 18, respectively.

Day 1 (7th September 2003)

Lower gabbroic rocks of the northern part of the Hidaka metamorphic belt in the upper stream of Pankenushi River

Chitose Airport→*expressway*→*Route 274*→Hidaka town →*wilderness rough road*→Pankenushi River→Stops 1 and 2 →Hidaka town→*Route 274/237/235*→Shizunai Spa (suburb of Shizunai town)

Stop 1: (Day 1-1). Syn-metamorphic igneous activity in the northern area of the Hidaka metamorphic belt

The upper stream of Pankenushi River is underlain by the Pankenushi suite (Ol-bearing Px gabbro) and Memurodake complex (Hbl diorite) from west to east (Fig. 10). At this stop, we can observe the Ol-bearing Px gabbro with layered structure of the Pankenushi suite. The well-developed layered structure is made up from thin alternation of troctolite and Phl- and Hbl-bearing Ol-Px gabbro. The width of each layer is several cm to tens cm. The anorthositic thin layer is locally observed within the layered structure.

The troctolite shows coarse-grained cumulous texture but locally granoblasitic recrystallization, and consists mainly of Pl and Ol with Oq as an accessory mineral. Brown Hbl and Phl surrounding Ol, Cpx and Opx are found in the Phl- and Hbl-bearing Ol gabbro.

Stop 2: (Day 1-2). Foliated two Px gabbro in the mylonite zone

At this stop, we observe the layered gabbro with mylonitic foliations. The gabbro consists of Pl, Opx locally porphyroclastic, Cpx and brown Hbl with Oq and Ap as accessory minerals. The fine two Pxs and Pl grains and the elongated Opx porphyroclasts form the foliations. The brown Hbl grains coexist with Opx and Cpx. From the textural point of view, the recrystallization during the mylonite formation of the Pankenushi suite may have proceeded under the granulite facies condition.

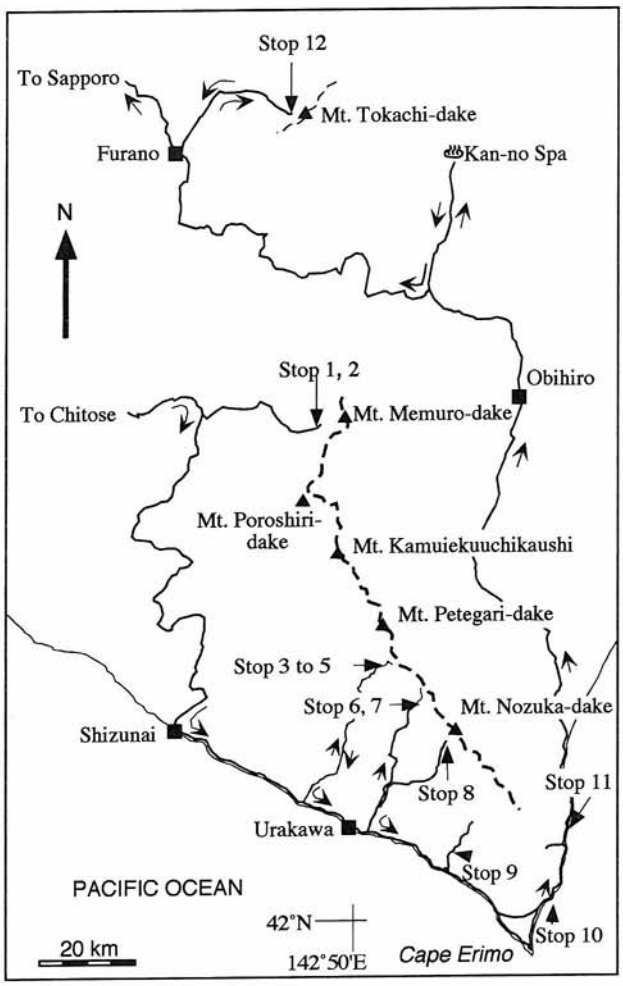

Fig. 18. Routes and stops of the Field trip B1.

Day 2 (8th September 2003)

Crustal anatexis in the lower crust of the central part of the Hidaka metamorphic belt in the upper stream of Motourakawa River

Shizunai Spa (suburb of Shizunai town)→*Route 235*→ Ogifushi village→*wilderness rough road along* Motourakawa River→Nishu-omanai River (Kamui mountain hut)→*trail and river walk*→Stops 3, 4 and 5→*wilderness rough road*→ *Route 235*→Aeru guest house (suburb of Urakawa town, capital of the Hidaka district)

Today if we are lucky, we can see wild brown bears along the trail and river!!

Stop 3: (Day 2-1). Western marginal mylonite zone along the Hidaka Main Thrust

In this area the most narrow western marginal mylonite zone is exposed with a thickness of approximately 100 m, whereas both Hbl-mylonite of Qtz-diorite or mafic granulite origin and Bt-mylonite of the basal tonalite origin (often Grt-bearing) are seen in the river. Just along the Hidaka Main Thrust (HMT), these mylonites are indicating cataclastic

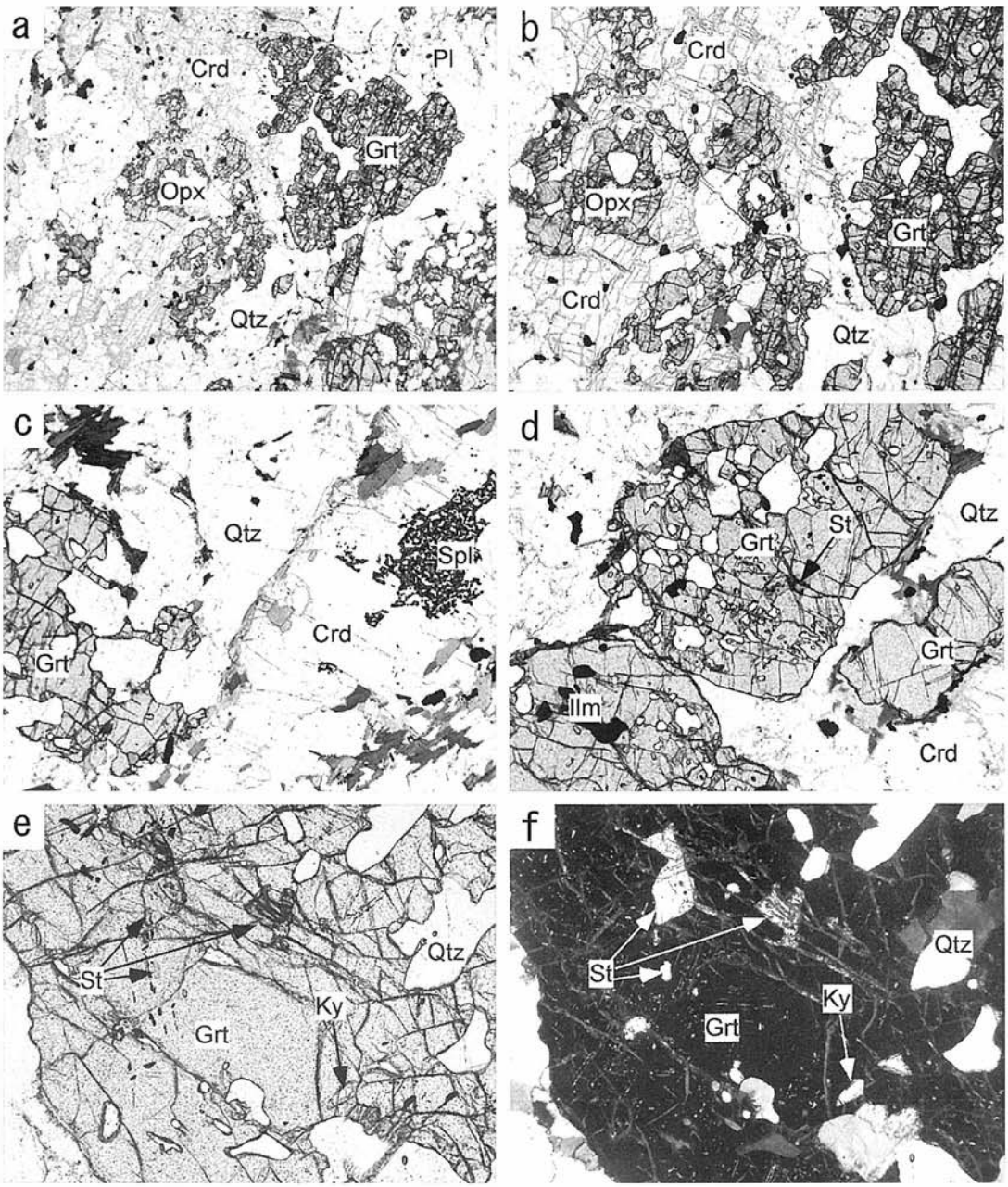

Fig. 19. Photomicrographs of the pelitic granulite. Note that Ky and St as relict minerals included in a porphyroblastic Grt grain (f).

features.

Stop 4: (Day 2-2). Basal tonalite intrusion in granulite unit of Zone IV

Weakly mylonitized Opx-Crd and Grt-Opx-Crd tonalites with S-type peraluminous affinity are observed as intrusion into granulite-facies metamorphic rocks of Zone IV, next to the mylonite zone. These tonalites are often saved from mylonitization, in which characteristic inclusion-free euhedral Crd still remains as an igneous mineral crystallized from tonalitic magma. Not only here but also upper streamside, these S-type tonalites include ultramafic xenoliths (Spl-lherzolite or harzburgite).

Stop 5: (Day 2-3). Thin alternation of mafic granulite and pelitic granulie

At this exposure thin alternation of mafic and pelitic granulites including Opx-Hbl granulite (Opx-bearing amphibolite), Grt-Opx-Crd gneiss, Opx-Crd-Bt gneiss and Grt-Crd-Bt gneiss is observed. So-called agmatitic amphibolite is the well-foliated veined mafic granulite (Opx-Hbl granulite). Veins of the agmatitic amphibolite are Qtz-norite or Opx-bearing diorite in composition and assemblage. Opx-concentrated reaction zone is formed at the boundary between veins and mafic granulite. Mafic and pelitic granulites frequently show the evidence of partial melting to

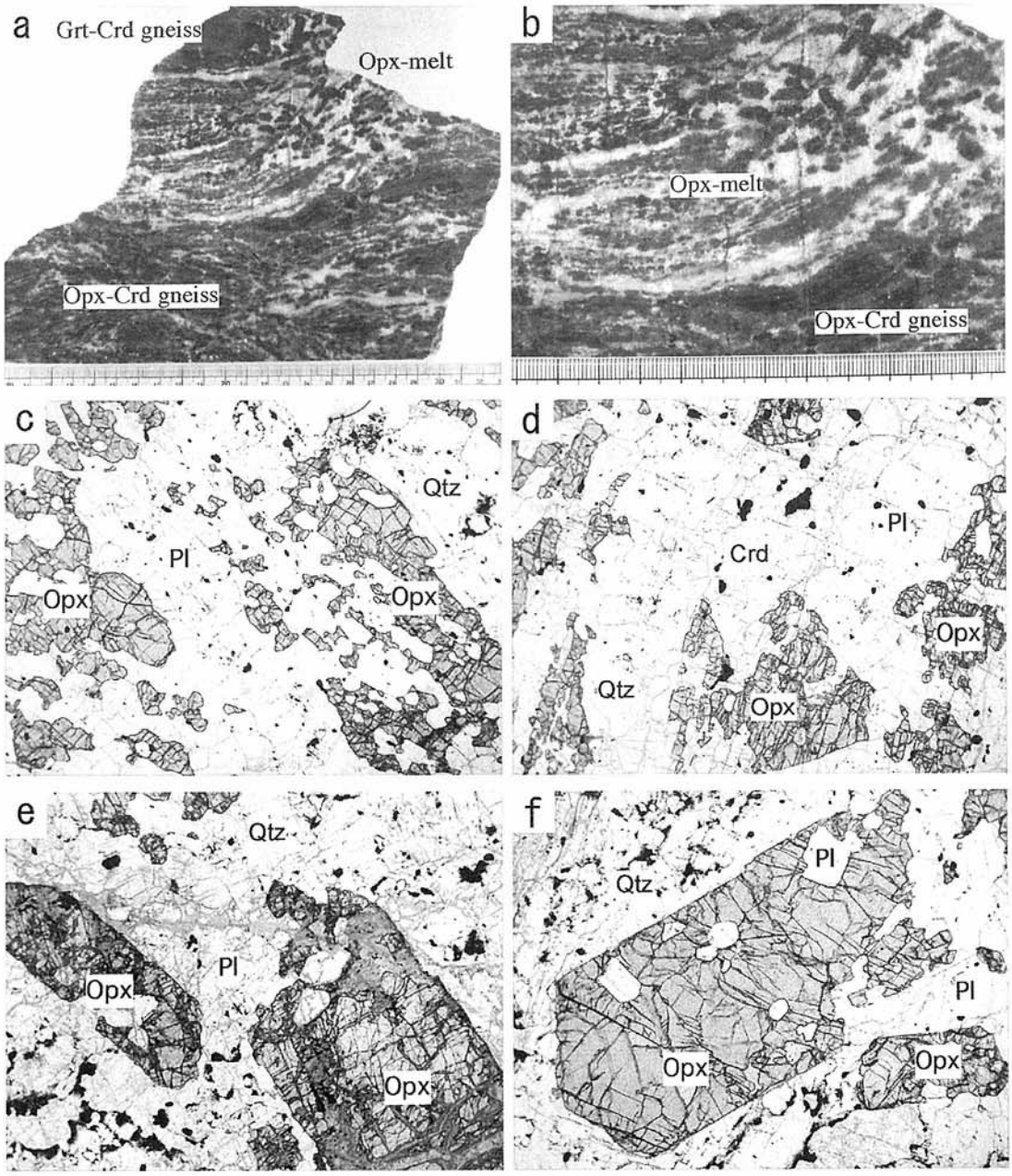

Fig. 20. Polished slabs of the mafic and pelitic granulites with agmatitic nature (a, b). Photomicrographs (c-f) of the leucocratic vein in the Opx-Crd gneiss. Note that euhedral Opx includes calsic-Pl.

form highly euhedral Opx-bearing melt pod (Fig. 14).

The mafic granulite is mainly Cum-bearing Opx-Hbl granulite containing Opx, Hbl, Pl with subordinate Qtz, Ilm and secondary Cum. Opx-bearing melt pod derived from partial melting of mafic granulite consists of Opx, Pl and Qtz, which also contains Hbl as inclusions in Opx and Cum and as a secondary phase around Opx. Grt-Opx-Crd gneiss contains mainly Grt, Opx, Crd, Pl and Qtz with subordinate Kfs, Bt, Gr, Ap, Ilm and Po and Grt-Crd-Bt gneiss is containing Grt, Crd, Bt, Pl and Qtz with minor Sil and Hc inclusions in Crd. Accesory minerals are Gr, Ilm, Po and Ap. Opx±Crd-bearing anatectic melt is often seen in both pelitic garnulites.

Day 3 (9th September 2003)

High-grade granulites and related magmatism of the central area of the Hidaka metamorphic belt in the upper stream of Horobetsu River and Niobetsu River areas

Aeru guest house (suburb of Urakawa town)→*wilderness rough road*→Horobetu River→*bush and river walk*→Stops 6 and 7→Urakawa→*Route 236*→Niobetsu River→*on foot*→ Stop 8→Urakawa (Aeru guest house)

Today if we are lucky, we can meet wild brown bears again!!

Stop 6: (Day 3-1). Basal mylonite zone along the Hidaka Main Thrust

The exposure is situated at the eastern border of the western marginal (basal) mylonite zone of the Hidaka metamorphic belt. At this stop, we can observe Hbl mylonite of Qtz-diorite or mafic granulite origin and mylonitized S-type tonalites (Bt mylonite) with their inclusions of Opx-bearing brown Hbl amphibolite and rare ultramafic rocks (meta-harzburgite ?).

Stop 7: (Day 3-2). The highest-grade granulites of the Hidaka metamorphic belt

At this exposure, we can observe the details of mode of occurrences of various granulite-facies rocks in Zone IV. It consists mainly of Grt-Crd-Bt gneiss, Grt-Opx-Crd gneiss, Opx-Crd gneiss, Opx-Pl gneiss, and Opx-bearing amphibolite (mafic granulite) with rare Oam-bearing mafic gneiss. These granulites are often obliquely cut by euhedral Opx-bearing anatexite. These granulites show an NW-SE trending foliations and an NNE-SSW trending mineral lineations.

The constituents of the Opx-bearing amphibolite are Opx, brown Hbl, Pl, Ilm with or without Qtz and Cum. Opx is often replaced by secondary Oam. Grt-Opx-Crd gneiss contains Grt, Opx, Crd, Pl, Qtz with rare Bt (Figs. 19a,b). Grt-Crd-Bt gneiss contains Grt, Crd, Bt, Pl, and Qtz with minor Sil and Hc as inclusions in Crd, and St and Ky in Grt (Figs. 19c-f). In Zone IV, anatectic melts consisting mainly of Opx, Pl and Qtz intruded obliquely into these amphibolite and genisses with agmatitic features displayed by a mixture of host rock and leucocratic veins or lenses (Fig. 20). Partly leucocratic Opx-bearing anatectic veins also include Crd.

Opx-free brown Hbl amphibolite is also seen in the upper stream side of these granulites. The brown Hbl amphibolite consists mainly of Hbl and Pl with subordinate Cpx, Cum and Qtz, but no Opx. The amphibolite shows an NW-SE trending foliation and an NW-SE trending mineral lineation. Some of the amphibolites show weakly shear deformation affected by the southward thrusting. Thin intercalations of Ged-Crd gneiss and Ath gneiss are also observed in the amphibolite.

Stop 8: (Day 3-3). The second stage igneous activity and the low-pressure granulite facies xenoliths

The Mt. Nozuka-dake area is underlain by various kinds of igneous rocks with small amounts of metamorphic rocks (Fig. 11). In the second stage the Niobetsu complex cuts the foliation of the host mylonitic rocks, and is no sings of any mylonitic deformation. The magma activity of the Niobetsu complex occurred at 18.3 ± 2.7 Ma (Owada *et al*., 2002).

The Niobetsu complex includes the xenoliths derived from the host S-type tonalite. These xenoliths show recrystallized-granoblastic texture with locally remaining mylonitic foliation, and consist of Pl, Opx, Crd, Qtz, Bt, Kfs, Spl, Ap, Oq and Grt. The metamorphic grade reached up to the low pressure granulite facies in terms of mineral parageneses. The second stage igneous activity took place at the post-D3 event, probably post-collisional events in the Hidaka Collision Zone.

If we are lucky, we can find the Grt-bearing fayalite- and almandine-bearing Bt-Qtz norite (a member of the Niobetsu complex) as bolders in the stream.

Day 4 (10th September 2003)

Mantle peridotite, the metamorphosed pelitic rocks and intrusive rocks in middle to upper crustal level of the southern end of the Hidaka metamorphic belt

Aeru guest house→*Route 336*→Horoman Peridtite sheet→*Route 336*→Cape Erimo→*Route 336*→Ruran-Chipira shore reef→*Route 336*→Tan-neso plutonic complex→*Route 336*→Obihiro station→*Local Route*→Kan-no Spa.

Stop 9 (Day 4-1). Horoman Peridoite sheeted complex

The Pl-lherzolite contains much greater amounts of Pl, and commonly is intercalated with thin layers of pyroxenites and gabbros with green Spl. The peridotite generally shows a granular texture. The pyroxenite and Pl-free lherzolite locally occur as along the fringe of the Pl lhrzolite. Some pyroxenite layers are boudinaged, and are slightly rotated due to shearing. The gabbro layer or vein are mainly composed of coarse Pl and Opx, minor amounts of Ol, Cpx and Ti-Parg.

Stop 10 (Day 4-2). Biotite gneiss to schist of the Upper sequence and cordierite-muscovite tonalite of the Ruran-Chipira shore reef and the Saruru River

In the southern end of the Hidaka metamorphic belt, we can observe the field relationship between the Bt gneiss assigned to Zone II and the Crd-bearing two mica granodiorite (S-type granitic rock). The Crd-bearing two mica granodiorite intrudes the Bt gneiss. The Bt gneiss is composed mainly of Pl, Bt, Qtz, Ms, alumino-silicate and a small amount of opaque minerals. On the other hand, the Crd-bearing two mica granodiorite consists mainly of Pl, Qtz, Bt, Ms, Kfs and small amounts of Crd and opaque minerals.

Stop 11: (Day 4-3). Various igneous rocks at the Oshirabetsu complex

The I-type zoned pluton intrudes the Oshirabetsu gabbro to diorite complex, and locally includes the Phl-bearing Ol gabbro as xenoliths. The zoned pluton locally contains various kinds of metamorphic rocks, as a diatreme. The matrix granitic rock in this zone shows reddish brown in color, and contains Opx and abundant graphite and sulphide minerals compared to the other parts of the body. The Opx grains may be derived from anatectic peraluminous melt of the xenolithic materials. The K-Ar Bt dating of the norlite from the Oshirabetsu complex gives an age of 35.3 ± 1.1 Ma (Ishihara and Tershima, 1985).

Day 5 (11th September 2003)

Tokachi-dake volcano in central Hokkaido

Kan-no Spa→*Route 38*→Furano town→*Route 237*→Tokachi-dake spa→*Route 237*→Furano town→*Route 38*→Takikawa city→*Express way*→Sapporo city

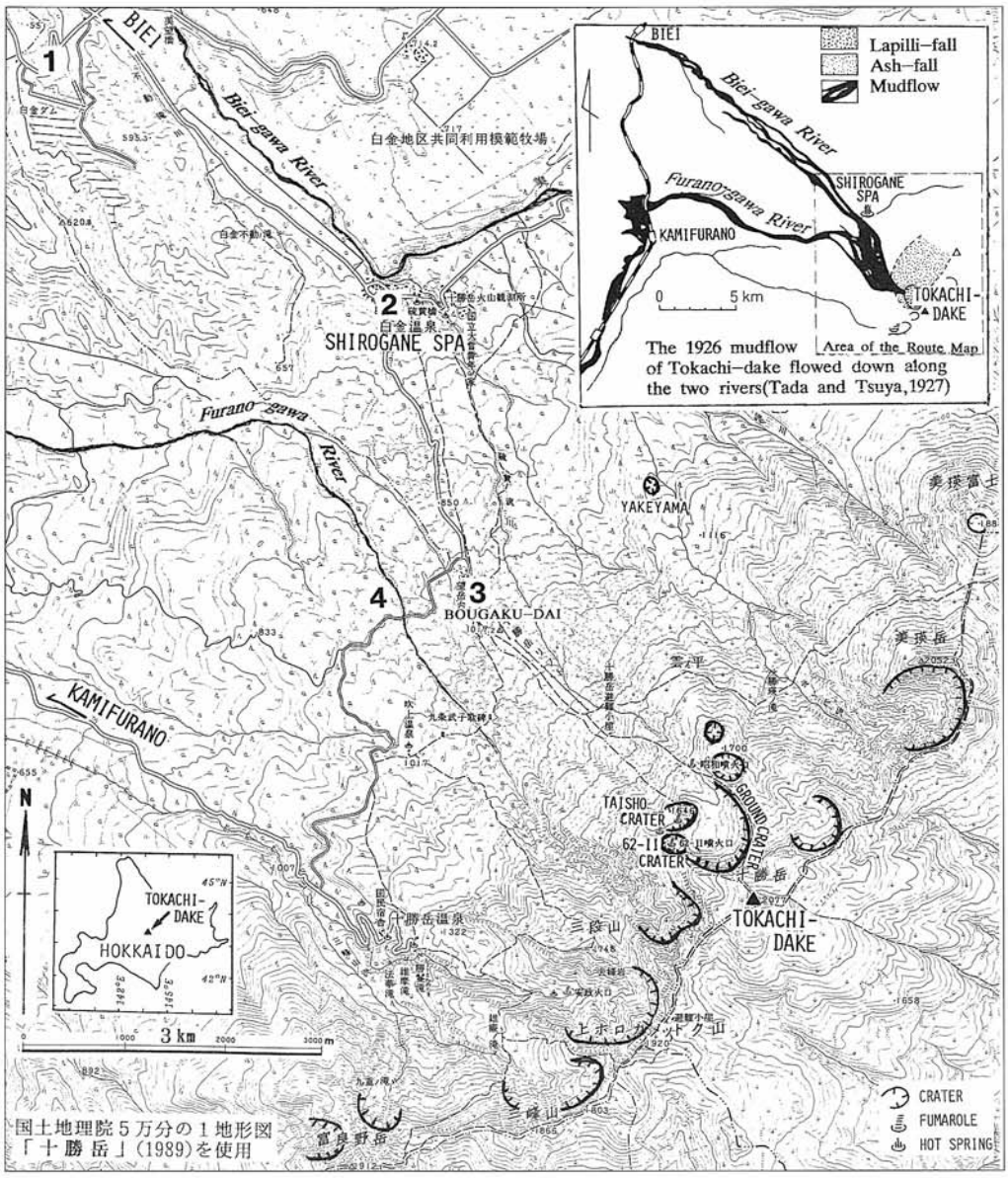

Fig. 21. Route map of Tokachi-dake Volcano. Numbers 1-4 are recommended stops.
1: Outcrops of felsic pyroclastic flow deposits (welded) of early Pleistocene. 2: Shirogane Spa, reconstructed after the 1988-89 eruption. 3: Whole view of the volcano and outcrops of lavas and pyroclastic flow deposits of the younger volcano group. 4: Sabo works against volcanic mudflow (lahar).

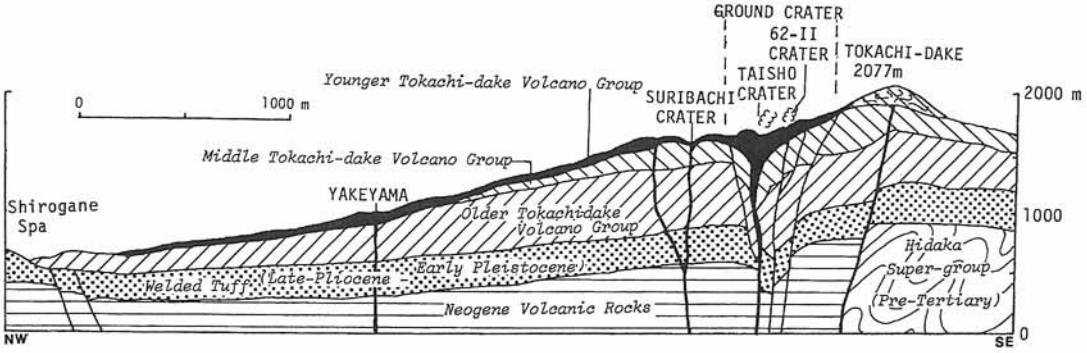

Fig. 22. NW-SE cross-section of Tokachi-dake Volcano (Katsui et al., 1990).

Table 2. Volcanic eruptions of Tokachi-dake in historic times (Katsui et al., 1990).

Year A.D.	Events
ca.1670*	A lava flow descended to Bougaku-dai, 3km NW of the central cone.(*radiocabon date)
1857	An eruption column observed.
ca.1887	Eruption columns and ash-falls observed.
1926	On May 24, the first explosion occurred and caused mudflow which destroyed an inn at the place of Shirogane Spa. Then, the second explosion occurred and the NW sector of the central cone collapsed, producing a hot volcanic avalanche which triggered disastrous mudflow by snow melting. The mudflow reached Kamifurano village, 25km NW of the crater, with an average velosity of 60km/h. In total 144 people were killed and 5080 houses were destroyed mostly by the mudflow. In September the activity renewed, and 2 people were lost near the new crater (Taisho Crater).
1962	On June 29, the first eruption (phreatic) occurred and killed 5 sulfur-miners by ballistic blocks. Then, 3 hours later, the second eruption (magmatic) started. The eruption column reached 12km high, and ash fell toward the E. This strong eruption lasted for 11 hours. New craters (62-0～III) opened along the SW rim of Ground Crater.
1988 -89	On Dec. 16, phreatic explosions started from 62-II Crater. Then, the activity changed into phreato-magmatic explosions and continued intermittently until March 1989, being frequntely accompanied with small-scale pyroclastic surges and flows. No casualty.

Stop 12: (Day 5-1) Tokachi-dake Volcano

Tokachi-dake (2077m), one of the most active volcanoes in Japan, is situated in the central highlands of Hokkaido. It forms the SW part of the Daisetsu-Tokachi volcanic chain, which represents the SW end of the Kuril volcanic arc.

This volcano is built on a wide plateau of felsic pyroclastic flow deposits of late-Pliocene to early-Pleistocene, and consists of many strato-volcanoes of basalt and andesite which were formed in middle-Pleistocene to Holocene.

As shown in Figures 21 and 22, the volcanic edifices of Tokachi-dake are arranged mainly in a direction of NE-SW, and are divided into three groups; the Older, Middle and Younger Tokachi-dake Volcano Groups. The Holocene eruption centers of the Younger Tokachi-dake Volcano Group together with fumaroles and hot-springs, are located on the NW side of the main trend of volcano arrangement. Such structural features of Tokachi-dake suggest the presence of a concealed cauldron or volcano-tectonic depression which was formed through repeated eruptions of the large felsic pyroclastic flows.

The products of the Young Tokachi-dake Volcano Group are mostly mafic andesite. Eruptions of scoria with or without lava flows are the most common activity throughout this period. However, pyroclastic flow and sector collapse of the volcanic edifice occurred also, as evidenced by the prehistoric eruption (*ca.* 240 B.C.) and the 1962 eruption, respectively.

Tokachi-dake has been very active and hazardous during historic times (Table 2). The regular repetition of historic eruptions at an interval of 30-40 years attracts our attention in regard to the prediction of eruption in near future. Prior to the 1988-1989 eruption, hazard maps of Tokachi-dake were prepared, which led to successful evacuation. Then, together with improvement of the volcano monitoring system, various measures for mitigation of volcanic disasters have been introduced (Katsui *et al.*, 1990).

Acknowledgements: The authors wish to thank Mrs. T. Yamasaki, T. Nakano and S. Kawanami for help the field work. Thanks due to Prof. Y. Hiroi for improvement of the manuscript.

References

Arita, K., Toyoshima, T., Owada, M., Miyashita, S. and Jolivet, L. (1986) Tectonic movements of the Hidaka metamorphic belt, Hokkaido, Japan. *Monogr. Assoc. Geol. Collab. Japan*, **31**, 247-263.*

Arita, K., Shingu, H. and Itaya, T. (1993) K-Ar geochronological constraints on tectonics and exhumation of the Hidaka metamorphic belt, Hokkaido, northen Japan. *Jour. Mineral. Petrol. Econ. Geol.*, **88**, 101-113.*

Arita, K., Ikawa, T., Ito, T., Yamamoto, A., Saito, M., Kimura, G., Watanabe, T., Ikawa, T. and Kuroda, T. (1998) Crustal structure and tectonics of the Hidaka Collision Zone, Hokkaido (Japan), revealed by vibroseis seismic reflection and gravity surveys. *Tectonophysics*, **290**, 197-210.

Beard, J. S. and Lofgren, G. E. (1991) Dehydration melting and water-saturated melting of basalic and andesitic greenstones and amphibolites. *Jour. Petrol.*, **32**, 356-401.

Bhattacharya, A. and Sen, S. K. (1985) Energetics of hydration of cordierite and water barometry in cordierite - granulites. *Contrib. Mineral. Petrol.*, **89**, 370-378.

Brey, G. P. and Köler, T. (1990) Geothermometry in four-phase lherzolites II. New thermobarometers, and practical assessment of existing thermobarometers. *Jour. Petrol.*, **31**, 1353-1378.

Dutrow, B. L. and Holdaway, M. J. (1989) Experimental determination of the upper thermal stability of Fe-staurolite+quartz at medium pressures. *Jour. Petrol.*, **30**, 229-248.

Ferry, J. M. (1981) Petrology of graphitic sulfide-rich schists from South-Central Maine: an example of desulfidation during progradereglonal metamorphism. *Amer. Mineral.*

66, 908-930.

Ganguly, J. and Saxena, S. K. (1984) Mixing properties of aluminosilicate garnets: constraints from natural and experimental data, and applications to geothermo-barometry. *Amer. Mineral.*, **69**, 88-97.

Graham, C. M. and Powell, R. (1984) A garnet - hornblende geothermometer: caliblation testing, and application to the Pelona Schist, Southern California. *Jour. Metamorphic Geol.*, **2**, 13-31.

Harley, S. L. (1984) An experimental study of the partitioning of Fe and Mg between garnet and orthopyroxene. *Contrib. Mineral. Petrol.*, **86**, 359-373.

Hensen, B. J. and Osanai, Y. (1994) Experimental study of dehydration melting of F-biotite in model pelitic compositions. *Mineral. Mag.*, **58A**, 410-411.

Himmelberg, G. R., Brew, D. A. and Ford, A. B. (1994) Evaluation and application of garnet amphibolite thermobarometry, Western Metamorphic Belt near Juneau, Alaska. *USGS Bull.*, **2107**, 185-198.

Holdaway, M. J., Mukhopadhyay, B., Dyar-M-D, M. D., Guidotti, C.V. and Dutrow, B.L. (1997) Garnet-biotite geothermeter revised; new Margules parameters and a natural specimen data set from Maine. *Amer. Mineral.*, **82**, 582-595.

Ikeda, Y. (1984) Trace elements of granitic rocks from Hidaka belt, Hokkaido. *Magma*, **70**, 9-14.**

Ishihara, S. and Terashima, S. (1985) Cenozoic granitoids of central Hokkaido, Japan - an example of plutonism along collision belt. *Bull. Geol. Surv. Japan*, **36**, 653-680.

Ito, T., Moriya, T., Ikawa, H., Ikawa, T., Arita, K., Tsumura, N., Shinohara, M., Miyauchi, T., Kimura, G., Okuike, S., Shimizu, N. and Ikawa, T. (1999) Delamination-wedge tectonics of the Hidaka Collision Zone. *Earth Monthly (Gekkan chikyu)*, **21**, 130-136.**

Katsui, Y., Kawachi, S., Kondo, Y., Ikeda, Y., Nakagawa, M., Gotoh, Y., Yamagishi, H., Yamazaki, T. and Sumita, M. (1990) The 1988-1989 eruption of Tokachi-dake, central Hokkaido, its sequence and mode. *Bull. Volcanol. Soc. Japan, Ser. 2*, **35**, 111-129.

Komatsu, M., Miyashita, S., Maeda, J., Osanai, Y., Toyoshima, T., Motoyoshi, Y. and Arita, K. (1982) Petrological constitution of the continental type crust upthrust in the Hidaka belt, Hokkaido. *Jour. Japan. Assoc. Mineral. Petrol. Econ. Geol., Spec. Pap.*, no. 3, 220-230.*

Komatsu, M., Miyashita, S., Maeda, J., Osanai, Y. and Toyoshima, T. (1983) Disclosing of a deepest section of continental-type crust up-thrust as the final event of collision of arcs in Hokkaido, north Japan. *In* Hashimoto, M. and Uyeda, S., eds. *Accretion Tectonics in the Circum-Pacific Regions*, TERRAPUB, Tokyo, 149-165.

Komatsu, M., Miyashita, S. and Arita, K. (1986) Composition and structure of the Hidaka metamorphic belt, Hokkaido-historical review and present status-. *Monogr. Assoc. Geol. Collab. Japan*, **31**, 189-203.*

Komatsu, M., Osanai, Y., Toyoshima, T. and Miyashita, S. (1989) Evolution of the Hidaka Metamorphic Belt, Northern Japan. *In* Daly, J. S., Cliff, R. A. and Yardley, B. W. D., eds., *Evolution of Metamorphic Belts*. Geol. Soc. Spec. Pub., no. 43, 487-493.

Komatsu, M., Toyoshima, T., Osanai, Y. and Arai, M. (1994) Prograde and anatectic reactions in the deep arc crust exposed in the Hidaka metamorphic belt, Hokkaido, Japan. *Lithos*, **33**, 31-49.

Lal, R. K. (1993) Internally consistent recalibrations of mineral equilibria for geothermobarometry involving garnet-orthopyroxene-plagioclase-quartz assemblages and their application to the South Indian granulites. *Jour. Metamorphic Geol.*, **11**, 855-866.

Landis, C. A. (1971) Graphitization of dispersed carbonaceous material in the metamorphic rocks. *Contrib. Mineral. Petrol.*, **30**, 34-45.

Lee, H. Y. and Ganguly, J. (1988) Equilibrium compositions of coexisting garnet and orthopyroxene: Experimental determinations in the system FeO - MgO - Al_2SiO_5 - SiO_2, and applications. *Jour. Petrol.*, **29**, 93-113.

Maeda, J. (1990) Opening of the Kuril Basin deduced from the magmatic history of central Hokkaido, north Japan. *Tectonophysics*, **174**, 235-255.

Maeda, J. and Kagami, H. (1994) Mafic igneous rocks derived from N-MORB source mantle, Hidaka magmatic zone, central Hokkaido: Sr and Nd isotopic evidence. *Jour. Geol. Soc. Japan*, **100**, 185-188.*

Maeda, J. and Kagami, H. (1996) Interaction of a spreading ridge and an accretionary prism: Implications from MORB magmatism in the Hidaka magmatic zone, Hokkaido, Japan. *Geology*, **24**, 31-34.

Maeda, J. and Saito, K. (1997) Role of mantle-derived primitive magma for generation of continetal crust: Inferences from the Hidaka metamorphic belt, central Hokkaido. *Mem. Geol. Soc. Japan*, no. 47, 75-85.*

Maeda, J., Suetake, S., Ikeda, Y., Tomura, S., Motoyoshi, Y. and Okamoto, Y. (1986) Tertiary plutonic rocks in the axial zone of Hokkaido-distribution, age, major element chemistry, and tectonics-. *Monogr. Assoc. Geol. Collab. Japan*, **31**, 223-246.*

Martignole, J. and Sisi, J. (1981) Cordierite-garnet-H_2O equilibrium: A geological thermometer, barometer and water fugacity indicator. *Contrib. Mineral., Petrol.*, **77**, 38-46.

Miyoshi, M. (1986) Geology and metamorphism of the Main Zone of the Hidaka metamorphic belt in the Rekifune River area of the middle part of the Hidaka range, Hokkaido. *In* Komatsu, M., ed., *Tectonic Belts in Hokkaido, No.1*. Report of research project, Grant-in-Aid for Scientific Research (No. 60302031) from the Ministry of Education, Japan, 29-33.**

Newton, R. C. and Haselton, H. T. (1981) Thermodynamics of the garnet - plagioclase - Al_2SiO_5 - quartz geobarometer. *In* Newton, R. C., Navrotsky, A., and Wood, B. J., eds., *Advances in physical geochemistry, vol. 1*, Springer-Verlag, New York, 131-147.

Newton, R. C. and Perkins, III D. (1982) Thermodynamic caliblation of geobarometers based on assemblages garnet - plagioclase - orthopyroxene (clinopyroxene) - quartz. *Amer. Mineral.*, **67**, 203-222.

Osanai, Y. (1985) Geology and metamorphic zoning of the Main Zone of the Hidaka Metamorphic Belt in the Shizunai River region, Hokkaido. *Jour. Geol. Soc. Japan*, **91**, 259-278.*

Osanai, Y. and Owada, M. (1990) Finding of staurolite in pelitic granulites from the Hidaka metamorphic belt, Hokkaido, Japan. *Jour. Geol. Soc. Japan*, **96**, 549-552.

Osanai, Y. and Owada, M. (1994) High temperature metamorphism and related crustal anatexis in the Hidaka metamorphic belt, Hokkaido, north Japan. *Geology News*, no. 478, 34-44.*

Osanai, Y., Miyashita, S., Arita, K. and Bamba, M. (1986) The metamorphism and thermal structure of the collisional terrain of a continental and oceanic crusts: a case of the Hidaka metamorphic belt, Hokkaido, Japan. *Monogr. Assoc. Geol. Collab. Japan*, **31**, 205-222.*

Osanai, Y., Owada, M. and Takasu, I. (1989) Original rock constitution of the Main Zone of the Hidaka metamorphic belt, Hokkaido, Japan. *Bull. Fukuoka Univ. Educ., ser. III*, **38**, 71-91.*

Osanai, Y., Komatsu, M. and Owada, M. (1991) Metamorphism and granite genesis in the Hidaka Metamorphic Belt, Hokkaido, Japan. *Jour. Metamorphic Geol.*, **9**, 111-124.

Osanai, Y., Owada, M. and Kawasaki, T. (1992) Tertiary deep crustal ultrametamorphism in the Hidaka metamoprhic belt, northern Japan. *Jour. Metamorphic Geol.*, **10**, 401-414.

Osanai, Y., Owada, M., Shimura, T., Kawasaki, T. and Hensen, B.J. (1997) Crustal anatexis and related acidic magma genesis in the Hidaka metamorphic belt, Hokkaido, northern Japan. *Mem. Geol. Soc. Japan*, no. 47, 29-42.*

Owada, M. and Osanai, Y. (1989) Genesis of granitic rocks in the Hidaka metamorphic belt. *Earth Monthly (Gekkan Chikyu)*, **11**, 252-257.**

Owada, M., Osanai, Y. and Kagami, H. (1991) Timing of anatexis in the Hidaka metamorphic belt, Hokkaido, Japan. *Jour. Geol. Soc. Japan*, **97**, 751-754.

Owada, M., Osanai, Y. and Kagami, H. (1992) Timing of granitic magma genesis under the lower crustal condition-an example of the Hidaka metamorphic belt-. *Earth Monthly (Gekkan Chikyu)*, **14**, 291-295.**

Owada, M., Osanai, Y. and Kagami, H. (1997) Rb-Sr isochron ages for hornblende tonalite from the southeastern part of the Hidaka metamorphic belt, Hokkaido, Japan: Implication for timing of peak metamorphism. *Mem. Geol. Soc. Japan*, no. 47, 21-27.

Owada, M., Yamasaki, T., Yoshimoto, K. and Osanai, Y. (2002) Impact of arc-arc collision on formation of granitic magma and crustal evolution: Evidence from the Nozuka-dake granite in the Hidaka metamorphic belt, Hokkaido, Japan. *Abstr. Japan. Assoc. Mineral. Petrol. Econ. Geol.*, 241.**

Perchuk, L. L. (1991) Delivation of a thermodynamically consistent set of geothermometers and geobarometeres for metamorphic and magmatic rocks. *In* L. L. Perchuk ed. *Progress in Metamorphic and Magmatic Petrology*, Cambridge Univ. Press, Cambridge, 93-111.

Perchuk, L. L. and Lavrent'eva, I. V. (1983) Experimental investigation of exchange equilibria in the system cordierite-garnet-biotite. *In* Saxsena, S. K., ed. *Kinetics and Equilibrium in Mineral Reactions*. Springer-Verlag, New York, 199-239.

Perchuk, L. L., Aranovich, l. Ya, Podlesskii, K. K., Lavrent'eva, I.V., Gerasimov, V.Y., Kitsul, V.I., Korsakov, L.P. and Berdnikov, N.V. (1985) Precambrian granulites of the Aldan Shield, eastern Siberia, the USSR. *Jour. Metamorphic Geol.*, **3**, 265-310.

Perkins, III D. and Chipera, S. J. (1985) Garnet-orthopyroxene-plagioclase-quartz barometry: refinement and application to the English River subprovince and the Minnesota River valley. *Contrib. Miner. Petrol.*, **89**, 69-80.

Powell, R. and Evans, J. A. (1983) A new geobarometer for the assemblage biotite-muscovite-chlorite-quartz. *Jour. Metamorphic Geol.*, **1**, 331-336.

Powell, R. and Holland, T.J.B. (1988) An internally consistent thermodynamic dataset with uncertainties and correlations: 3. Applications to geobarometry, worked examples and a computer program. *Jour. Metamorphic Geol.*, **6**, 173-204.

Richardson, S. W. (1968) Staurolite stability in part of the system Fe-Al-Si-O-H. *Jour. Petrol.*, **9**, 467-488.

Saeki, K., Shiba, M. and Itaya, T. (1995) K-Ar ages of metamorphic and igneous rocks in the Hidaka metamorphic belt. *Jour. Mineral. Petrol. Econ. Geol.*, **86**, 177-178.*

Shimura, T. (1992) Intrusion of granitic magma and uplift tectonics of the Hidaka metamorphic belt, Hokkaido. *Jour. Geol. Soc. Japan*, **98**, 1-20 .*

Shimura, T. (1999) Genesis of the pyroxene-bearing I-type tonalite and melting degree of the source rock, in the Hidaka Metamorphic Belt, northern Japan. *Jour. Geol. Soc. Japan*, **105**, 536-551.*

Shimura, T., Komatsu, M. and Iiyama, T. (1992) Genesis of the lower crustal garnet-orthopyroxene tonalites (S-type) of the Hidaka Metamorphic Belt, northern Japan. *Trans. Roy. Soc. Edinburgh, Earth Sci.*, **83**, 259-268.

Shimura, T., Komatsu, M., Tsutai, T., Owada, M. and Takahashi, Y. (1997) Thermal and chemical interaction between granitic magmas and wall rocks in the Hidaka metamorphic belt, northern Japan. *Mem. Geol. Soc. Japan*, no. 47, 1-12.*

Tada, F. and Tsuya, H. (1927) The eruption of the Tokachidake volcano, Hokkaido, on May 24th, 1926. *Bull. Earthq. Res. Inst., Tokyo Imp. Univ.* **2**, 49-84.

Tagiri, M. (1997) An estimation of the degree of crustal melting in the Hidaka metamorphic belt. *Mem. Geol. Soc. Japan*, no. 47, 13-20.*

Tagiri, M. and Oba, T. (1983) Synthesis of graphite from bituminous coal at 0.5-2kb water pressure and 300-600 °C. *Jour. Japan. Assoc. Mineral. Petrol. Econ. Geol.*, **78**, 190-193.

Tagiri, M. Shiba, M. and Onuki, H. (1989) Anatexis and chemical evolution of pelitic rocks during metamorphism and migmatization in the Hidaka metamorphic belt, Hokkaido. *Geochem. Jour.*, **23**, 321-337.

Takahashi, T. (1983) The Oshirabetsu gabbroic mass in the southern part of the Hidaka metamorphic belt, Hokkaido, Japan. *Jour. Fac. Sci. Hokkaido Univ. Ser. IV*, **20**, 203-224.

Takahashi, T. and Sasaki, A. (1983) Isotopic composition of sulfer in the Oshirabetsu gabbro complex and the associated nickeliferous pyrrhotite ore - Magmatic sulfide mineralization and the external source of sulfer. *Mining Geol.*, **33**, 399-409.*

Thompson, A. B. (1976) Mineral reactions in pelitic rocks: II. Calculation of some P-T-X(Fe-Mg) phase reactions. *Amer. Jour. Sci.*, **276**, 425-454.

Toyoshima, T., Komatsu, M. & Shimura, T. (1994) Tectonic evolution of lower crustal rocks in relations to magmatic activities in the Hidaka metamorphic belt, Hokkaido, northern Japan. *The Island Arc*, **3**, 182-198.

Toyoshima, T., Komatsu, M. and Shimura, T. (1997) Tectonics of the Hidaka metamorphic belt, Hokkaido, northern Japan. *Mem. Geol. Soc. Japan*, no. 47, 259-277.*

Tsuchiya, N., Suzuki, S. and Chida, T. (1991) Origin of graphite in the Oshirabetsu gabbroic body, Hokkaido Japan. *Jour. Mineral. Petrol. Econ. Geol.*, **86**, 264-272.*

Tsumura, N., Ikawa, H., Ikawa, T., Shinohara, M., Ito, T., Arita, K., Morita, T., Kimura, G. and Ikawa, T. (1999) Delamination-wedge structure beneath the Hidaka Collision Zone, Central Hokkaido, Japan: inferred from seismic reflection profiling. *Geophys. Res. Lett.*, **26**, 1057-1060.

Usuki, T., Kaiden, H., Misawa, K. and Shiraishi, K. (2002) Overgrowth ages of zircons in pelitic granulites from the central part of the Hidaka Metamorphic Belt, Hokkaido, Japan. *Abstr. Japan. Assoc. Mineral. Petrol. Econ. Geol.*, 248.**

Vielzeuf, D. and Holloway, R. (1988) Experimental determination of the fluid-absent melting relations in the pelitic system. Consequences for crustal differentiation. *Contrib. Mineral. Petrol.*, **98**, 257-276.

Wells, P. R. A. (1977) Pyroxene thermometry in simple and complex systems. *Contrib. Mineral. Petrol.*, **62**, 129-139.

Wells, P. R. A. (1979) Chemical and thermal evolution of Archean sialic crust, southern west Greenland. *Jour. Petrol.*, **20**, 187-226.

White, A.J.R. and Chappell, B.W. (1977) Ultrametamorphism and granitoid genesis. *Tectonophysics*, **43**, 7-22.

Wolf, M. B. and Wyllie, P. J. (1994) Garnet growth during amphibolite anatexis: Implication of a garnetiferous restite. *Jour. Geol.*, **101**, 357-373.

Wood, B. J. and Banno, S. (1973) Garnet-orthopyroxene and orthopyroxene- clinopyroxene relationships in simple and complex systems. *Contrib. Mineral. Petrol.*, **42**, 109-124.

Yamasaki, T., Owada, M. and Osanai, Y. (2000) Partial melting of peraluminous xenoliths and production of granitic melt: Implications for crustal melting in the deeper part of volcanic arcs. *WPGM 2000*, *EOS*, **81**, 203.

* In Japanese with English abstract.

** In Japanese.

Received May 26, 2003
Accepted July 9, 2003

Hutton Symposium V, Field Guidebook
Geological Survey of Japan, Interim-Report no.28, p.103－114, 2003

Trip M1

Ryoke granitoids and metamorphic rocks in the eastern Mikawa district, central Japan

Toshio KUTSUKAKE[1], Akira MIYAKE[2] and Yukiko OHTOMO[3]

Abstract: This field trip conveys to the participants an overview of the Ryoke Belt, which represents a middle-crustal section of the Cretaceous Eurasian continental margin. Some Ryoke granitoid plutons of both the Older and Younger groups and also the Ryoke metamorphic rocks including staurolite-bearing schists and migmatites are examined. An outcrop of the Median Tectonic Line, the greatest fault in the Japanese Islands, is also observed.

Keywords: Aichi Prefecture, central Japan, Cretaceous, field excursion, geochemistry, Hutton Symposium, Kiyosaki Granodiorite, Median Tectonic Line, migmatization, Mitsuhashi Granite, petrography, Ryoke granitoids, Ryoke metamorphic rocks, Shinshiro Tonalite, staurolite-bearing schist.

1. Introduction

The Ryoke Belt is well known as high-*T*/low-*P*, Miyashiro's (1973) andalusite-sillimanite type, metamorphic belt. However, the granitoids are far more extensively developed than the metamorphic rocks. In the Cretaceous time, the Inner Zone where is the Japan Sea side of southwest Japan, divided by the Median Tectonic Line, was situated at the Eurasian continental-margin, and constituted a segment of the batholithic belt of Pacific Asia. The Ryoke Belt represents the magmatic front of this arc magmatism that formed this batholithic belt (Kutsukake, 1993). Geothermobarometric calibrations indicate that the present level of exposures of the Ryoke Belt is of the middle-crustal section of the Cretaceous Eurasian continental margin.

The purpose of this field trip is to convey to the participants a general geological and petrological features of the Ryoke Belt, by showing some representative granitoids and metamorphic rocks, distributed in the eastern Mikawa district, central Japan.

2. Tectonic setting of the Ryoke Belt

Before the Miocene opening of the Japan Sea, southwest Japan was situated between the Shikhote-Alin, Russia and the Korean peninsula (Fig. 1). During the late Cretaceous to Paleogene Periods, the Inner Zone of southwest Japan had been a segment of the batholithic belt of Pacific Asia. These batholithic granitoids are the products of continental-margin arc magmatism, formed by the oblique subduction of now-consumed oceanic plates (Kula and Pacific plates) and/or Kula-Pacific ridge under the Eurasian plate (Kinoshita and Ito, 1986). The Ryoke Belt extends for more than 700 km along the Median Tectonic Line (MTL), which divides southwest Japan into the Inner and Outer Zones. A lateral displacement along the MTL, estimated to be more than 2,000 km (Osozawa, 1998), had started in the late-Cretaceous time (*ca.* 100 Ma) and had brought the Sambagawa metamorphic belt to the present position, alongside of the Ryoke Belt. The Sambagawa Belt is a metamorphosed subduction complex of low-*T*/high-*P*. The parallel arrangement of these two contrasting metamorphic belts has led to the idea of 'paired metamorphic belts' by Miyashiro (1973).

3. Geological outline of the Ryoke Belt in the Mikawa district

The geological map of the Ryoke Belt in the Mikawa district is shown in Figure 2. The eastern half of the Ryoke metamorphic rocks is of andalusite-sillimanite type (Koide, 1958; Kutsukake, 1977). However, the western half is of somewhat different with metamorphic conditions of lower-*T*/higher-*P*, characterized by the presence of staurolite (Asami, 1971; Asami and Hoshino, 1980; Asami *et al.*, 1982). In the high-grade zones, a partial melting took place within the metamorphic rocks and the migmatites were formed.

The Ryoke granitoids have been classified into the Older and Younger groups (Ryoke Research Group, 1972). The Older Ryoke granitoids are syn- to late-tectonic plutons and distributed in the high-grade zones. They occur as elongate bodies conformable to the general trend of the Ryoke metamorphic rocks, and have been strained and recrystallized together with the host metamorphic rocks. Thus, they exhibit gneissic banding and are properly called "orthogneiss". In this area, the Kamihara Tonalite, Tenryukyo Granite and Kiyosaki Granodiorite belong to the Older group, whereas, the Younger Ryoke granitoids are post-tectonic plutons, truncating the structures of both the metamorphic rocks and Older granitoids, and are accompanied by the formation of contact aureoles. The Mitsuhashi Granite and Shinshiro

[1] Laboratory of Geological Sciences, Science Hall, Aichi University, Toyohashi 441-8522 Japan. E-mail: kutukake@vega.aichi-u.ac.jp
[2] Department of Earth Sciences, Aichi University of Education, Kariya 441-8542 Japan. E-mail: akmiyake@auecc.aichi-edu.ac.jp
[3] Department of Earth Sciences, Faculty of Education, Yamagata University, Yamagata 990-8560 Japan. E-mail: yukiko@kescriv.kj.yamagata-u.ac.jp

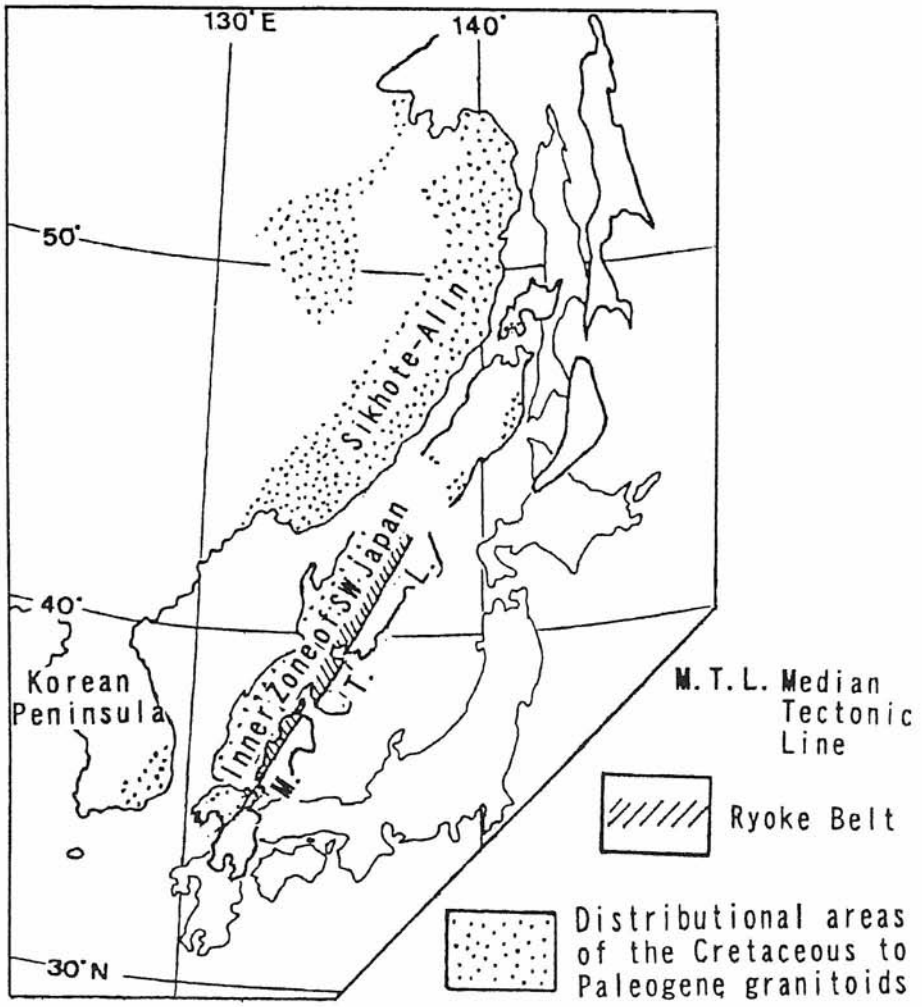

Fig. 1. Geotectonic reconstruction of the eastern margin of the Eurasian continent before the opening of the Japan Sea, and the distribution of Cretaceous to Paleogene granitoids (Kutsukake, 1993). The Japanese Islands drawn by thin lines show their present position.

Tonalite are representative Younger Ryoke granitoids in this area.

Mafic rocks occur as smaller bodies, of which the calcic gabbros, such as olivine-hornblende norite, are quite similar to those of the Peninsular Ranges batholith, North America and the Pervian batholith, South America (Kutsukake, 2000).

Along the MTL, the Ryoke granitoids were mylonitized to varying degrees, and also the phyllonites of unknown origin are distributed in narrow strip (Ohtomo, 1993).

4. Geology of Each Area and Petrographic Features

4.1 Ryoke metamorphic rocks in the Hongu-san area

The Ryoke Belt in this area consists mainly of medium- to high-grade metamorphic rocks, derived from shale, sandstone and chert, and subordinately of meta-mafic rocks. These metamorphic rocks are intruded by the Younger Ryoke granitoids; the Shinshiro Tonalite in the northwestern part and the Busetsu Granite in the northern part.

The CHIME monazite age yields *ca.* 100 Ma for the metamorphic rocks, *ca.* 85 Ma for the Shinshiro Tonalite and 77 Ma for the Busetsu Granite, respectively (Suzuki *et al.*, 1994; Morishita and Suzuki, 1995). These ages denote the time of monazite crystallization, and represent the initial attainment to the lower amphibolite facies for the metamorphic rocks and the consolidation time for the granitoids (Suzuki *et al.*, 1994).

4.1.1 Mineral assemblages of pelitic rocks and metamorphic zoning

Based on the mineral assemblages in pelitic rocks, the following four metamorphic zones are recognized: andalusite zone, lower sillimanite zone, upper sillimanite zone and contact metamorphic zone (Fig. 3). The boundaries between the andalusite zone and lower sillimanite zone (sillimanite isograd), and between the lower sillimanite zone and upper sillimanite zone (cordierite isograd) are subparallel to the general trend of the original bedding, whereas, the contact aureoles around the Shinshiro Tonalite and Busetsu Granite cut across the sillimanite isograd.

Andalusite zone

The dominant mineral assemblage in pelitic rocks of this zone is muscovite + biotite + plagioclase + quartz.

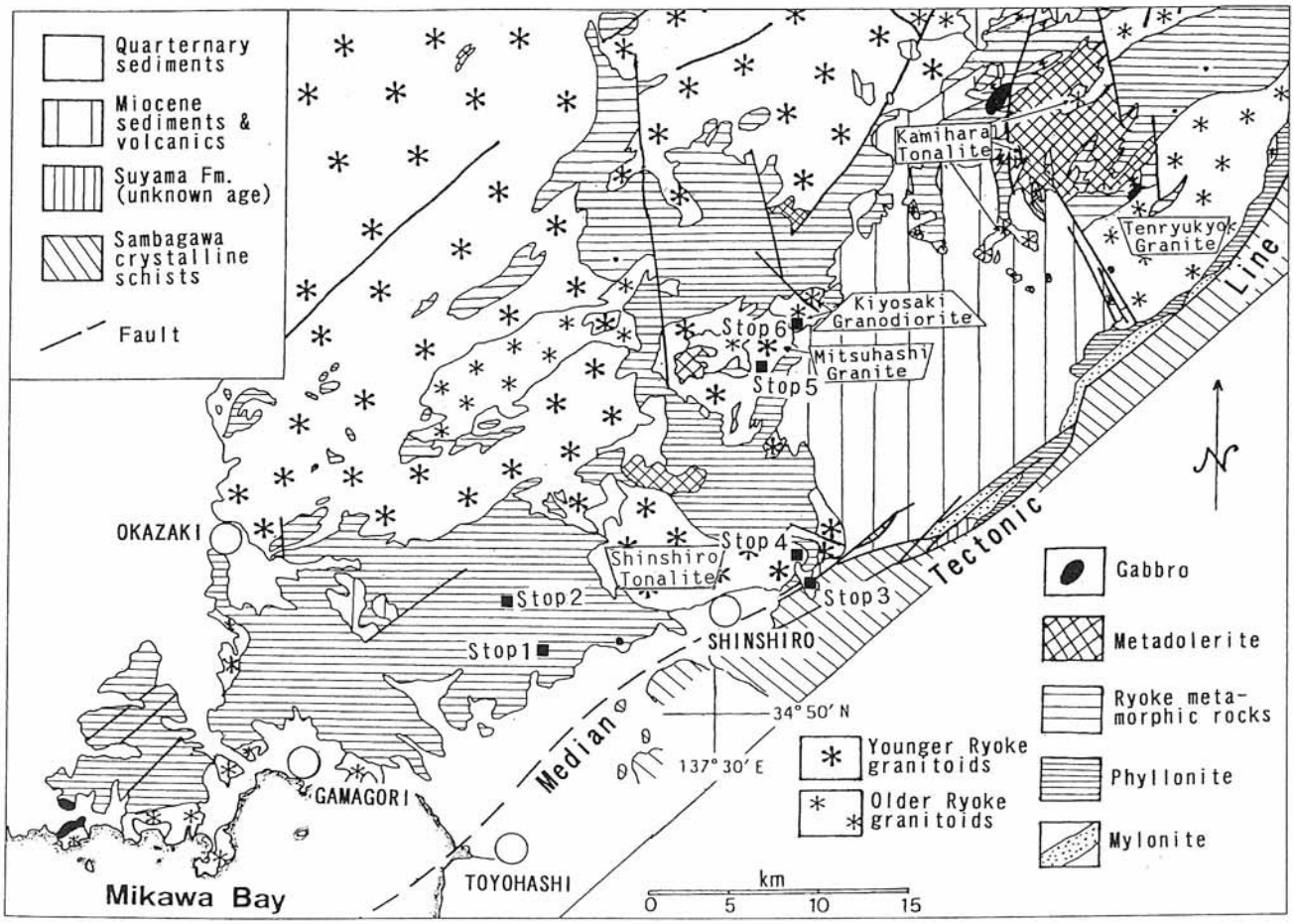

Fig. 2. Geological out-line map of the Ryoke Belt in the Mikawa district, showing the stop points of this field trip.

Sometimes andalusite, garnet, K-feldspar and small amounts of cordierite are added to this assemblage although the coexistence of andalusite + K-feldspar or cordierite + K-feldspar is never observed. Andalusite and garnet, in some cases biotite occur as porphyroblasts. Rare small grains of staurolite occur as inclusions within the porphyroblasts (Asami and Hoshino, 1980; Asami *et al.*, 1982; Seo, 1985). Muscovite shows remarkable preferred orientation, and the schistosity of pelitic rocks is defined by its arrangement.

Lower sillimanite zone

The common mineral assemblage in pelitic rocks of this zone is muscovite + biotite + sillimanite (fibrolite) + K-feldspar + plagioclase + quartz. Garnet and trace of andalusite are sometimes observed to this assemblage. With increasing metamorphic grade within this zone, muscovite markedly decreases in abundance, coupled with the modal increase of sillimanite and K-feldspar. The inferred reaction caused this modal change is:

muscovite + quartz → sillimanite + K-feldspar + H_2O (1)

Upper sillimanite zone

This zone is distinguished from the lower sillimanite zone by the existence of cordierite. The dominant assemblage in pelitic rocks is biotite + cordierite + sillimanite + K-feldspar + plagioclase + quartz. In many cases, garnet coexists with this assemblage. Cordierite occurs as porphyroblasts and contains inclusions of tiny sillimanite crystals. This suggests the transition from the lower to upper sillimanite zones characterized by the reaction:

biotite + sillimanite + quartz →
cordierite + K-feldspar + H_2O (or melt) (2)

Contact metamorphic zone

This zone is characterized by the coexistence of large amounts of cordierite and K-feldspar in pelitic rocks, and the dominant mineral assemblage is biotite + cordierite + K-feldspar + plagioclase + quartz. In addition, andalusite and/or sillimanite sometimes appear. The transition from the andalusite and lower sillimanite zones to contact metamorphic zone is clearly defined, but to distinguish between the upper sillimanite zone and this zone is not always easy, as their mineral assemblages are quite similar.

The transition from the andalusite zone to contact zone is marked by the following reaction:

muscovite + biotite + quartz →
cordierite + K-feldspar + H_2O (3)

The frequent occurrence of andalusite and occasional appearance of sillimanite in the contact zone suggest the reaction:

muscovite + quartz →

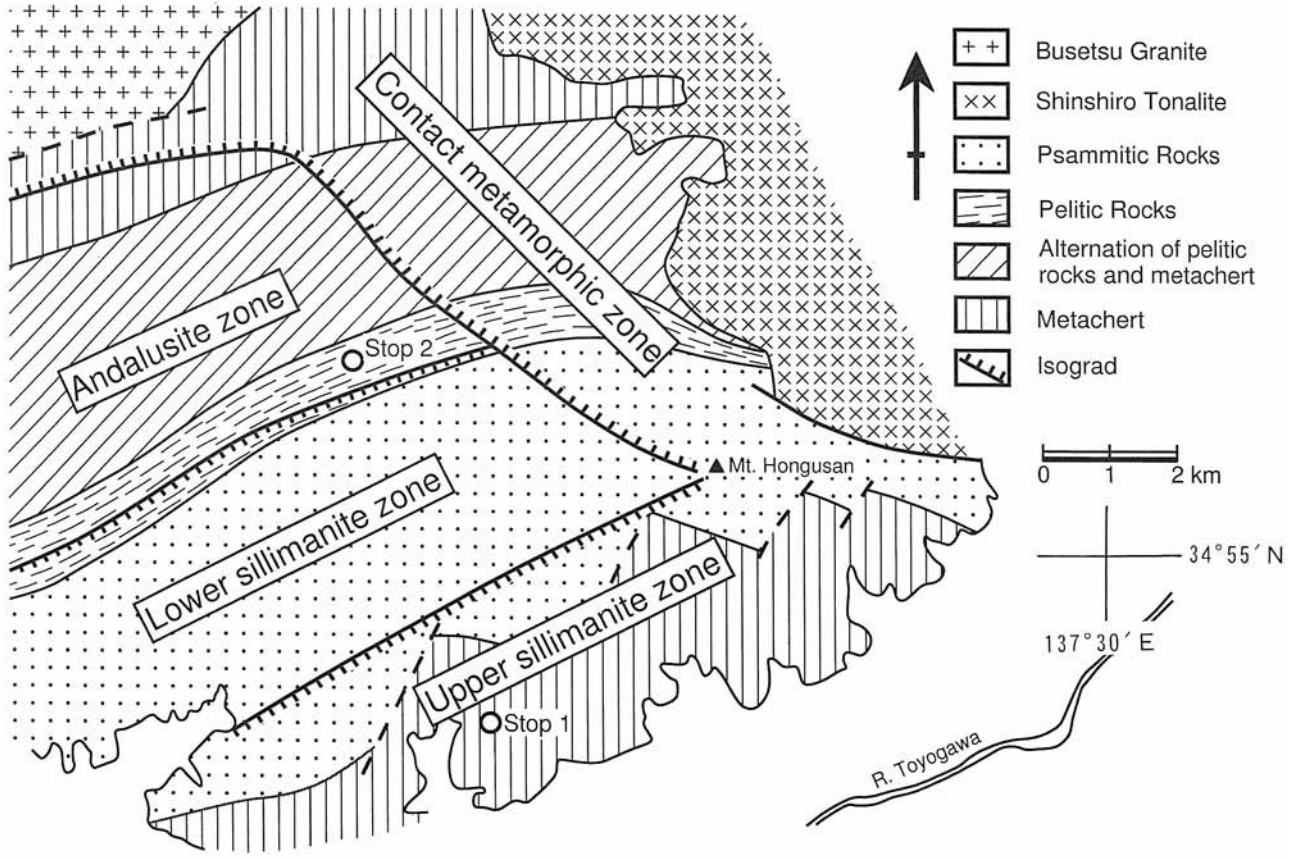

Fig. 3. Geological map of the Hongu-san area.

andalusite (or sillimanite) + K-feldspar + H_2O (1')

This reaction (3) is regarded to take place under low-pressure conditions compared to the reaction (2) (Pattison and Tracy, 1992), suggesting a significant pressure decrease before the emplacement of the Shinshiro Tonalite.

4.1.2 Porphyroblasts in the andalusite zone and contact metamorphic zone

The porphyroblasts of andalusite, garnet and biotite in the andalusite zone seem to be formed under relatively static conditions before the development of schistosity. The reasons are as follows:

(i) Preferred lattice orientation of biotite porphyroblasts is very weak, although the preferred dimensional orientation is moderately developed. This is contrasting to muscovite which shows both the preferred orientations (Seo and Hara, 1981; Miyake, 1993).

(ii) Andalusite and garnet porphyroblasts sometimes show sector structure (Fig. 4a), which is regarded to have been formed in a static environment (Rice and Mitchell, 1991).

(iii) Andalusite, garnet and muscovite porphyroblasts sometimes include a lot of tiny minerals, such as graphite. These inclusions essentially show straight arrays (*Si plane*). Frequently *Si* is not continuously linked and discordant to the matrix schistosity (*Se*), suggesting a discontinuous formation between these porphyroblasts and matrix minerals. The schistosity (*Se*) wraps around porphyroblasts and asymmetric pressure shadows are seen by the side (Fig. 4b). If the porphyroblast rotation occurred during the schistosity-forming deformation, the porphyroblast formation must have preceded the schistosity development.

In the contact metamorphic zone, post-tectonic growth of andalusite porphyroblast can be recognized. In some cases entirely new porphyroblasts were produced, where *Si* is continuously linked and in parallel to *Se* (Fig. 4c). In other cases post-tectonic andalusite domain overgrew the matrix foliation on a pre-existing syn-tectonic porphyroblast, keeping its lattice orientation. In the latter cases, the post-tectonic domain developed along the curve of mica-rich matrix wrapping a syn-tectonic domain leaving quartz-rich pressure shadow behind, and *Si* in the post-tectonic domain sharply cuts across that in the syn-tectonic domain (Fig. 4d). These post-tectonic andalusites should have been produced by the reaction (1') during the contact metamorphism (Miyake *et al.*, 1992).

4.1.3 Migmatites and pegmatites in the upper sillimanite zone

Pelitic rocks in the upper sillimanite zone show a migmatitic appearance more or less: granitic coarse-grained layers (leucosome) of millimeter to centimeter order in thickness are intercalated with biotite-rich aluminous layer (paleosome). The migmatites are frequently folded in a complex manner with several to some tens of centimeter order wavelength.

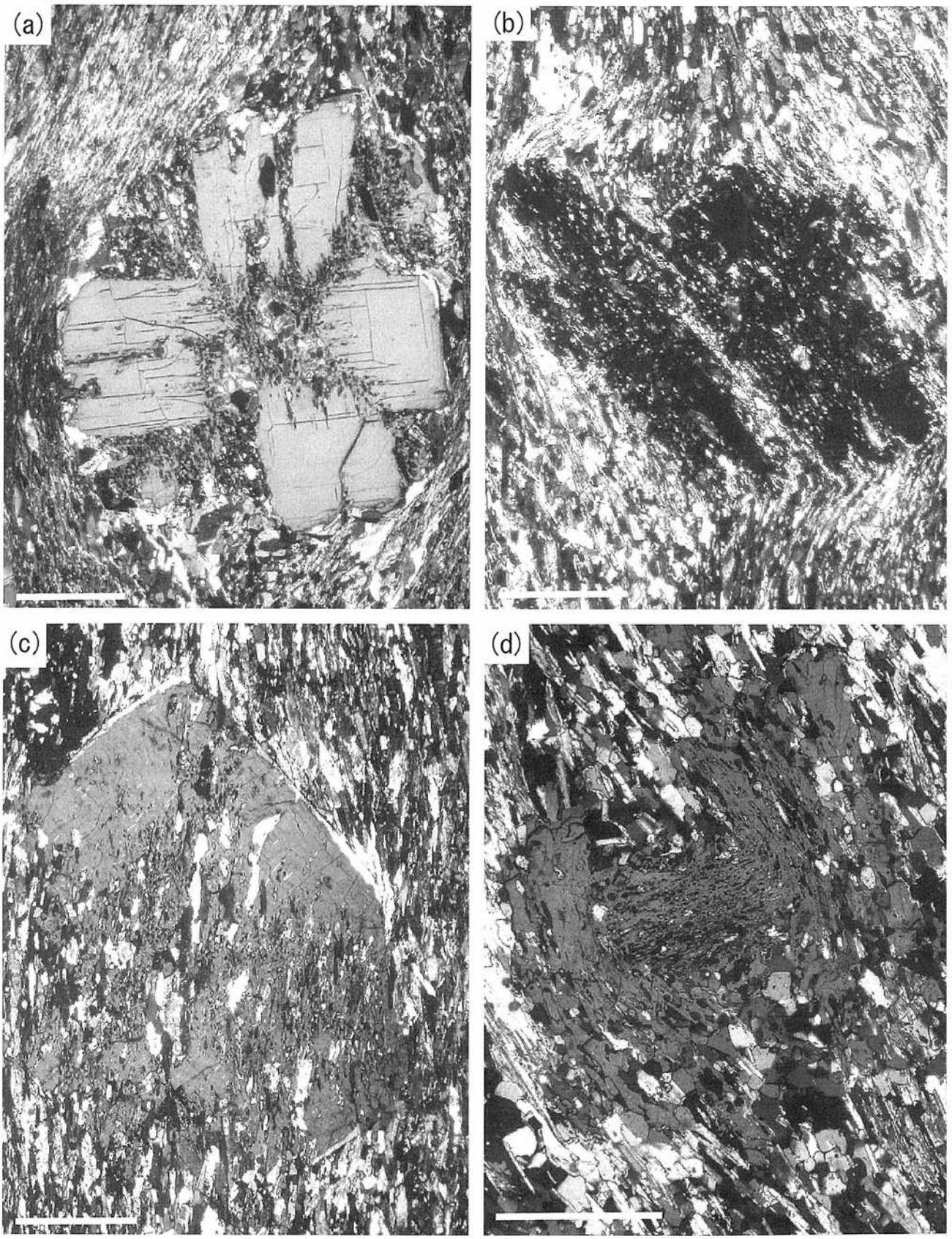

Fig. 4. Andalusite porphyroblasts from the andalusite zone and contact metamorphic zone. Scales as 500 μ m. (a) Pre-tectonic andalusite showing a sector structure (chiastolite) from the andalusite zone. (b) Pre-tectonic andalusite with a lot of inclusions from the andalusite zone. (c) Post-tectonic andalusite from the contact metamorphic zone, showing overgrowth of post-tectonic domains on a pre-tectonic domain. (d) Andalusite porphyroblast from the contact metamorphic zone, showing overgrowth of post-tectonic domains on a pre-tectonic domain.

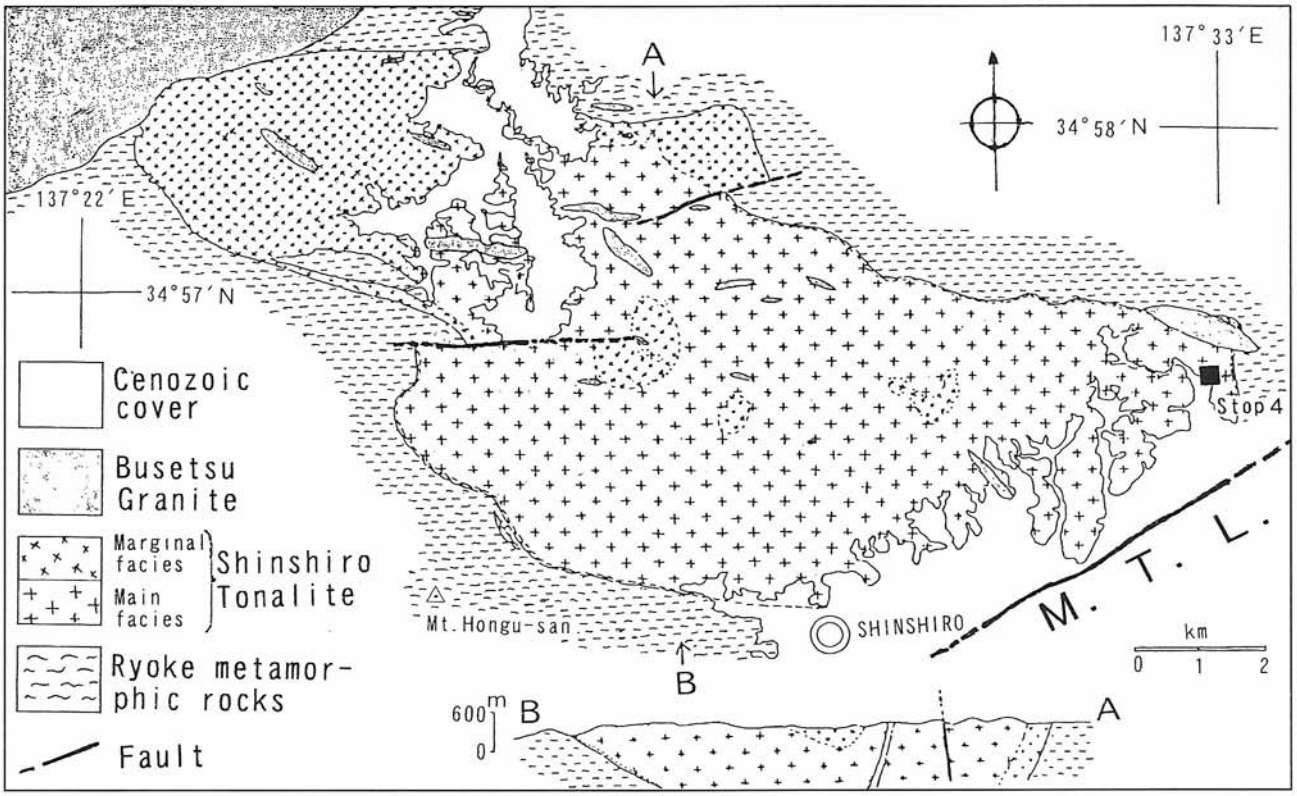

Fig. 5. Geological map and cross-section of the Shinshiro Tonalite pluton (Ohtomo, 1985). M.T.L: Median Tectonic Line.

Cordierite in the paleosome fulfills the space between acicular or prismatic sillimanite crystals, and strongly tends to elongate in parallel to the fold axis. Such elongated crystals are sometimes fragmented into several segments without any evidences of retrograde reaction, suggesting the deformation of the migmatites proceeded under the upper amphiolite-facies condition.

Apart from the granitic layer in migmatites, pegmatitic veins and pools of various scales from several centimeters to several meters are seen throughout the upper sillimanite zone. These pegmatites contain a lot of K-feldspar over quartz and plagioclase. Many pegmatite veins are boudinaged or folded in varying degrees, or have wavy boundaries. The foliation of the host metamorphic rocks becomes parallel to or in harmony with the boundary of pegmatite, indicating the intrusion of pegmatite to have been pre- or syn-tectonic.

CHIME age at the margin of well-faced monazite crystals in the leucosome yielded 95 to 96 Ma (Suzuki *et al.*, 2000), which is almost the same as the Kamihara Tonalite, the oldest Ryoke granitoid in central Japan (Nakai and Suzuki, 1996).

4.2 Ryoke granitoids

4.2.1 Shinshiro Tonalite pluton

The Shinshiro Tonalite is one of the Younger Ryoke granitoids, and an elliptical-shaped pluton of 14 km (NW-SE) × 6 km (NE-SW), emplaced within the Ryoke metamorphic rocks (Fig. 5). The maximum width of the contact aureoles around this pluton attains 4 km, and the highest-grade rocks are characterized by the associations of cordierite-K-feldspar

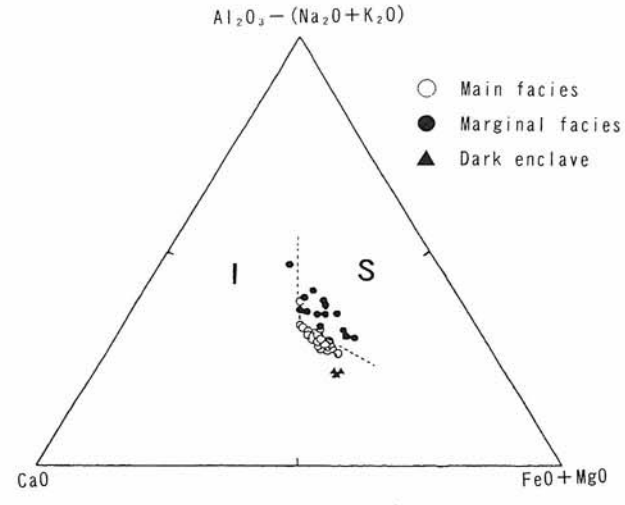

Fig. 6. ACF-diagram for the Shinshiro Tonalite. I: I-type, S: S-type.

and andalusite-K-feldspar within several tens of meters immediately from the contact. In several places, thin dykes of the Busetsu Granite are seen. K-Ar mineral ages of 73.3±2.9 Ma (hornblende) and 68.0±2.1 Ma (biotite) have been reported by Uchimi *et al.* (1990), and CHIME monazite age yields *ca.* 85 Ma (Morishita and Suzuki, 1995).

The major lithology is coarse- to medium-grained hornblende-biotite tonalite (main facies). A marginal facies comprises medium- to fine-grained biotite tonalite and two-mica granite. Cummingtonite occurs in close association with the hornblende. The foliation, which is defined by the parallel

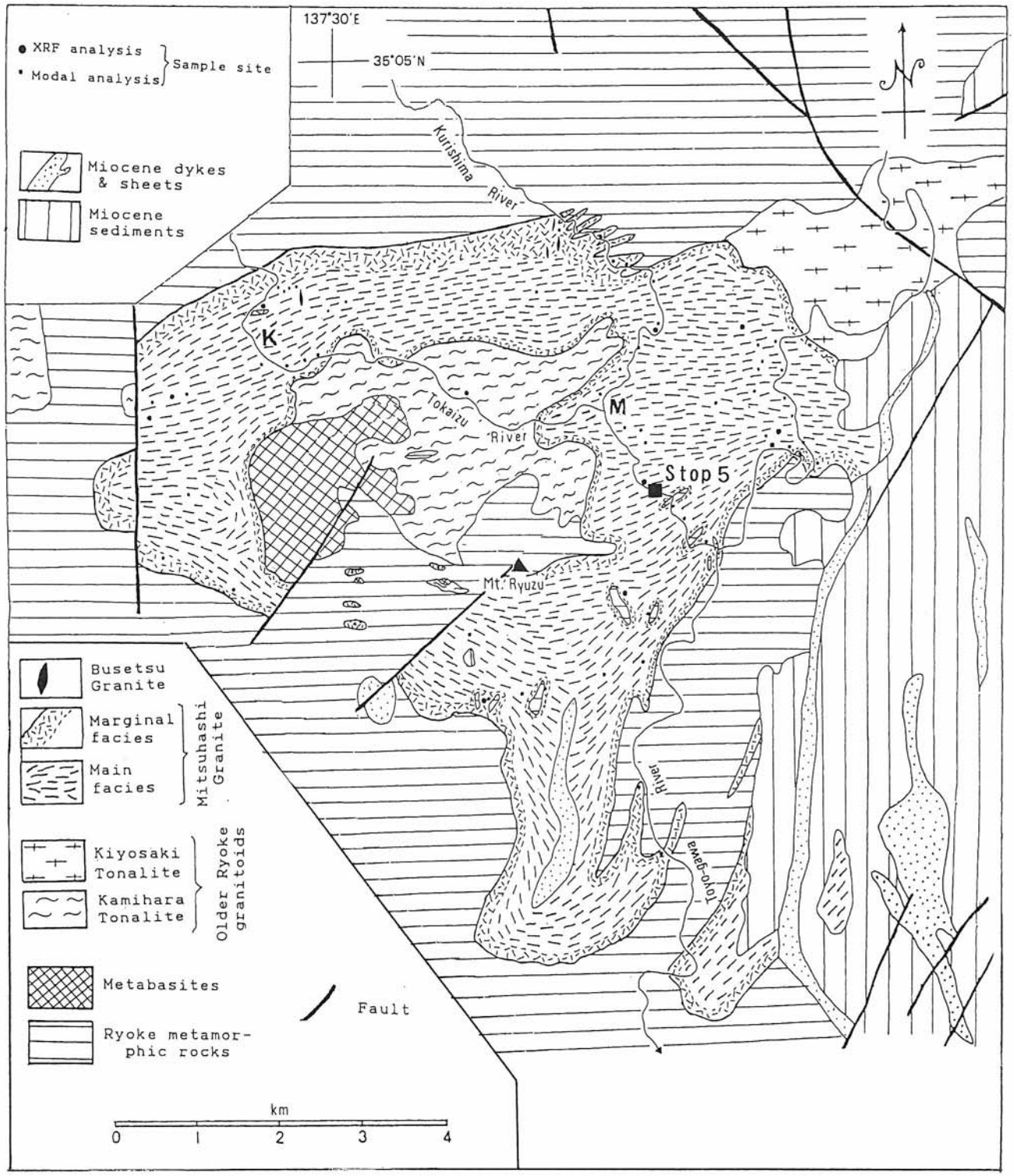

Fig. 7. Geological map of the Mitsuhashi Granite pluton (Kutsukake, 1997a).

alignment of prismatic hornblende (8-15 mm in length) and also by the elongation of dioritic enclaves, is well developed within the main facies. These foliations should have developed during the emplacement of this pluton. To trace the foliation and to examine the distributional pattern of color index, two stretched basin and one semi-dome structures are inferred within this pluton. The main axes of the basins and semi-dome are parallel to the elongation of the pluton. Color index gradually decreases toward the center of each basin. The internal structures and contact relations to the host rocks indicate this pluton to have an asymmetrical funnel shape.

With regard to the whole rock chemistry, the main facies is rather uniform with the average of SiO_2=65wt%, whereas, the marginal facies is quite variable in SiO_2 content from 62 to

Table 1. Radiometric datings for the Mitsuhashi Granite and Kiyosaki Granodiorite (Kutsukake, 1997a, 2001).

	Dating method	Age (Ma)	Reference
Mitsuhashi Granite	K-Ar (biotite)	71.6, 69.6, 69.0	Ozima et al. (1967)
	Rb-Sr (whole rock & mineral isochron) $(^{87}Sr/^{86}Sr)_0$=0.7075	75.5	Ozima et al. (1967)
	CHIME (monazite)	83.8	Suzuki et al. (1994)
	U-Pb (zircon)	78	Banks & Shimizu (1969)
Kiyosaki Granodiorite	K-Ar (biotite)	69.5, 70.0	Ozima et al. (1967)
	CHIME (monazite)	86.6, 87.0	Morishita et al. (1996)
	U-Pb (zircon)	100, 105	Banks & Shimizu (1969)

73wt%. The main facies rocks are plotted exclusively in the I-type field, whereas, most of the marginal facies rocks fall within the S-type field in the ACF-diagram (Fig. 6). As the marginal facies frequently includes xenolithic metasediments, the muscovite-bearing granodiorite and granite can be regarded as an assimilation product of these xenoliths.

4.2.2 Mitsuhashi Granite pluton

The Mitsuhashi Granite is a representative Younger Ryoke granitoid in this area (Koide, 1958). This pluton (8 km × 8 km) was emplaced within the Ryoke metamorphic rocks (Fig. 7). It is a horseshoe-shaped pluton with the Older Ryoke granitoids and metamorphic rocks in the core. Within 50 m-100 m from the contact, a marginal facies is developed: medium-grained garnet-bearing biotite granite and granodiorite.

The main facies is coarse-grained hornblende-biotite tonalite and low-K_2O granodiorite, with subordinate cummingtonite-bearing hornblende-biotite quartz diorite. The Mitsuhashi Granite is fairly calcic (Peacock's index～65) and high in Fe/Mg ratio. They fall within the tholeiitic field in the AFM-diagram. Very low Fe^{3+}/Fe^{2+} ratio (～0.1) and frequent occurrence of almandine-rich garnet indicate the crystallization under the low oxygen-fugacity condition.

Geobarometric calibrations indicate the emplacement of this pluton to have taken place at *ca.* 15 km in depth (Kutsukake, 1997b). Radiometric datings are summarized in Table 1.

4.2.3 Kiyosaki Granodiorite pluton

The Kiyosaki Granodiorite pluton, 5 km × 4 km, was emplaced within the Ryoke metamorphic rocks, and is intruded by the Mitsuhashi Granite to the southwest (Fig. 8). In many places, thin dykes and small stocks of the Mitsuhashi Granite can be seen.

Within some tens to two hundred meters from the contact, a leucocratic marginal facies is developed, including the xenoliths of host metamorphic rocks.

Gneissic foliation, defined by the parallel alignment of mafic minerals, is not so distinct in the southern portion, whereas, it fairly develops in the northern portion of the pluton. Porphyritic alkali feldspar crystals, 2 cm or more across, are frequently seen.

Available radiometric ages are summarized in Table 1.

4.3 Median Tectonic Line

The Median Tectonic Line (MTL) is the greatest fault dividing southwest Japan into the Inner and Outer Zones, and situated as the southern limit of the Ryoke Belt (Fig. 2). In its western half it is running in E-W, and in the Chubu district it bends to N-S. The activity of the MTL had started in the late-Mesozoic Era, and has been continuous for a long time even until today. It is an active fault in some parts, especially in Shikoku.

In the Chubu and Kinki districts, mylonite zones are developed along the MTL, with a shear sense of a top to the west. This sense should represent the initial shape of the MTL. This mylonitization took place after the peak of the Ryoke metamorphism (Ohtomo, 1993), mainly between 90 Ma and 70 Ma (Takagi, 1992; Takahashi, 1992). The Ryoke metamorphic belt uplifted during this time. The present MTL cuts through the initial mylonite zones.

In the eastern Mikawa district, the MTL runs in NE-SW. In the northeastern part of this district, the rocks of the Ryoke Belt accompanied with the pile nappe juts out onto the Sambagawa Belt (Ohtomo, 1993). The oldest and next oldest Ryoke granitoids, distributed along the MTL, had suffered the mylonitization. The mylonites derived from the Hiji Tonalite, one of the oldest Ryoke granitoids, occur beneath the nappe composed of the mylonitized Ryoke metamorphic rocks.

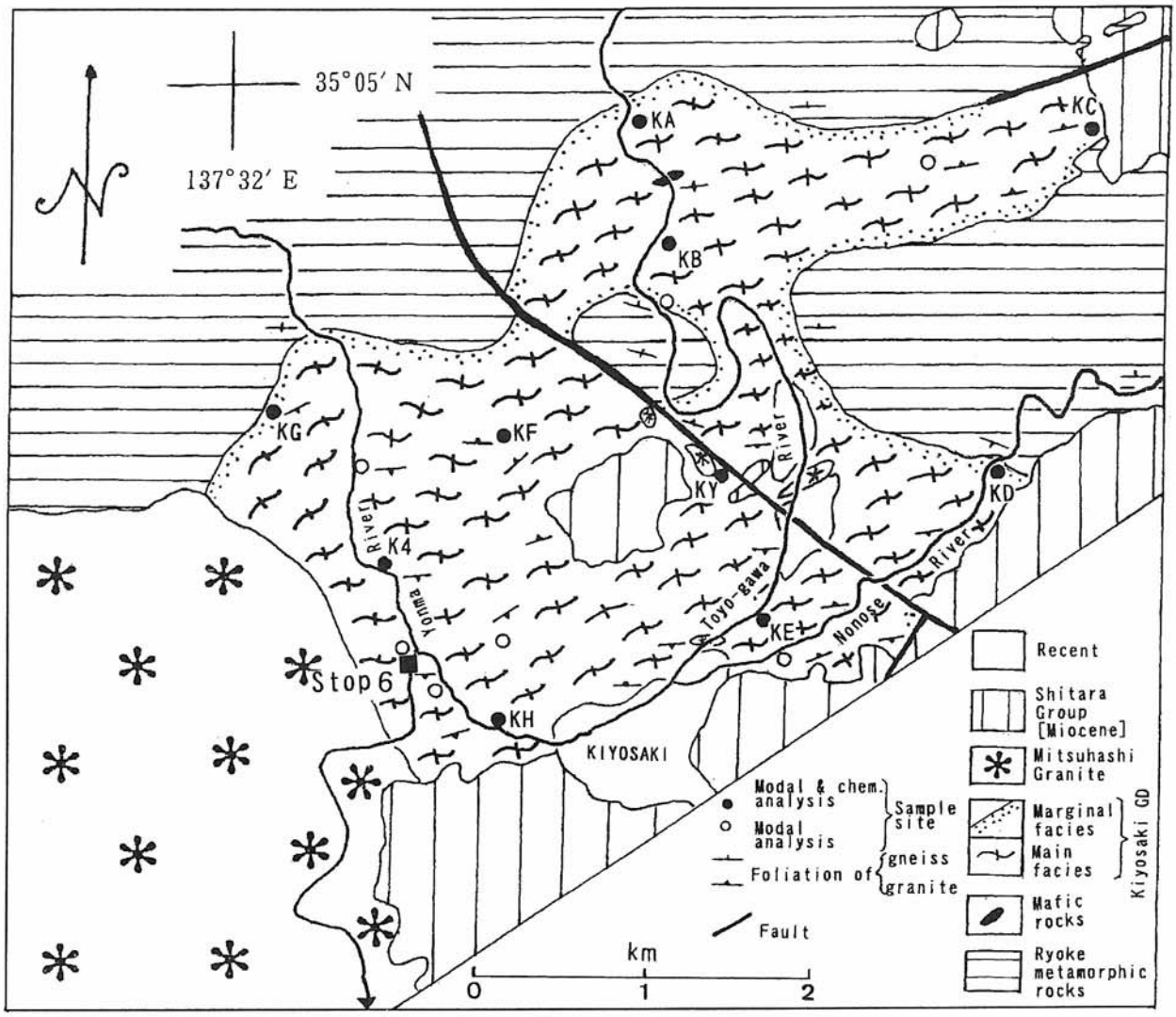

Fig. 8. Geological map of the Kiyosaki Granodiorite pluton (Kutsukake, 2001).

5. Explanation for stop points

Stop 1. Ryoke metamorphic rocks and migmatites [Roadcut along the woodland path in Chigiri-cho, Toyokawa City]

There are nice exposures of pelitic migmatites along the route, as shown in Figure 9.

Migmatites of stop 1-1 are repeatedly folded (Fig. 10a). The melanosome is composed of biotite, sillimanite, cordierite, garnet, plagioclase, K-feldspar and quartz. The mineral assemblage of the leucosome is essentially the same as the melanosome, except for the dominance of feldspar and quartz.

The migmatite at stop 1-1 includes a block of meta-mafic rock, with 0.3 m × 1.5 m (Fig. 10b). The boundary between the meta-mafic rock and the host migmatite is very sharp and straight. This block can be regarded to be a piece of the fragmentation of a dyke, disrupted by the deformation. This rock is petrographically quite similar to the metamafic rock, occurring as a larger body at stop 1-2. They are massive and homogeneous rocks, composed mainly of plagioclase, biotite and hornblende with small amounts of quartz.

At stop 1-3, a lenticular pegmatite block is included in the migmatite. The foliation of the host migmatite curves around the block when it was wrapped (Figs. 10c and d). The monazite CHIME age of this pegmatite is 96±4 Ma.

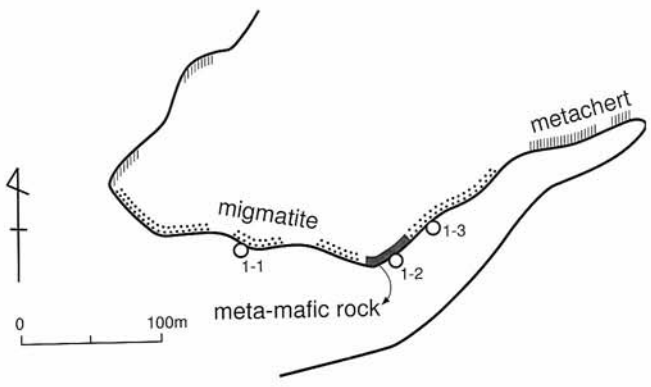

Fig. 9. Route-map for stops 1-1 through 1-3.

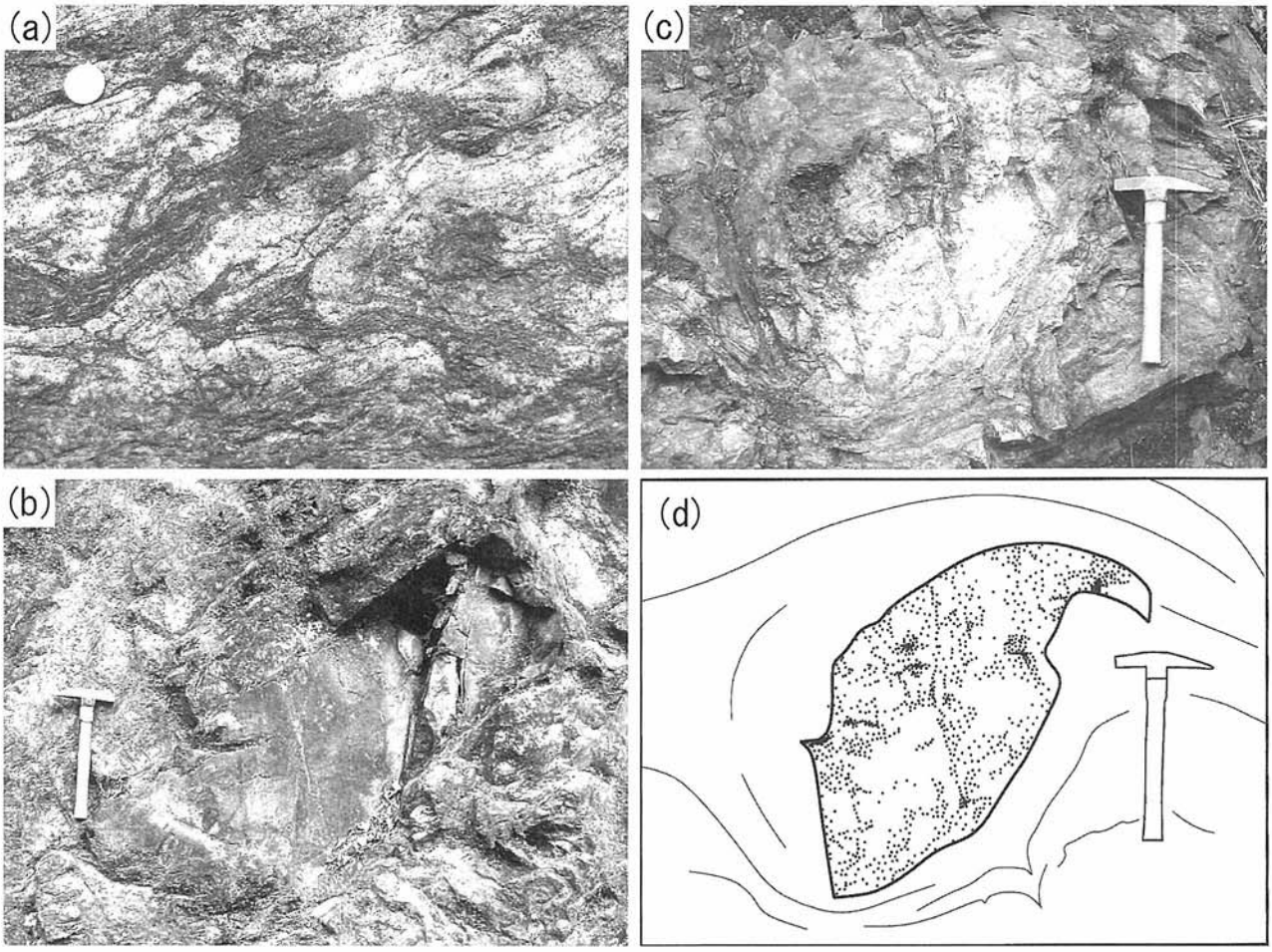

Fig. 10. Outcrops at stop 1. (a) Folded migmatite, (b) Meta-mafic rock block in migmatite, (c) Lenticular pegmatite block in migmatite, (d) Schematic sketch of (c).

Stop 2. Andalusite schist [Riverbed of the Otome-gawa in Nukata Town]

In this large outcrop, the pelitic schists of the andalusite zone are observed. The schist is composed of andalusite, biotite, muscovite, garnet, plagioclase and quartz with small amounts of cordierite, graphite and ilmenite. Andalusite occurs as large porphyroblasts with several centimeters in long diameter. The long axis (c-axis) of the andalusite weakly tends to arrange, parallel to the schistosity defined by the mica flakes' alignment. It is observed with the naked eye that the schistosity wrap those porphyroblasts.

Stop 3. Median Tectonic Line [Riverside of the Toyo-gawa under the Nagashino-Ohashi Bridge in Horai Town]

An outcrop of the MTL is seen on the left riverside of the Toyo-gawa. Here, the granitoid mylonites of the Ryoke Belt, in the upper hanging wall, are in contact with the Sambagawa crystalline schists in the lower wall. The fault plane strikes N82° E and dips 61° N. No fault gauges are seen. In the riverbed, a narrow disturbed zone with a width of 20 to 30 cm is developed striding both the belts. The vertical open cracks (NNW-SSE) and also tiny faults, subparallel to the MTL, had displaced the MTL by several centimeters in many places. The light-colored mylonites are derived from the medium-grained leucocratic granodiorite, and subordinately the dark-colored mylonites, derived from the fine-grained tonalite, occur as small lens and thin bands within the leucocratic ones. They have a uniform mylonitic foliation (S_m), striking N7° W to N20° E and dipping 40° to 45° N and a mylonitic lineation (L_m), plunging *ca.* 20° N or NNE. Folded veinlets of a coarse-grained leucocratic granite cut across the mylonites. Immediately near the MTL, these rocks are highly cataclasized by the later fault movements.

Stop 4. Shinshiro Tonalite [Riverside of the Toyo-gawa near the Hananoki Park in Shinshiro City]

This stop point is situated near the eastern margin of the Shinshiro Tonalite pluton. In this outcrop a typical lithology, coarse-grained hornblende-biotite tonalite, of the main facies of the Shinshiro Tonalite is seen. The foliation, defined by the alignment of prismatic hornblende crystals and elongation of dark enclaves, is fairly developed.

Stop 5. Mitsuhashi Granite [Riverside of the Tokaizu River in Shitara Town]

In this outcrop, we can see a typical lithology of the main facies of the Mitsuhashi Granite: coarse-grained hornblende-

Table 2. Major and trace element analyses of the Mitsuhashi Granite (1) and Kiyosaki Granodiorite (2) (Kutsukake, 1997a, 2001).

	1	2
SiO_2	63.73	65.89
TiO_2	0.76	0.58
Al_2O_3	16.92	15.60
Fe_2O_3	0.12	1.11
FeO	5.52	3.52
MnO	0.11	0.08
MgO	1.37	2.10
CaO	5.07	3.95
Na_2O	3.69	2.95
K_2O	1.63	3.10
P_2O_5	0.24	0.15
L.O.I.	1.05	1.24
Total	100.17	100.27
Trace elements (in ppm)		
Rb	45	96
Sr	417	282
Ba	851	848
Th	7	10.9
Nb	17	12
Zr	301	189
Ga	17	19
Cr	15	52.1
V	39	77
Ni	8	-
Zn	96	-
Pb	11	14
Y	18	16
Sc	10.9	10.5
U	1.5	1.0
La	44.9	28.1
Ce	89	51
Nd	37	19
Sm	5.90	3.38
Eu	2.00	1.12
Tb	0.7	0.4
Yb	1.80	1.39
Lu	0.26	0.20

－: not determined

1. Hornblende-biotite tonalite (Specimen No.94021005).
2. Hornblende-augite-biotite granodiorite (Specimen No.KH).

biotite tonalite. Magmatic foliation, trending N35° E and dipping 45° N, is well developed, and also layering is seen: thin (< 1 cm) mafic-rich layers are alternating with thick (5-10 cm) quartzofeldspathic layers.

Mafic minerals and plagioclase are all euhedral and show a preferred orientation parallel to the layering.

Under the microscope, plagioclase (An_{54-36}), hornblende (ferrohornblende with Mg#=0.25) and biotite (Mg#=0.25) are euhedral, and quartz and K-feldspar (Or_{94-99}) fill their interstices. As accessory minerals, zoned allanite, apatite, ilmenite and zircon are common.

An analysis of the sample collected near this outcrop is shown in Table 2 (No.1).

Stop 6. Kiyosaki Granodiorite [At the confluence of the Toyo-gawa River and Yonma River in Shitara Town]

In this outcrop, a typical lithology of the Kiyosaki Granodiorite is seen: a medium-grained weakly foliated hornblende-augite-biotite granodiorite.

Ovoidal and/or lenticular dark enclaves, several to ten centimeters across, are ubiquitous throughout the outcrop. A leucocratic granitic dyke with a width of 5-10 cm traverses, which could have been derived from the adjoining Mitsuhashi Granite.

This granodiorite is composed mainly of plagioclase, alkali feldspar, quartz, biotite, augite and hornblende.

Plagioclase is subhedral, tabular and zoned with An_{45} to An_{32}. Augite (Mg#=0.57) has an abnormal composition of subcalcic augite with the high alumina and alkalies contents. This probably represents a 'transitional' composition to hornblende, due to the replacement by the latter. The hornblende, mostly replaced the augite, is of magnesiohornblende (Mg#=0.65), and close to actinolite. Biotite (Mg#=0.46) is grayish brown in Z-axial color. Apatite, monazite, allanite, zircon and pyrite are common accessory minerals.

An analysis of the granodiorite collected near this outcrop is shown in Table 2 (No.2).

Dark enclaves are tonalitic in composition, and consist mainly of plagioclase, quartz, biotite and hornblende.

References

Asami, M. (1971) Finding of staurolite-bearing pelitic schist in the Ryoke metamorphic belt of central Japan. *Proc. Japan Acad.*, **47**, 511-516.

Asami, M. and Hoshino, M. (1980) Staurolite schists from the Hongu-san area in the Ryoke metamorphic belt, central Japan. *Jour. Geol. Soc. Japan*, **86**, 581-591.

Asami, M., Hoshino, M., Miyakawa, K. and Suwa, K. (1982) Metamorphic conditions of staurolite schists of the Ryoke metamorphic belt in the Hazu-Hongu-san area, central Japan. *Jour. Geol. Soc. Japan*, **88**, 437-450.*

Banks, P. O. and Shimizu, N. (1969) Isotopic measurements on zircons from Japanese granitic rocks. *Geochem. Jour.*, **8**, 25-34.

Kinoshita, O. and Ito, H. (1986) Migration of Cretaceous igneous activity in southwest Japan related to ridge subduction. *Jour. Geol. Soc. Japan*, **82**, 723-735.*

Koide, H. (1958) *Dando granodioritic intrusives and their associated metamorphic complex*. Japan Soc. Prom. Sci., 311p.

Kutsukake, T. (1977) Petrological studies on the Ryoke metamorphic rocks in the Toyone-mura area, Aichi Prefecture, Japan. *Mem. Fac. Sci., Kyoto Univ., Ser. Geol. Mineral.*, **43**, 49-110.

Kutsukake, T. (1993) An initial continental-margin plutonism — Cretaceous Older Ryoke granitoids, southwest Japan. *Geol. Mag.*, **130**, 14-28.

Kutsukake, T. (1997a) Petrology and geochemistry of a calcic and ferrous granitoid pluton: the Mitsuhashi Granite in the Ryoke Belt, southwest Japan. *Jour. Mineral. Petrol. Econ. Geol.*, **92**, 231-244.

Kutsukake, T. (1997b) The depth of emplacement of the Mitsuhashi Granite pluton in the Ryoke Belt, southwest Japan — as inferred from some geobarometric calibrations. *Jour. Geol. Soc. Japan*, **103**, 604-607.

Kutsukake, T. (2000) Petrographic features of the gabbroic rocks in the Ryoke Belt of the Mikawa district, southwest Japan. *Sci. Rept. Toyohashi Mus. Nat. Hist.*, **10**, 1-12.

Kutsukake, T. (2001) Geochemistry of the Kiyosaki Granodiorite in the Ryoke Belt, central Japan. *Sci. Rept. Toyohashi Mus. Nat. Hist.*, **11**, 1-12.

Miyake, A. (1993) Rotation of biotite porphyroblasts in pelitic schist from Nukata area, central Japan. *Jour. Struct. Geol.*, **15**, 1303-1313.

Miyake, A., Murata, E. and Morishita, O. (1992) Growth stages of andalusite in the Ryoke metamorphic rocks from the Nukata area, Aichi Prefecture. *Jour. Mineral. Petrol. Econ. Geol.*, **87**, 478-480.*

Miyashiro, A. (1973) *Metamorphism and Metamorphic Belts*. George Allen & Unwin, London, 492p.

Morishita, T. and Suzuki, K. (1995) CHIME ages of monazite from the Shinshiro Tonalite of the Ryoke Belt in the Mikawa area, Aichi Prefecture. *Jour. Earth Sci., Nagoya Univ.*, **42**, 45-53.

Morishita, T., Suzuki, K. and Nasu, T. (1996) CHIME ages of monazites from granitoids in the Mikawa-Tono area, central Japan. *Abstr. 103rd Ann. Meet. Geol. Soc. Japan*, 282.**

Nakai, Y. and Suzuki, K. (1996) CHIME monazite ages of the Kamihara Tonalite and the Tenryukyo Granodiorite in the eastern Ryoke Belt of central Japan. *Jour. Geol. Soc. Japan*, **102**, 431-439.

Ohtomo, Y. (1985) Zonal structure of the Shinshiro Tonalite pluton. *Magma*, **73**, 69-73.**

Ohtomo, Y. (1993) Origin of the Median Tectonic Line. *Jour. Sci. Hiroshima Univ., Ser. C*, **9**, 611-669.

Osozawa, S. (1998) Major transform duplexing along the eastern margin of Cretaceous Eurasia. *In* Flower, M. F. J., Chung, S. L., Lo, C. H. and Lee, T. Y., eds., *Mantle dynamics and plate interactions in East Asia*. Amer. Geophys. Union, Washington, D.C., 245-257.

Ozima, M., Ueno, N., Shimizu, N. and Kuno, H. (1967) Rb-Sr and K-Ar isotopic investigations of Shidara granodiorites and their associated metamorphic belt, central Japan. *Japan. Jour. Geol. Geogr.*, **38**, 159-162.

Pattison, D. R. M. and Tracy, R. J. (1992) Phase equilibria and thermobarometry of metapelites. *In* Kerrick, D. M. ed., *Contact Metamorphism.* Mineral. Soc. Amer. Rev. Mineral., **26**, 105-206.

Rice, A. H. and Mitchell, J. I. (1991) Porphyroblast textural sector-zoning and matrix displacement. *Mineral. Mag.*, **102**, 431-439.

Ryoke Research Group (1972) The mutual relations of the granitic rocks in the Ryoke metamorphic belt in central Japan. *Earth Sci.* (*Chikyu Kagaku*), **26**, 205-216.*

Seo, T. (1985) A study of the Ryoke metamorphism in view of metamorphic history and conditions - as illustrated in the metamorphic terrain of the southeastern part of Mikawa plateau. *Geol. Rep. Hiroshima Univ.*, **27**, 93-155.*

Seo, T. and Hara, T. (1981) The development of schistosity in biotite schists from southwestern part of Mikawa plateau, central Japan. *Jour. Geol. Soc. Japan*, **86**, 817-826.

Suzuki, K., Morishita, T., Kajizuka, I., Nakai, Y., Adachi, M. and Shibata, K. (1994), CHIME ages of monazites from the Ryoke metamorphic rocks and some granitoids in the Mikawa-Tono area, central Japan. *Bull. Nagoya Univ. Furukawa Mus.*, **10**, 17-38.*

Suzuki, K., Miyake, A., Kakehi, M. and Kato, T. (2000) Thermal history of Ryoke metamorphic rocks and granitoids in the Mikawa area on the basis of CHIME monazite ages. *Earth Monthly* (*Gekkan Chikyu*), *Gogai*, **30**, 22-27.**

Takagi, H. (1992) Mylonites along the Median Tectonic Line in central Japan. *29th IGC field trip, B16*, 327-335.

Takahashi, Y. (1992) K-Ar ages of the granitic rocks in Awaji Island — with an emphasis on timing of mylonitization —. *Jour. Mineral. Petrol. Econ. Geol.*, **97**, 291-299.*

Uchimi, S., Uto, K. and Shibata, K. (1990) K-Ar age results - 3: New data from the Geological Survey of Japan. *Bull. Geol. Surv. Japan*, **41**, 567-575.*

* in Japanese with English abstract.
** in Japanese.

Received May 22, 2003
Accepted July 9, 2003

Hutton Symposium V, Field Guidebook
Geological Survey of Japan, Interim-Report no.28, p.115－124, 2003

Trip M2

Post-tectonic two-mica granite in the Okazaki area, central Japan: a field guide for the 2003 Hutton Symposium

Yutaka NAKAI[1] and Kazuhiro SUZUKI[2]

Abstract: The Busetsu Granite belongs to the Ryoke Metamorphic Belt in the Okazaki area, and comprises fine- to medium-grained biotite granodiorite, medium-grained two-mica monzogranite and fine-grained two-mica granodiorite. Individual lithologies have gradual and intrusive contacts. Outcrops are dominated by extensive medium-grained two-mica monzogranite, which formed *c.* 77 Ma. Zircon, xenotime and monazite grains in the Busetsu Granite are euhedral, and show internal compositional variations typical of crystallization from magmatic liquids. This supports the assumption that whole-rock analyses represent true melt compositions. All lithologies are peraluminous, with differing trends of element concentrations. Individual magmas are inferred to derive from two or more discrete sources, or from a single heterogeneous source characterized by intrinsic differences in trace elements. Intrusions were emplaced successively over a short period in a post-tectonic setting.

Keywords: Hutton Symposium, field excursion, Peraluminous two-mica granite, Busetsu Granite, CHIME dating, Ryoke Belt.

1. Introduction

Okazaki is a modern prosperous city with strong automotive, mechanical and chemical industries, but is traditionally famed for it's stone products. Stone masonry in this area goes back more than five hundreds years, and it's success is partially due to the high quality of local biotite and muscovite-biotite granites. Fine- and medium-grained biotite granites, known as *Ao-ishi* (blue stone) and *Chu-me* (medium-grained), respectively, are mainly used for gravestones and statues, and muscovite-biotite granite, known as *Usu-ishi* (mortar stone), is used for mortar, torii (Shinto shrine archways), fencing and building. Similar granites outcrop along a hundred kilometer-long belt, from Okazaki through Inabu and Kadoshima to Komagane in Nagano Prefecture. The granites belong to the highest-grade part of the high *T*/*P* Ryoke Metamorphic Belt, where paragneiss occurs with a sillimanite plus K-feldspar assemblage (Fig. 1). The granites have been named as the Busetsu Granite (Koide, 1958) in the Okazaki and Inabu areas, the Kadoshima Granite (Koide, 1942) in the Kadoshima area and the Otagiri Granite (Murayama and Katada, 1957) in the Komagane area. These units are distinguished from other granitoids in the Ryoke Belt by the fine-grained massive texture, the presence of muscovite, garnet, monazite and xenotime, and the occasional presence of sillimanite or cordierite.

2. Timing of the Busetsu Granite

The intrusive relationships between granitoids in the Ryoke Belt have been determined by the Ryoke Research Group (1972). The Kamihara Tonalite is the earliest pluton and possesses a strong gneissosity. The second oldest unit is the Tenryukyo Granodiorite, which is characterized by a moderate to weak foliation and phenocrysts of plagioclase and K-feldspar up to 2-3 cm in size. Unlike the Kamihara Tonalite, the Tenryukyo Granodiorite is associated with a contact aureole characterized by reaction of muscovite and quartz to form fibrolitic sillimanite and K-feldspar (Yokoi, 1983). The Tenryukyo Granodiorite was intruded successively by the Kiyosaki Granodiorite, the Mitsuhashi Granodiorite and the Inagawa Granodiorite. The Shinshiro Tonalite is older than the Mitsuhashi Granodiorite, and is intruded discordantly into the andalusite-sillimanite transition zone of the Ryoke Belt, with a distinct contact aureole characterized by the reaction of muscovite and quartz to form andalusite and K-feldspar (Asami and Hoshino, 1985, Miyake *et al.*, 1992). The Busetsu Granite is intruded into the Inagawa Granodiorite, which in turn is intruded into the Nohi Rhyolite, a Late Cretaceous sequence of ignimbrite (Sakai *et al.*, 1965). This suggests that both the Inagawa Granodiorite and the Busetsu Granite were emplaced at shallow crustal levels, in tectonic conditions that differ from those for older plutons like the Kamihara Tonalite and the Tenryukyo Granodiorite.

The metamorphic rocks and granitoids in the map area have been dated by CHIME (the chemical Th-U-total Pb isochron method, Suzuki and Adachi, 1991). Averages of reported monazite ages are summarized in Fig. 2 (Suzuki *et al.*, 1994a, 1994b; Morishita and Suzuki, 1995; Suzuki *et al.*, 1995; Nakai and Suzuki, 1996; Suzuki and Adachi, 1998). Monazites in pelitic gneisses have yielded *c.* 100 Ma CHIME ages. Smith and Barreiro (1990) have argued that monazite forms as metamorphic mineral at lower amphibolite facies conditions and that the Th-U-Pb system records the timing of monazite formation, even with subsequent thermal effects at

[1] Aichi University of Education, Kariya 448-8542, Japan. E-mail: sy-nakai@m2.catvmics.ne.jp
[2] Nagoya University Center for Chronological Research, Nagoya 464-8602, Japan. E-mail: suzuki@nendai.nagoya-u.ac.jp

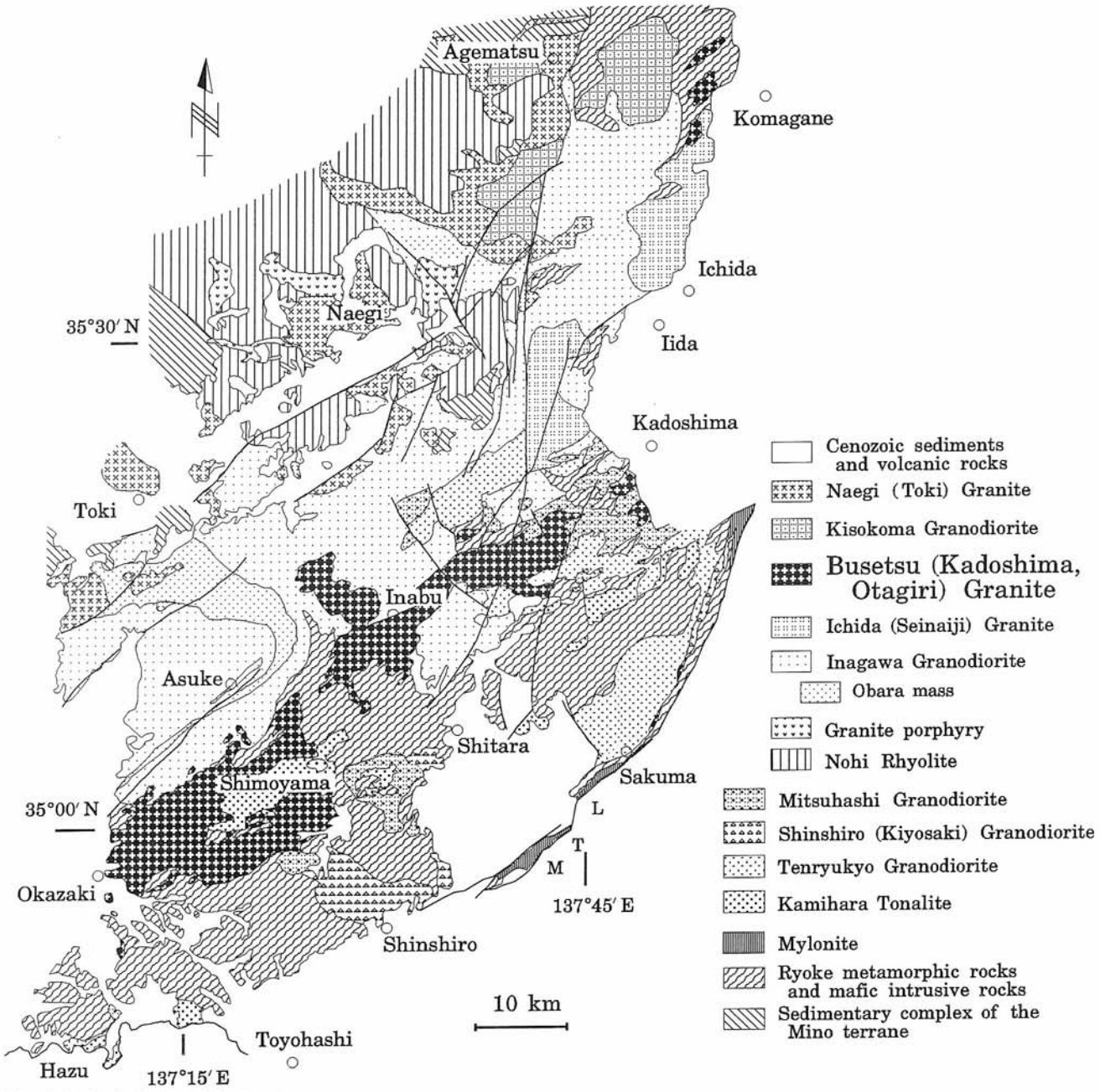

Fig. 1 Geological map of the Ryoke metamorphic belts in the area from Nagano to Aichi Prefectures (simplified from Ryoke Research Group, 1972)

upper amphibolite facies. If this is the case, then the ages from pelitic gneiss represent the timing of prograde metamorphism at amphibolite facies conditions. The *c.* 100 Ma gneiss age is similar to the CHIME monazite ages of 98.2-99.6 Ma for Ryoke Belt gneisses (Suzuki *et al.*, 1996) in the Iwakuni area, 500 km west of the Okazaki area. This is not consistent with a view that timing of the Ryoke metamorphism and plutonism become younger towards the east. The simple model that Ryoke metamorphism and plutonism were caused by the eastward migration of a heat source such as a subducting ridge is thus in question.

The CHIME monazite ages are in agreement with the intrusive relations of granitoids. The oldest Kamihara Tonalite yields a *c.* 95 Ma monazite age and the Tenryukyo Granodiorite *c.* 92 Ma. These ages can be interpreted as the timing of syn- to late-tectonic plutonism. The discordant Shinshiro Tonalite, Kiyosaki Granodiorite and Mitsuhashi Granodiorite yield a narrow range of ages from 85.2±2.1 to 84.4±0.8 Ma. Further CHIME monazite ages for the Busetsu Granite (77.6±0.6 Ma) and the Inagawa Granodiorite (82.5±0.9 Ma), are in agreement with the sequence of granitoid emplacement determined from field relationships. The Busetsu Granite was first dated by the K-Ar method at 73 Ma (Kawano and Ueda, 1966; recalculated age is 74.6 Ma using the decay constant of Steiger and Jager, 1977). Subsequent radiometric dating includes Rb-Sr whole-rock isochron ages of 82.5±3.9 Ma ($Sr/$=0.7096±0.0002, Shibata and Ishihara, 1979) and 74.9±8.0 Ma ($Sr/$=0.7095±0.0006, Nakai, 1982;

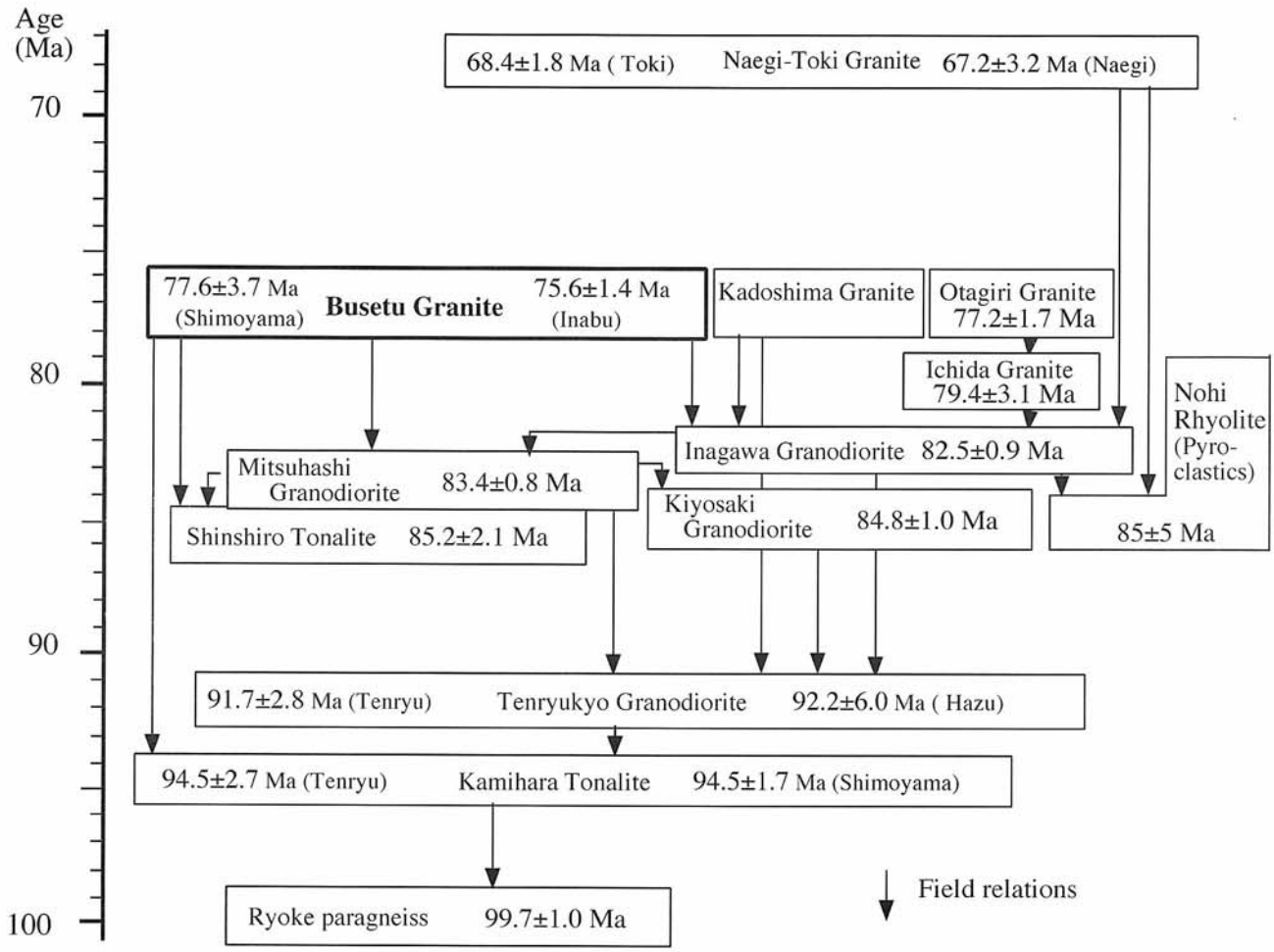

Fig. 2 Summary of CHIME monazite ages in context of intrusive relations of granitoids in the Ryoke metamorphic belt within the area from Nagano to Aichi Prefectures. The intrusive relations follow the synthesis of Ryoke Research Group (1972) with a slight modification.

Nakai *et al.*, 1985, originally 71.7±1.4 Ma, it was recalculated by discarding 3 data points for metamorphosed diabase), K-Ar mica ages of 68.2±3.4 and 66.0±3.3 Ma (Nakai, 1982) and a Re-Os age of 76.4±0.3 Ma for molybdenite in an associated pegmatite (Ishihara *et al.*, 2002).

Figure 3 shows CHIME ages for monazite in three samples of medium-grained two-mica monzogranite from the Okazaki area. The CHIME ages, 75.3±4.9, 75.9±6.1 and 77.2±4.1 Ma, coincide well with previous determinations. If we combine all analytical data for three samples on a single isochron, we obtain an age of 77.0±2.8 Ma. This age can be regarded as the time of magmatic crystallization for medium-grained two-mica monzogranite. Ishihara *et al.* (2002) interpreted the 76.4±0.3 Ma Re-Os date as the time of intrusion of late pegmatite dikes into medium-grained two-mica monzogranite, and the 74Ma K-Ar biotite age as the time of cooling through 300±50°C.

3. Rock types in the Busetsu Granite

The Busetsu Granite in the Okazaki area includes at least four rock types: fine-grained biotite granodiorite, medium-grained biotite granite/granodiorite (with tonalite), medium-grained two-mica monzogranite and fine-grained two-mica granodiorite (Nakai, 1976 ; Nakai *et al.*, 1985). Although boundaries between the rock types are hard to place exactly owing to insufficient outcrop, medium-grained two-mica monzogranite is the most widespread (Fig. 4). Medium-grained biotite granite/granodiorite is also abundant, including rocks of tonalitic composition developed in close association with metamorphic rocks in northern and southeastern parts of the map area. Fine-grained granodiorite occurs as xenolithic bodies in the map center, and fine-grained two-mica granodiorite forms small bodies.

The boundary between fine- and medium-grained biotite granodiorite can be seen at Yamasen Quarry (Stop 1), where medium-grained biotite granodiorite intrudes into fine-grained biotite granite. Medium-grained biotite granodiorite is intruded by medium-grained two-mica monzogranite at Tokai Quarry (Stop 2). According to Nakai *et al.* (1985), medium-grained biotite granodiorite is intruded by medium-grained two-mica monzogranite at Okuyamada, and medium-grained two-mica monzogranite is intruded by fine-grained two-mica granodiorite at Yasudo.

Fine-grained biotite granodiorite, light bluish colored and massive, has an average mode of 36.5% quartz, 39.0%

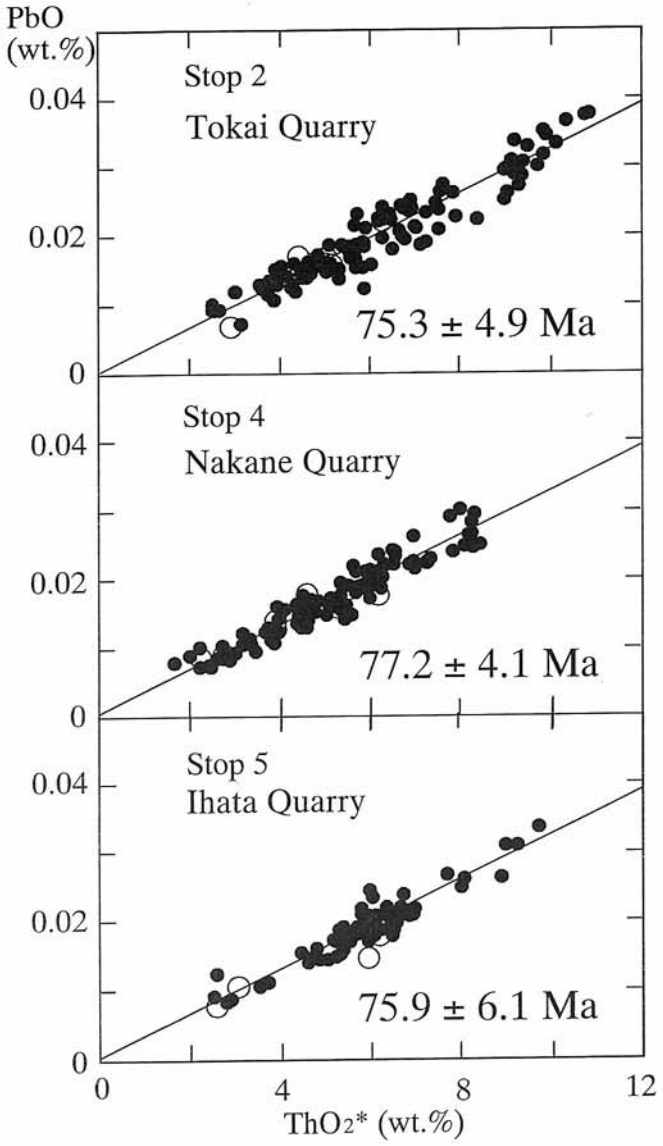

Fig. 3 Plots of PbO vs. ThO_2* of monazite in medium-grained two-mica monzogranite from Tokai (Stop 2), Nakane (Stop 4) and Ihata (Stop 5) quarries. ThO_2* represents sum of the measured ThO_2 and ThO_2 equivalent of the measured UO_2. Open circles represent data points for spots with detectable amounts of sulfur, and are not used for age calculation. Error given to the age is of 2 σ .

plagioclase, 14.5% K-feldspar, 9.5% biotite and 0.5% muscovite. Muscovite is barely visible on close inspection. Accessory minerals include ilmenite, zircon, apatite, garnet, allanite, xenotime and monazite. Monazite is very sparse in most samples. Quartz grains are typically around 0.4 mm across and have wavy extinctions. Plagioclase occurs as euhedral or subhedral grains, typically zoned with distinct boundaries between core and rim. Core compositions are calcic andesine (*An*=40-45), and rims range from calcic to sodic oligoclase. Cores are partly sericitized.

Medium-grained biotite granodiorite is lighter colored and coarser grained than fine-grained biotite granodiorite. The average size of quartz grains is around 1mm. Most samples consist of 40% quartz, 30% plagioclase, 20% K-feldspar and 10% biotite, but some samples collected from the northern and southeastern parts contain 30-40% quartz, 50-60% plagioclase and 4-10% K-feldspar. Plagioclase grains are normally zoned from andesine in cores to oligoclase in rims. In the related tonalites the plagioclase is labradorite. Calcic cores are partly sericitized.

Medium-grained two-mica monzogranite is leucocratic, and consists of 32-38% quartz, 23-39% plagioclase, 18-33% K-feldspar, 3-9 % biotite and 2-6% muscovite. Quartz grains, 0.5-3.0 mm in diameter, are anhedral, with inclusions of plagioclase and biotite. Plagioclase grains, 1-3mm in size, have subhedral forms with oscillatory-zoned calcic cores (*An*=45-30) and sodic rims (*An*=20-10). K-feldspar grains, up to 2.5 mm in diameter, have traces of fine-grained microperthitic intergrowth, and inclusions of plagioclase and quartz. Biotite and muscovite occur as subhedral to anhedral plates of up to 1 mm long. Muscovite is found mainly in intergranular spaces between the major constituents. Accessory minerals include garnet, ilmenite, apatite, monazite, xenotime and zircon. Of these, garnet is fairly abundant. Samples from Nakane Quarry (Stop 4) contain significant amounts of monazite, with the relative abundance of monazite, xenotime and zircon approximately 20:4:1. Monazite and xenotime occur as euhedral to subhedral prisms up to 0.3 mm long, and zircon forms well-faceted prisms 0.1-0.2 mm long. Most zircon grains have concentric zoning (Suzuki *et al.*, 1992). Monazite grains have core to rim decreases in La and Ce with counterbalancing increases in Nd and heavier rare earth elements. Zircon grains have core to rim increases in Y and Hf/(Zr+Hf) ratio. The zoning patterns, coupled with the morphology, contrast with what is expected for "restite" components.

Fine-grained two-mica granodiorite occurs as small bodies in medium-grained two-mica monzogranite. Apart from differences in grain size, the two can hardly be discriminated from one another in the field. Under the microscope, fine-grained two-mica granodiorite is characterized by the presence of rounded quartz grains within poikilitic K-feldspar.

4. Chemistry

Thirty-four fresh samples were analyzed by XRF under identical experimental conditions to show the small compositional variation among rock types (Table 1). SiO_2 contents vary from 71 to 74 wt% for fine and medium-grained biotite granodiorite (solid circles in Fig. 5), and from 73 to 75 wt% for medium-grained two-mica monzogranite (open circles). K_2O (2.6-4.3 wt%), Rb (67-198 ppm) and A/CNK (1.08-1.31 with an exceptional value of 1.45) increase, whereas FeO (2.8-1.0 wt%), MgO (0.5-0.21 wt%), CaO (2.8-0.9 wt%), Sr (365-114 ppm) and Zr (189-55 ppm) decrease with increasing SiO_2. Al_2O_3 (14.1-14.9 wt%) and Na_2O (3.0-3.5 wt%) are relatively constant. As mentioned above, accessory zircon, xenotime and monazite are euhedral, and show intra-grain REE distributions typical for cotectic crystallization from a finite reservoir. This suggests that the

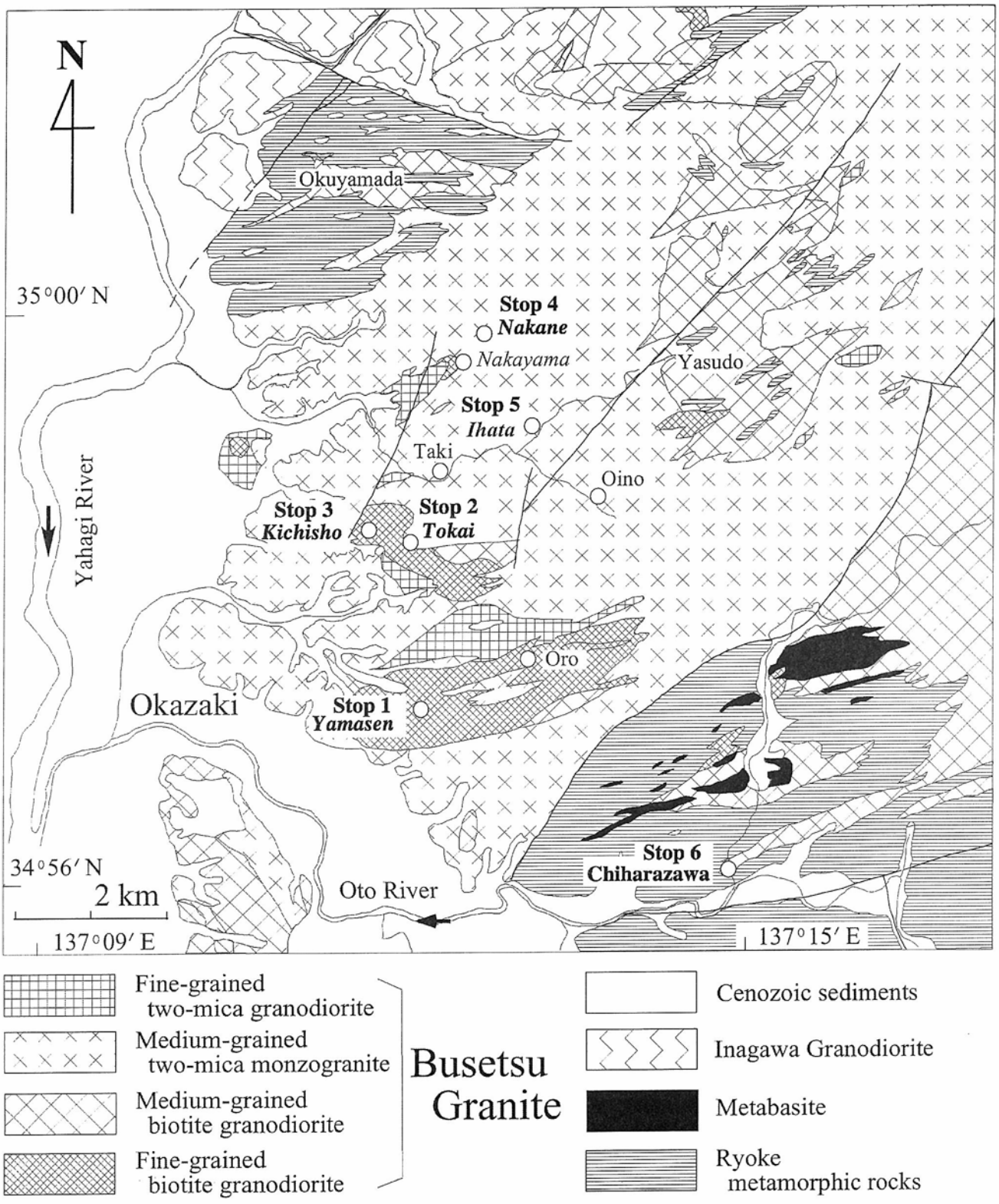

Fig. 4 Geologic map of the Okazaki area (simplified and modified from Nakai et al., 1985) showing localities of Stops (Stops 1 to 6) and sample localities (Oro, Taki, Oino and Nakayama quarry).

accessory minerals did not originate as a restite component or as xenocrysts, but crystallized from magmatic melt. Since the magmatic accessory minerals are included in early-formed plagioclase cores as well as later-formed constituents, bulk analyses can be assumed to represent compositions of magmatic melts. Fractionation of biotite and plagioclase may explain, at least partially, the evolutionary trends. There is, however, a significant difference in the TiO_2, FeO, Zr and Y trends between the granodiorite and the monzogranite.

The composition of medium-grained two-mica monzogranite

Table 1 XRF analysis of fine-grained (f) and medium-grained (m) biotite granodiorite (bt), medium-grained two-mica monzogranite (2m) and biotite-rich enclave (clot) from the Busetsu Granite in the Okazaki area. A/CNK shows molar $Al_2O_3/(CaO+Na_2O+K_2O)$ ratios.

	Stop 1 (*Yamasen*)								Oro	Stop 2 (*Tokai*)				Stop 3 (*Kichisho*)			Taki
	A1	A2	A3	A4	B	C	D	E		A	B	C	D	A	B	C	
(wt.%)	bt,f	bt,f	bt,m	bt,m	bt,m	bt,f	bt,f	bt,f	bt,f	bt,f	bt,f	2m	2m	bt,f	bt,f	bt,f	2m
SiO_2	71.70	72.00	72.77	74.03	72.78	72.86	71.25	72.56	72.82	70.78	70.67	74.77	74.48	72.28	72.82	72.48	74.17
TiO_2	0.27	0.31	0.20	0.20	0.24	0.27	0.30	0.27	0.25	0.30	0.31	0.10	0.10	0.29	0.30	0.25	0.11
Al_2O_3	14.64	14.79	14.23	14.30	14.62	14.70	14.85	14.81	14.72	14.54	14.58	14.57	14.39	14.71	14.83	14.48	14.62
FeO	2.37	2.75	1.82	1.84	1.99	2.26	2.39	2.28	2.11	2.57	2.63	1.02	1.00	2.22	2.36	2.07	1.07
MnO	0.05	0.06	0.04	0.04	0.05	0.05	0.06	0.05	0.05	0.06	0.06	0.05	0.07	0.06	0.06	0.05	0.03
MgO	0.47	0.53	0.37	0.35	0.46	0.50	0.51	0.49	0.47	0.52	0.54	0.21	0.21	0.49	0.48	0.39	0.27
CaO	2.27	2.53	1.93	1.89	2.07	2.21	2.44	2.27	2.23	2.75	2.78	0.94	0.98	2.38	2.46	2.22	0.99
Na_2O	3.16	3.23	3.01	3.04	3.10	3.12	3.12	3.20	3.04	3.23	3.17	3.37	3.50	3.16	3.16	3.10	3.32
K_2O	3.07	2.56	3.64	3.71	3.61	3.25	2.99	3.17	3.57	2.95	2.94	3.95	3.89	3.18	3.13	3.38	4.21
P_2O_5	0.10	0.11	0.05	0.05	0.07	0.09	0.09	0.09	0.08	0.08	0.08	0.12	0.11	0.09	0.08	0.06	0.11
Total	98.10	98.87	98.06	99.45	98.99	99.31	98.00	99.19	99.34	97.78	97.76	99.10	98.73	98.86	99.68	98.48	98.90
A/CNK	1.16	1.17	1.15	1.15	1.14	1.16	1.16	1.16	1.14	1.08	1.08	1.26	1.22	1.13	1.14	1.13	1.23
Cr (ppm)	22	16	12	18	21	6	16	13	7	< 3	< 3	3	3	7	19	17	12
Co	4	5	4	4	4	2	5	2	3	3	4	2	2	3	3	3	2
Ni	8	11	3	9	8	7	10	8	7	7	7	12	12	6	8	7	11
Zn	71	94	57	56	56	65	65	68	59	65	62	52	49	57	65	57	47
Rb	94	84	94	97	95	90	86	86	105	78	89	198	196	109	106	111	136
Sr	339	339	298	293	302	365	343	343	312	356	343	115	114	292	317	290	161
Y	21	21	19	25	20	19	18	18	24	26	29	16	18	20	29	22	14
Zr	134	146	134	139	115	142	136	135	124	168	189	56	55	133	148	133	65
Nb	11	13	8	10	8	9	9	9	9	10	11	11	13	9	10	9	9
Ba	878	826	1004	1027	893	884	691	863	884	780	704	429	351	658	806	770	732
Pb	19	22	35	25	23	21	20	15	21	17	17	24	20	14	17	18	32
Th	6	7	10	9	9	9	6	7	6	4	6	5	5	3	5	7	7

	Oino	Stop 4 (*Nakane*)								Stop 5 (*Ihata*)			*Nakayama*				Stop 6
		A	B	C	D	E	F	G1	G2	A	B	C	A	B	C	D	
(wt.%)	2m	2m	2m	2m	2m	2m	2m	2m	clot	2m	2m	2m	bt,f	bt,f	bt,f	bt,f	2m
SiO_2	74.49	73.45	73.78	72.91	74.50	73.16	72.92	73.46	61.62	75.09	73.4	73.91	74.18	73.51	72.66	72.89	74.20
TiO_2	0.14	0.15	0.18	0.17	0.14	0.14	0.15	0.13	0.76	0.13	0.14	0.13	0.20	0.20	0.20	0.20	0.07
Al_2O_3	14.48	14.66	14.74	14.56	14.60	14.58	14.55	14.42	17.93	14.61	14.19	14.13	14.49	14.36	14.26	14.25	14.52
FeO	1.25	1.46	1.70	1.66	1.37	1.43	1.41	1.34	8.00	1.18	1.25	1.17	1.75	1.69	1.68	1.76	0.71
MnO	0.04	0.05	0.06	0.06	0.04	0.05	0.05	0.05	0.19	0.04	0.04	0.04	0.06	0.06	0.06	0.06	0.08
MgO	0.30	0.37	0.42	0.39	0.34	0.35	0.35	0.33	1.77	0.28	0.30	0.28	0.35	0.32	0.32	0.34	0.18
CaO	1.04	1.59	1.74	1.64	1.54	1.54	1.47	1.37	0.17	1.13	1.17	1.13	1.94	1.96	1.89	1.95	0.83
Na_2O	3.29	3.43	3.39	3.39	3.24	3.37	3.25	3.35	0.26	3.02	3.15	3.05	3.18	3.02	3.19	3.13	2.93
K_2O	4.12	3.40	3.32	3.37	3.30	3.19	3.44	3.68	6.94	3.85	4.24	4.26	3.34	3.37	3.82	3.67	4.44
P_2O_5	0.11	0.17	0.20	0.17	0.09	0.18	0.16	0.08	0.13	0.07	0.06	0.06	0.06	0.05	0.06	0.05	0.09
Total	99.26	98.73	99.53	98.32	99.16	97.99	97.75	98.21	97.77	99.40	97.94	98.16	99.55	98.54	98.14	98.30	98.05
A/CNK	1.23	1.20	1.20	1.19	1.25	1.24	1.24	1.20	-	1.31	1.19	1.21	1.17	1.18	1.11	1.12	1.45
Cr (ppm)	8	< 3	< 3	7	< 3	9	15	4	13	7	< 3	6	< 3	< 3	< 3	< 3	12
Co	3	3	4	2	3	3	2	3	5	3	2	3	2	4	3	3	3
Ni	10	8	7	10	8	11	9	7	14	11	9	10	10	9	11	7	9
Zn	65	55	66	64	52	58	57	49	295	55	53	48	53	49	44	55	15
Rb	138	123	102	131	111	98	92	130	330	67	109	118	106	120	135	79	120
Sr	178	223	197	221	229	236	207	230	51	191	188	172	269	264	259	277	107
Y	13	14	15	16	16	10	10	16	66	19	18	22	26	26	28	23	12
Zr	74	84	119	102	87	82	82	74	181	72	74	70	114	108	109	115	53
Nb	9	10	13	12	9	10	10	9	54	10	10	9	10	9	10	10	8
Ba	873	680	447	597	800	590	645	649	351	905	895	788	685	694	710	722	438
Pb	33	20	19	20	23	21	20	26	5	30	33	33	19	21	17	22	38
Th	9	4	5	4	8	6	7	7	35	13	12	9	6	6	6	7	4

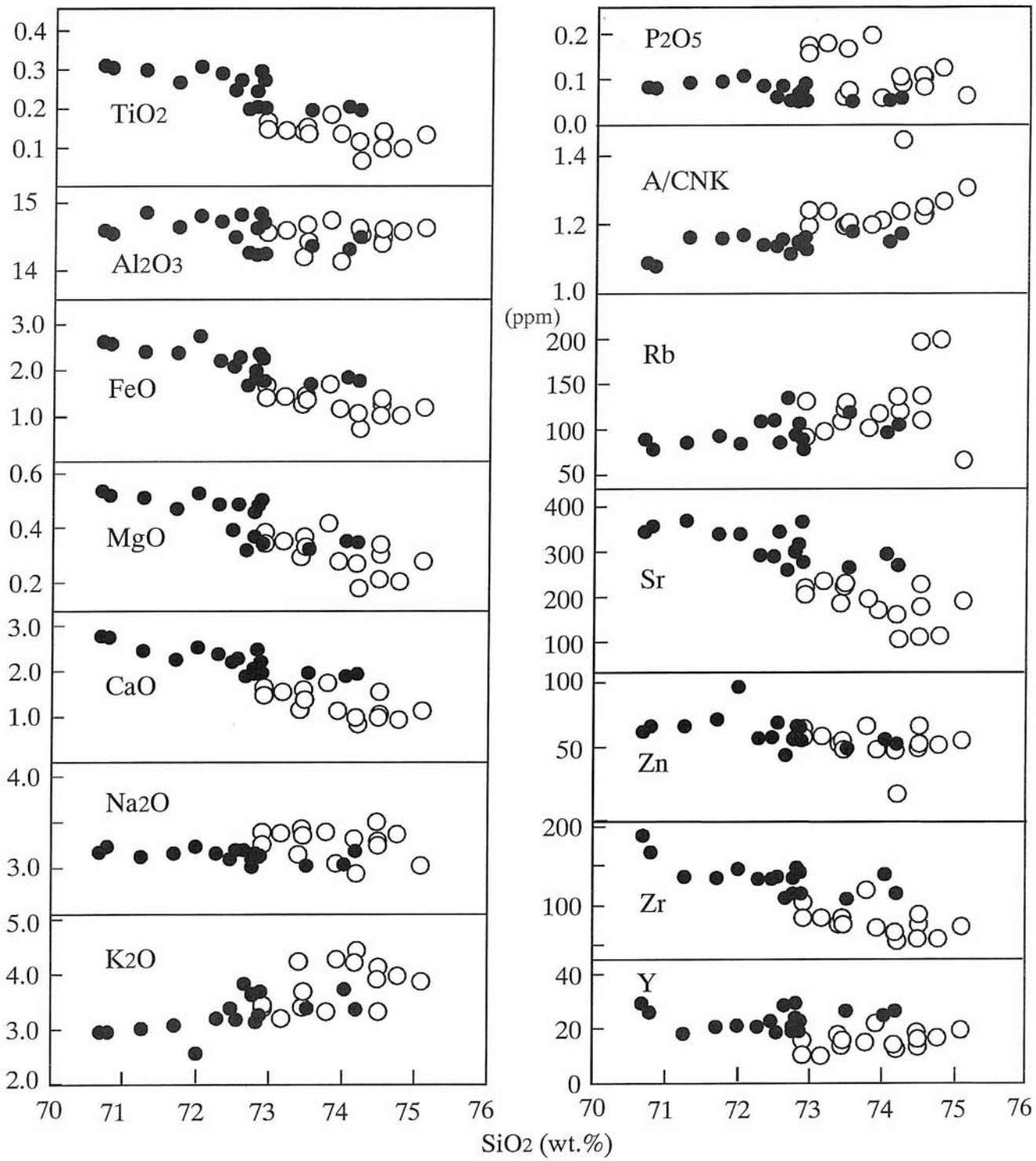

Fig. 5 Major and trace element variation diagrams of the Busetsu Granite. Solid circles represent data point for fine- and medium-grained biotite granodiorite, and open circles represent that for medium-grained two-mica monzogranite.

also differs between sites. Samples from Tokai Quarry (Stop 2) have >190 ppm Rb with Rb/Sr ratios of *c.* 1.7, whereas other monzogranite samples contain <130 ppm Rb with Rb/Sr ratios of around 0.6. Medium-grained two-mica monzogranite from Nakane Quarry has a high P_2O_5 content of around 0.2 wt%. This correlates with the high abundance of monazite. The predominance of monazite over zircon reflects a high REE/Zr ratio in the magma. Magmas that produced the differing rock-types are inferred to have been derived from two or more discrete source magmas with differing Rb/Sr and REE/Zr, or from a single heterogeneous source magma characterized by intrinsic differences in trace element concentrations.

The whole-rock $\delta^{18}O$ values are in the range from 10.5 to

12.5 % (Ishihara and Matsuhisa, 2002), and the $\delta^{34}S$ values of molybdenite are -5.7 and -6.0 (Ishihara and Sasaki, 2002). These values coupled with the high A/CNK ratios are favorable to derivation of the parental magmas from sedimentary (pelitic) sources. However, the initial $^{87}Sr/^{86}Sr$ ratios (0.7096±0.0002, Shibata and Ishihara, 1979; 0.7097±0.0001, Nakai, 1982) do not differ significantly from those for the metaluminous Inagawa, Mitsuhasi and Tenryukyo Granodiorites (0.7078-0.7095, Kagami, 1973) of the Ryoke metamorphic belt.

5. Excursion

Stop 1: Yamasen Quarry

This quarry exposes fine and medium-grained biotite granodiorite. In some places fine-grained biotite granodiorite contains indistinct compositional or textural laminations that probably represent flow banding. Medium-grained biotite granodiorite contains a foliation defined by a loose alignment of constituent minerals. Fine-grained biotite granodiorite occasionally contains decimeter-sized xenoliths of coarse-grained biotite granodiorite (Inagawa Granodiotite), biotite schist injected with veins of coarse-grained leucocratic granite (akin to the Inagawa Granodiorite), and medium-grained biotite tonalite with 1 to 2 mm biotite-rich selvages. The boundary between the two dominant rock-types can be observed on the broken surface of an excavated block. Although the boundary is not clear-cut, medium-grained biotite granodiorite appears to have intruded into the fine-grained type, because the foliation in the medium-grained type is roughly parallel to the boundary. Some may regard the fine-grained biotite granodiorite as a xenolith of granitoid related to the biotite tonalite rock-type, which is older than fine-grained biotite granodiorite. This is, however, unlikely, because of the significant difference in composition. We conclude that rocks grouped in Figure 4 as medium-grained biotite granodiorite can be subdivided into two: a tonalitic variety followed by fine-grained biotite granodiorite and a later granodioritic variety. If this is the case, the Busetsu Granite in the Okazaki area comprises the rock-types medium-grained biotite tonalite, fine- and medium-grained biotite granodiorite, medium-grained two-mica monzogranite and fine-grained two-mica granodiorite, in the order of emplacement.

Stop 2: Tokai Quarry

The purpose of this stop is to examine the intrusive relationship between fine-grained biotite granodiorite and medium-grained two-mica monzogranite. Critical observations include (1) that the boundary is remarkably straight and clear, (2) that the boundary is sharp, with only slight coarsening apparent in the adjacent medium-grained two-mica monzogranite, and (3) that fine-grained biotite granodiorite is intruded by a vein originating in the medium-grained two-mica monzogranite. Another point of interest is the presence of a biotite-rich enclave in fine-grained biotite granodiorite.

Fine-grained biotite granodiorite in this quarry is slightly coarser than that at Stop 1. It has higher FeO and CaO contents other outcrops of fine-grained biotite granodiorite. Medium-grained two-mica monzogranite in this quarry has unusually high Rb/Sr values compared with two-mica rocks from other quarries, including Stops 4 and 5.

Stop 3: Kichisho Quarry

This quarry provides more examples of fine-grained biotite granodiorite. The rocks look like those at Stop 2, but are slightly lower in the FeO, CaO and Sr contents and higher in K_2O and Rb. Unlike Stops 1 and 2, aplite dikes have intruded fine-grained biotite granodiorite at this quarry. A horizontal aplite dike around 60 cm wide is visible on the pit wall

Stop 4: Nakane Quarry

Most occurrences of medium-grained two-mica monzogranite are massive; at this site, however, sections of the outcrop have a 'marbled paper' appearance. A typical example can be seen on the surface of a block at the entrance to the quarry. The layers appear to be distinguished by differences in grain size rather than mineral proportions. Quartz and feldspar grains never exceed 2 mm in size in the darker laminations, whereas in lighter areas grains are as large as 4 mm. The crenulation of the layers suggests deformation during or after solidification. The layering is probably a form of flow banding, and the crenulation of layers in parts of the outcrop may represent slight deformation or flow movement in the late stages of crystallization.

Two-mica monzogranite in this quarry is characterized by a high concentration of P_2O_5 (0.16-0.20 wt%). This may be due to the abundant presence of monazite. Numerous pegmatite dikes are intruded into two-mica monzogranite. They range in width from a few centimeters to several decimeters, and have aplitic margins. Some dikes contain sparse molybdenite (Sato and Nakai, 1991) which has been dated through the Re-Os method at 76.4±0.3 Ma (Ishihara *et al.*, 2002). Monazite from the host monzogranite yields a CHIME age of 77.2±4.1 Ma (Fig. 3).

Stop 5: Ihata Quarry

This quarry provides the most representative type of *Usu-ishi* (medium-grained two-mica monzogranite). Unlike Stop 4, the monzogranite here is very homogeneous. The working face can only be viewed from the entrance road. The overhanging wall is a fault surface with slickensides. Excavated rocks have accumulated on the entrance road, and excellent samples can be taken.

Stop 6: Riverbed at Chiharazawa

Hornfels derived from mica schist is exposed on the riverbed. The mica schist formed from thinly-bedded argillite during Ryoke metamorphism, and contains biotite with muscovite. Andalusite occurs in a few pelitic layers. Sedimentary bedding is well preserved, but rotated parallel to the schistosity, trending NE-SW to E-W with steep dips. The mica schist at this locality has been metamorphosed into hornfelses through the intrusion of the Busetsu Granite.

Pelitic hornfels is characterized by porphyroblastic cordierite or andalusite. Reaction textures showing the breakdown of muscovite and quartz to form andalusite plus K-feldspar are common at the immediate contact with the Busetsu Granite.

Numerous dikes of Busetsu Granite intrude the hornfels on the riverbed. Most dikes are concordant with the sedimentary bedding, and range in width from a decimeter to 1 m Towards the east, individual dikes converge into a stock of medium-grained biotite granodiorite. Dike rock contains muscovite, and has a high A/CNK value of 1.45. Although sericitization of plagioclase core may have contributed to the high A/CNK value, contamination of a granodioritic magma by argillaceous host rocks is the most likely cause. The sharp boundary of the dikes against the host suggests that contamination took place well before emplacement.

References

Asami, M and Hoshino, M. (1985) Staurolite-bearing schists from the Hongu-san area in the Ryoke metamorphic belt, central Japan. *Jour. Geol. Soc. Japan*, **86**, 581-591.

Ishihara, S. and Matsuhisa, Y. (2002) Oxygen isotopic constraints on the geneses of the Cretaceous-Paleogene granitoids in the Inner Zone of Southwest Japan. *Bull. Geol. Surv. Japan*, **53**, 421-438.

Ishihara, S. and Sasaki, A. (2002) Paired sulfur isotopic belts: Late Cretaceous- Paleogene ore deposits of Southwest Japan. *Bull. Geol. Surv. Japan*, **53**, 461-477.

Ishihara, S., Stein, H.J. and Tanaka, R. (2002) Re-Os age of molybdenite from the Busetsu two-mica granite, central Japan. *Bull. Geol. Surv. Japan*, **53**, 479-482.

Kagami, H. (1973) A Rb-Sr geochronological study of the Ryoke granites in Chubu district, central Japan. *Jour. Geol. Soc. Japan*, **79**, 1-10.

Kawano, Y. and Ueda, Y. (1966) K-Ar dating on the igneous rocks in Japan (V) - Granitic rocks in southwestern Japan-. *Jour. Japan. Assoc. Mineral. Petrol. Econ. Geol.*, **56**, 191-211.*

Koide, H. (1942) On the granitic rocks of the Tenryukyo district, Nagano Prefecture. *Bull. Tokyo Univ. Forest*, No. 30, 69-95.

Koide, H. (1958) *Dando granodioritic intrusives and their associated metamorphic complex*. Japan Society for the Promotion of Science, Tokyo, 311p.

Miyake, A., Murata, E. and Morishita, O. (1992) Growth stages of andalusite in the Ryoke metamorphic rocks from the Nukata area, Aichi Prefecture. *Jour. Mineral. Petrol. Econ. Geol.*, **87**, 475-480.*

Morishita, T. and Suzuki, K. (1995) CHIME ages of monazite from the Shinshiro Tonalite of the Ryoke belt in the Mikawa area, Aichi Prefecture. *Jour. Earth Planet. Sci. Nagoya Univ.* **42**, 45-53.

Murayama, M. and Katada, M. (1957) *Explanatory text of the geological map of Japan*. With geological sheet map "Akaho" at 1:50,000. Geological Survey of Japan, 45p.

Nakai, Y. (1976) Petrographical and petrochemical studies of the Ryoke granites in the Mikawa-Tono district, central Japan. *Bull. Aichi Univ. Educ.* **25**, 97-112.

Nakai, Y. (1982) The Busetsu Granite in the Ryoke metamorphic belt. *Abstract 89th Ann. Meet. Geol. Soc. Japan*, 404.**

Nakai, Y. and Suzuki, K. (1996) CHIME monazite ages of the Kamihara Tonalite and the Tenryukyo Granodiorite in the eastern Ryoke belt of central Japan. *Jour. Geol. Soc. Japan*, **102**, 431-439.

Nakai, Y., Takeuchi, S., Suganuma, T., Ohta, S., Sakamoto, E., Yamamoto, N. and Uchida, Y. (1985) *Geography and geology of Okazaki City. History of Okazaki City, Nature 14*, Okazaki City, Okazaki, 209p.**

Ryoke Research Group: Hayama, Y., Ikeda, K., Jindo, O., Kagami, H., Kijima, T., Kutsukake, T., Morimoto, M., Nakai, Y., Nakasuji, A., Sekido, S., Suzuki, K., Yamada, N., and Yamada, T. (1972) The mutual relations of the granitic rocks of the Ryoke metamorphic belt in central Japan. *Earth Sci. (Chikyu Kagaku)*, **26**, 205-216.*

Sakai, E., Otani, M., Sugioka, K., Hayakawa, M., Mizutani, T., Noda, I., Miyoshi, K., Miura, H., Matsuoka, S., Hattori, Y. and Ito, R., (1965) Preliminary note on the order of intrusion of the Mesozoic igneous rocks in the three cities of Mizunami, Ena and Nakatsugawa and in the Ena district, Gifu Prefecture, central Japan. *Bull. Aichi Gakugei Univ., Nat. Sci.*, **14**, 61-71.*

Sato, K. and Nakai, Y. (1991) Okazaki-mikage; Busetsu two-mica granite in the Ryoke Belt. *Chishitsu News*, **441**, 46-59.**

Shibata, K. and Ishihara, S. (1979) Rb-Sr whole-rock ages and K-Ar mineral ages of granitic rocks in Japan. *Geochem. Jour.*, **13**, 113-119.

Smith, H. A. and Barreiro, B. (1990) Monazite U-Pb dating of staurolite grade metamorphism in pelitic schist. *Contrib. Mineral. Petrol.* **105**, 602-615.

Steiger, R.H. and Jager, E. (1977) Subcommission on geochronology: convention on the use of decay constants in geo- and cosmochronology. *Earth Planet. Sci. Lett.*, **36**, 359-362.

Suzuki, K. and Adachi, M. (1991) Precambrian provenance and Silurian metamorphism of the Tsubonosawa paragneiss in the South Kitakami terrane, Northeast Japan, revealed by the chemical Th-U-total Pb isochron ages of monazite, zircon and xenotime. *Geochem. Jour.*, **25**, 357-376.

Suzuki, K. and Adachi, M. (1998) Denudation history of the High *T/P* Ryoke metamorphic belt, southwest Japan: constraints from CHIME monazite ages of gneisses and granitoids. *Jour. Metamorphic Geol.* **16**, 23-37.

Suzuki, K., Adachi, M., Yamamoto, K. and Nakai, Y. (1992) Intra-grain distribution of REE and crystallization sequence of accessory minerals in the Cretaceous Busetsu Granite at Okazaki, central Japan. *Geochem. Jour.*, **26**, 383-394.

Suzuki, K., Adachi, M. and Kajizuka, I., (1994a), Electron microprobe observations of Pb diffusion in metamorphosed detrital monazites. *Earth Planet. Sci. Lett.*, **128**, 391-405.

Suzuki, K., Morishita, T., Kajizuka, I., Nakai, Y., Adachi, M. and Shibata, K. (1994b) CHIME ages of monazites from the Ryoke metamorphic rocks and some granitoids in the Mikawa-Tono area, central Japan. *Bull. Nagoya Univ. Furukawa Mus.*, No.10, 17-38.*

Suzuki, K., Nasu, T. and Shibata, K. (1995) CHIME monazite ages of the Otagiri and Ichida Granites in the Komagane area, Nagano Prefecture. *Jour. Earth Planet. Sci., Nagoya Univ.*, **42**, 17-30.

Suzuki, K., Adachi, M. and Nureki, T. (1996) CHIME age dating of monazites from metamorphic rocks and granitic rocks of the Ryoke belt in the Iwakuni area, Southwest Japan. *The Island Arc*, **5**, 43-55.

Yokoi, K. (1983) Fe_2O_3 content of co-existing andalusite and sillimanite in the Ryoke metamorphic rocks occurring in the Hiraoka-Kadoya area, central Japan. *Jour. Japan. Assoc. Mineral. Petrol. Econ. Geol.*, **78**, 246-254.*

* in Japanese with English abstract.
** in Japanese.

Received May 26, 2003
Accepted July 4, 2003

Hutton Symposium V, Field Guidebook
Geological Survey of Japan, Interim Report no.28, p.125－134, 2003

Trip M3

Koto Rhyolites and their related granitic rocks around Lake Biwa, southwest Japan

Yoshihiro SAWADA[1] and Satoshi NAKANO[2]

Abstract: A late Cretaceous volcano - plutonic complex is associated with the 60 km × 40 km Biwako Cauldron in the area around Lake Biwa. The complex is part of the San'yo belt. The granitoids were intruded along outer fractures of the cauldron. The subsided floor of the cauldron block was filled with volcaniclastic rocks named the Koto Rhyolites. These are mainly pyroclastic flow deposits. Igneous activity in the cauldron is divided into two stages, around 95 Ma and 80 - 66 Ma. The granitoids and rhyolites of the second stage are comagmatic. On this trip, we will observe part of the huge Cretaceous granitic ring complex, and the intra-caldera volcaniclastic deposits. We will also get a spectacular view of the entire Biwako Cauldron and the ring complex, and a panorama of Lake Biwa, the largest lake in Japan.

Keywords: Hutton Symposium, field excursion, granite, rhyolite, welded tuff, volcano-plutonic complex, cauldron, ring complex, petrology, radiometric age, Lake Biwa, San'yo belt, Southwest Japan, Cretaceous

1. Introduction

A number of Cretaceous to Paleogene igneous complexes consisting of granitoids and felsic volcanic rocks occur throughout the Inner Zone of Southwest Japan (Fig.1). The granitoids have been divided into three zones from a petrological viewpoint: the Ryoke, San'yo and San'in belts, from south to north. A late Cretaceous volcano - plutonic complex is associated with a huge cauldron (Biwako Cauldron) in the area around Lake Biwa. This complex is part of the San'yo belt.

The granitoids form a ring complex which was intruded along fracture zones around the 60 km by 40 km cauldron (Sawada *et al.*, 1994). The subsided floor of the cauldron block was filled with volcaniclastic rocks named the Koto Rhyolites, Which consist mainly of pyroclastic flow deposits (Collaborative Research Group for the Granites around Lake Biwa, 2000; hereafter abbreviated (CRGGLB); Research Group for the Basement Geology around Lake Biwa (RGBGLB), 2002). The complex represents typical modes of Cretaceous to Paleogene volcano-plutonism in southwest Japan.

This one-day field trip examines the huge Cretaceous volcano-plutonic complex around the southern area of Lake Biwa (Fig.1). On the trip, we will observe part of the Cretaceous granitic ring complex related to caldera collapse, and the intra-caldera volcaniclastic deposits. We will also get a spectacular view of the entire Biwako Cauldron and the ring complex, and a panorama of Lake Biwa.

2. Outline of Geology around Lake Biwa

Lake Biwa is situated in central Japan. Geologically the area around the lake belongs to the Tamba-Mino belt of Jurassic accretionary complexes, consisting of Permian oceanic rocks (limestone, basaltic rock, siliceous mudstone and bedded chert) and Jurassic terrigeneous rocks. The Jurassic accretionary complexes were intruded by late Cretaceous granitic rocks and dykes, and covered by welded tuffs of late Cretaceous age (the Koto Rhyolites), the Miocene Ayukawa Formation, the Pliocene to Pleistocene Kobiwako Group, terrace deposits and alluvium.

The above late Cretaceous granitoids and the Koto Rhyolites are distributed in and around Lake Biwa. The granitoid plutons are named the Kaizukiyama, Koujyaku, Hira, Ryozen, Ohgi, Hiei, Tanakami, Yasu, and Suzuka (Fig.2). They are subdivided into three groups, based on their geology, age and petrographical features. The first group comprises the Kaizukiyama and Koujyaku plutons, located to the north and northeast of Lake Biwa. The second group is formed by the Ryozen and Ohgi plutons, which consist of small scale granodiorite-tonalite distributed to the west of the southern part of Lake Biwa. The third comprises major plutons (Hira, Hiei, Tanakami, Suzuka and Yasu) consisting of biotite granite. These plutons surround the southern part of Lake Biwa, and characteristically show form a morphological feature extending along the ring-like outline.

The Koto Rhyolites, consisting of pyroclastic rocks (mainly welded) are distributed mainly in the western foot of the Suzuka Range, but scattered occurrences are also found in several hills on the Koto Plain and on islets in Lake Biwa (Fig.2). They are associated with several types of dykes, including granite porphyries, granodiorite porphyries and feeder pyroclastic rocks.

Lake Biwa is one of the oldest lakes in the world, with an origin dating back to the Pliocene (4 Ma). The Kobiwako

[1] Department of Geoscience, Faculty of Science and Engineering, Shimane University. 1060 Nishikawatsu, Matsue 690-8504, Japan. E-mail: sawada@riko.shimane-u.ac.jp
[2] Faculty of Education, Shiga University. 2-5-1 Hiratsu, Otsu 520-0862, Japan. E-mail: nakano@sue.shiga-u.ac.jp

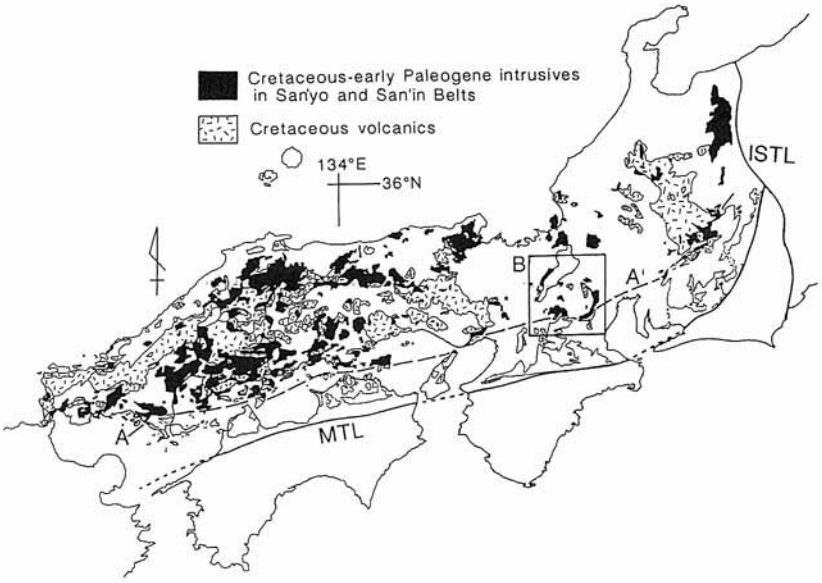

Fig.1. Distribution map of Cretaceous to Paleogene igneous rocks in the inner zone of southwest Japan. After the Geological Map of Japan (Yamada *et al.*, 1982).

Group, which was deposited in the ancestral lake, is widely distributed around Lake Biwa, especially to the southeast.

3. The granitoids

Nine granitic plutons occur around Lake Biwa, as outlined above (Fig.2). Locationally and morphologically, the plutons can also be divided into two groups. The first comprises cauldron related granitoids, whereas the second is distributed outside the cauldron. The former group is further subdivided into two subgroups. The first subgroup forms part of the ring complex intruded along ring fractures of the cauldron, and the second is distributed inside the cauldron block (Sawada *et al.*, 1994; CRGGLB, 1982, 1990, 1997, 2000).

Lithological variations are commonly observed in each pluton, ranging from coarse-grained biotite granite in the core to fine-grained porphyritic biotite granite at the margins. Rare hornblende-bearing facies occur in some plutons. Dykes are associated with all the plutons. Most of the dykes are granite - quartz porphyry, but some are granodiorite porphyry and rhyodacite. The intrusive orientation of the dykes is concordant with the plutonic ring complex, except for those in the Yasu pluton (Fig. 2).

Activity of the plutons around Lake Biwa is divided into three stages based on the age data.

Stage-1: Older granitoids occurring in the Hiei, Suzuka and Tanakami plutons (Fig.2). Sawada *et al.* (1994) reported a Rb-Sr whole rock isochron age of 96.1±17.5 Ma for the older Suzuka granite. K-Ar biotite ages of the older Hiei granite lie in the range 96.6 - 95.8 (±1.9 - 4.8) Ma (Sawada and Itaya, 1993). The Kaizukiyama pluton, which is distributed outside the Biwako Cauldron, yields Rb-Sr whole rock ages and K-Ar mica ages of 99-94 Ma (Sawada *et al.* 1994; Saito and Sawada, 2000).

Stage-2: The principal facies of these granitoids is biotite granite, but variable grain size is observed within each pluton, from porphyritic to equi-granular and from fine-grained to coarse-grained. Granitoids of this stage occur in the Hira, Hiei (younger), Tanakami, Suzuka (younger) and Yasu plutons. Rb-Sr whole rock isochron ages of the younger Hira and the younger Suzuka plutons are 78.2±3.9 Ma and 79.7±3.5 Ma, respectively (Sawada *et al.*, 1994). K-Ar biotite ages range from 73.3 to 69.7 (±1.5 - 3.5) Ma (Sawada and Itaya, 1993). After this event, dyke rocks, granodiorite porphyries and granites or quartz porphyries were intruded into the above granitoids and the Jurassic accretionary complex. K-Ar biotite ages of the porphyry dikes range between 72.3 and 66.3 Ma (±1.5 - 3.5) (Sawada and Itaya, 1993).

Stage-3: This stage is represented by a single younger granite pluton, the Koujyaku granite pluton to the north of Lake Biwa. Its Rb-Sr whole rock age is 57.4±5.1 Ma (Tainosho *et al.*, 1999).

4. The Koto Rhyolites

The Koto Rhyolites are widely distributed in the Ohmi Basin (Fig. 2). The main mass occurs at the foot of the Suzuka Range, but other occurrences are scattered in and around Lake Biwa (Mimura *et al.*, 1976; Nishikawa *et al.*, 1978; Ishida *et al.*, 1984; Harayama *et al.*, 1989).

The Koto Rhyolites of the main mass are divided stratigraphically into the two stages bounded by lacustrine and debris-flow deposits (the Fukadani deposits). The name of the lower unit is abbreviated as Koto-1, and that of the upper unit as Koto-2. The Koto-1 welded tuffs are rhyolites and silicic dacites, and are more than 350 m in thickness. The Rb-Sr whole rock isochron age of Koto-1 is 94.7±19.6 Ma (Sawada *et al.*, 1994).

The Koto-2 tuffs consist of rhyolitic or high-silica rhyolite

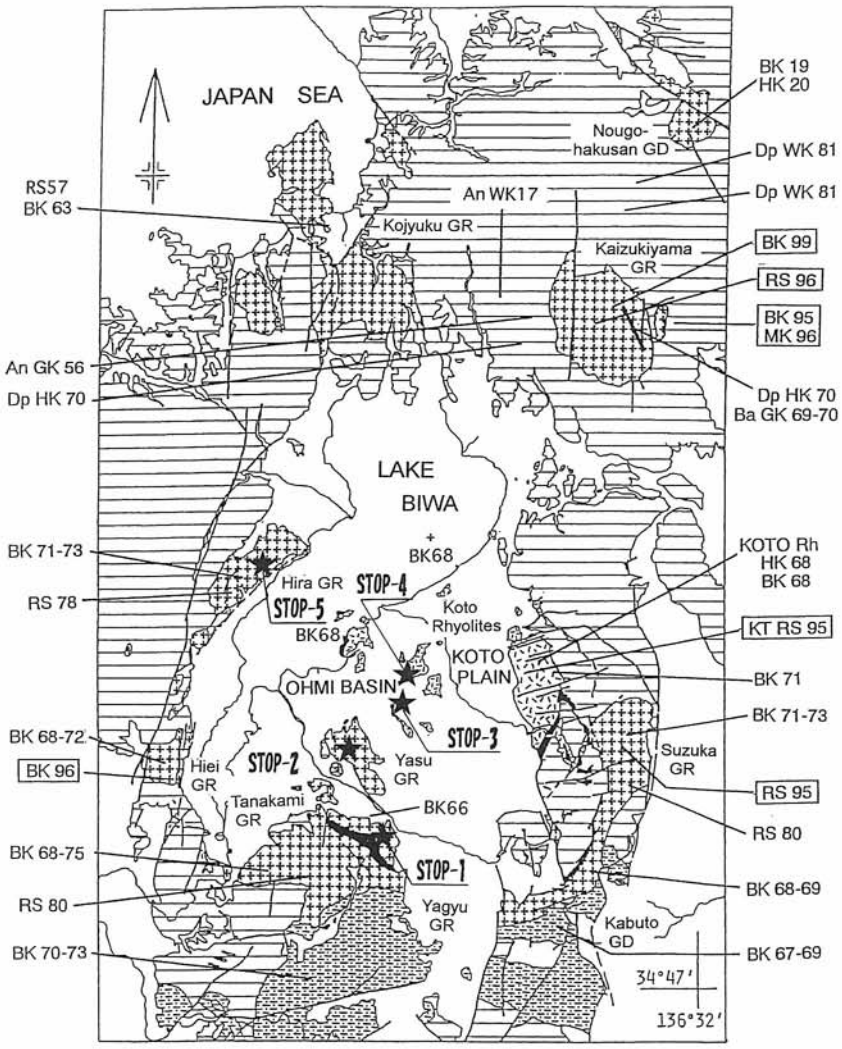

Fig.2. Geological map showing distributions of granitoids and Koto Ryolites with radiometric ages around Lake Biwa. The field stops of this excursion are shown as stars and stops 1 to 5. Numbers show radiometric ages. Abbreviations are as follows; K: K-Ar age; (B: biotite, H: hornblende, M: muscovite, G: groundmass, W: whole rock), and RS: Rb-Sr whole rock isochron age. Sources of data: Seki (1978), Miyamura *et al.* (1981), Harayama *et al.* (1989), Sawada and Itaya (1993), Sawada *et al.*, 1994, Koido *et al.* (1995), Kurimoto *et al.* (1999), Tainosho *et al.* (1999), Saito and Sawada (2000).

welded tuff or pumice tuffs, and are about 300 m in thickness. The Rb-Sr whole rock isochron age of Koto-2 is 75.8±2.4 Ma (Seki, 1978). The Inugami granite porphyry intrudes Koto-2, which shows an arc-shaped extension in the outside of the Hatasho quartz porphyry toward the Suzuka Range. The K-Ar biotite age of the Inugami granite porphyry is 72.1±3.6 Ma and 70.9±3.5 Ma (Harayama *et al.*, 1989, Sawada and Itaya, 1993). Finally, after the above eruptions and intrusive episodes, the Yuzurio pyroclastic dykes were intruded along the arc-shaped fractures (Nishikawa *et al.*, 1983). The Yuzurio pyroclastic dykes contain many accessory and accidental lithic fragments.

Koto Rhyolites and associated dyke rocks also occur on islets within Lake Biwa (Okinoshiraishi, Takeshima and Okishima) and in hills in the Koto Plain, east of Lake Biwa. The main facies comprises welded tuff of rhyolite - rhyodacite. Overall stratigraphy is not clear, as only one outcrop showing a succession of three welded tuff units is seen in the Azuchi Town district (Stop 4).

5. Geochemical features of the granitoids and the Koto Rhyolites

Correlation patterns between Ca, K, Rb, Sr, Y and Zr suggest that the Koto-1 and Koto-2 Rhyolites and their subvolcanic members are co-magmatic and products of fractional crystallization (Mimura *et al.*, 1976). Ikeda *et al.* (1980) pointed out that Koto-2 REE patterns are very similar to those of the younger Suzuka granites, and hence these magmas were probably supplied from the same magma chamber.

The geologic setting of the Koto Rhyolites, Suzuka

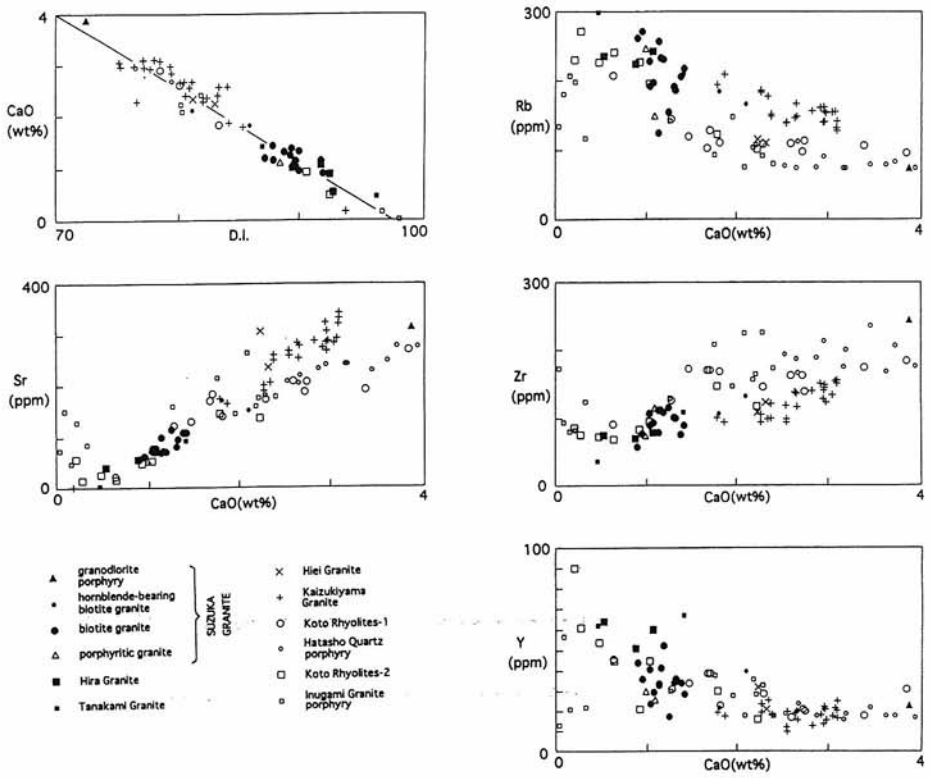

Fig.3. CaO - D.I.(normative sum Q+ab+or) and CaO-Sr, Rb, Zr, and Y diagrams for the granitoids, Koto Rhyolites and dykes.

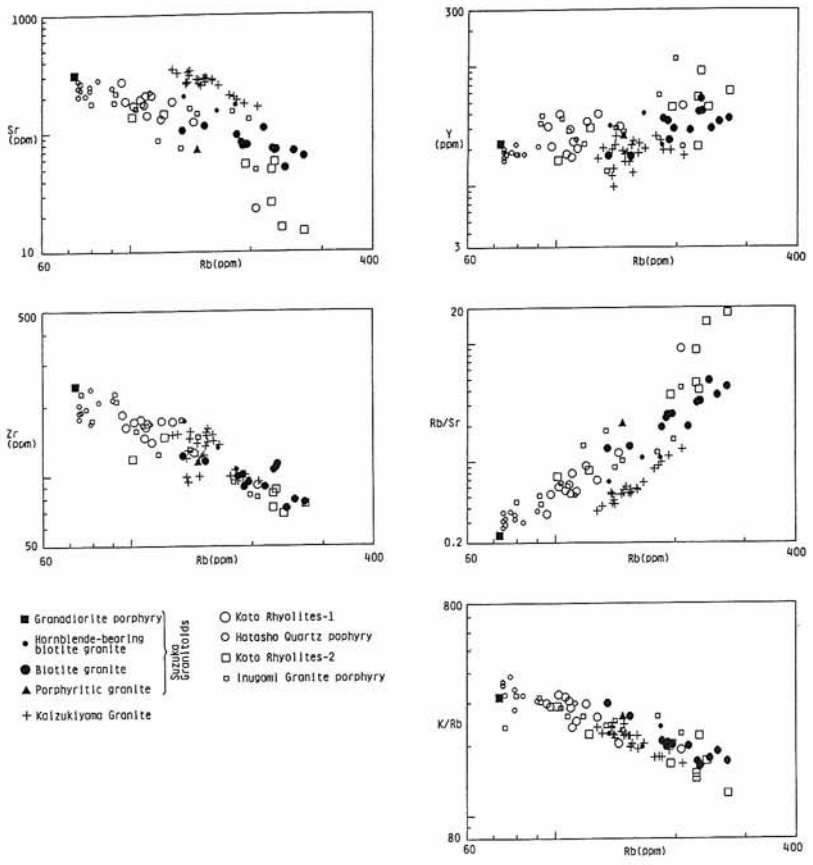

Fig. 4. Rb-Sr, Zr, Y, Rb/Sr and K/Rb plot for the Suzuka granitoids, Koto Rhyolites and their related dykes. On the diagram the data of the Cretaceous Kaizukiyama granite are also plotted for comparison of chemical characteristics. Sources of data: Mimura *et al.* (1976), Sawada *et al.* (1994), Sugii and Sawada (2000).

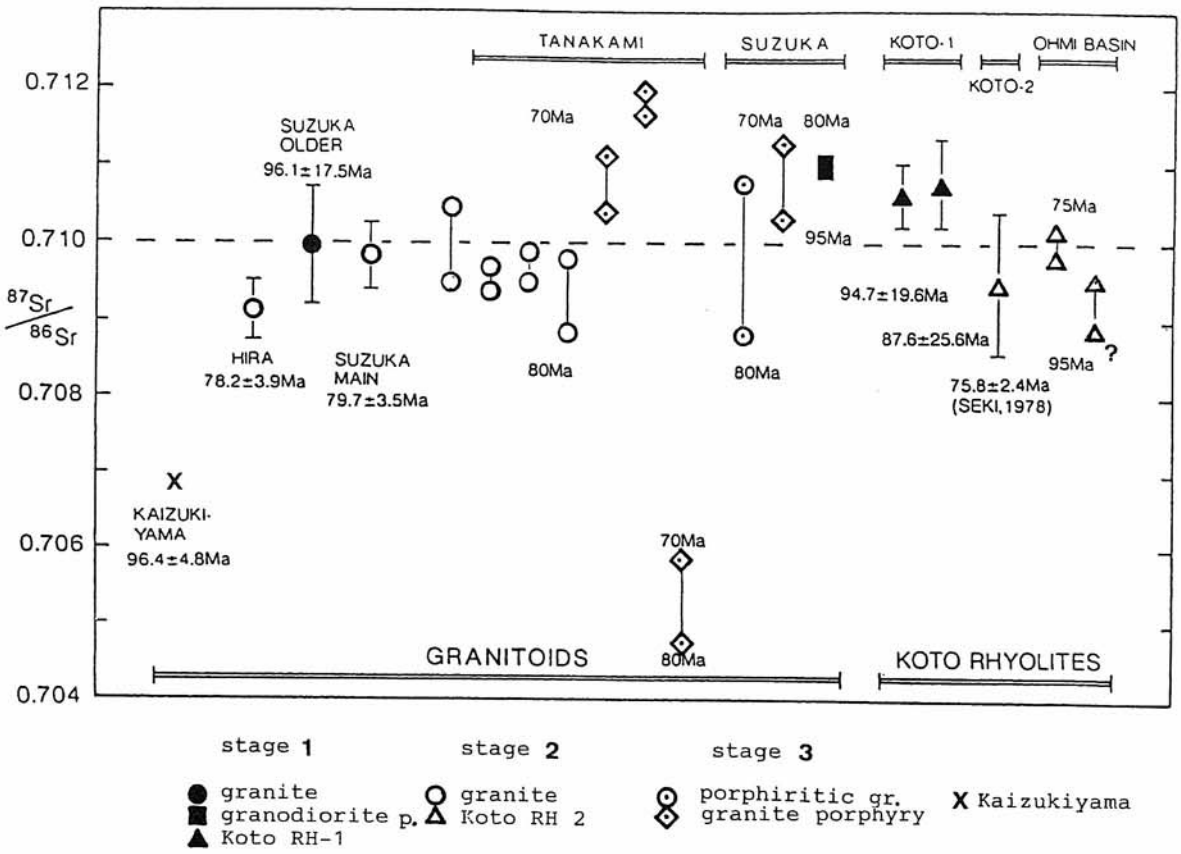

Fig. 5. Initial Sr isotopic ratios of the Cretaceous granitoids and the Koto Rhyolites around Lake Biwa (Sawada *et al.*, 1994). Lined bars with isochron age indicate error. Symbols with tine line and age show the value of Sr isotopic initial ratios at each estimated age.

granitoids and sub-volcanic dykes differs from that of the Kaizukiyama granite. That is, the former three members are part of the Biwako Cauldron, whereas the latter is distributed outside the Biwako Cauldron (granitic ring complex) (Fig.2). The differing geologic setting is supported by geochemical features. Rb vs Sr, Zr, Y, Rb/Sr and K/Rb diagrams of the Koto Rhyolites, Suzuka and Kaizukiyama granitoids, and sub-volcanic dykes are presented in Figures 3 and 4. The Rb vs Rb/Sr and K/Rb ratios of the Koto Rhyolites, Suzuka granitoids, and sub-volcanic dykes are similar to each other, but are distinct from those of the Kaizukiyama granite. Initial Sr isotopic ratios of the Kaizukiyama granite are very low compared with those of Koto Rhyolites and the granites forming the ring complex (Fig. 5) (Sawada *et al.*, 1994). Koto-1 initial Sr isotope ratios are slightly greater than those of the stage 2 granites including the Suzuka granites in (Fig.5), and are similar to stage 1 granodiorite porphyry. The stage 2 granitoids forming the ring complex are similar to each other, and to Koto-2 and Koto Rhyolites scattered around the Koto Plain.

6. The history of the Biwako Cauldron and the ring complex of granitoids

In summary, the granitoids around southern Lake Biwa have similar ages of formation and geochemical characters, close to those of the Koto Rhyolites. Combining the geology, geochronology and geochemistry suggests that the granitoids and the Koto Rhyolites are co-magmatic, and form a huge cauldron with granitic ring complex and mainly pyroclastic flow intra-caldera volcaniclastic deposits.

Voluminous eruptions of the Koto Rhyolites caused a huge Valles-type caldera collapse (Smith and Bailey, 1968; Nishikawa *et al.*, 1983). This cauldron was named "the Koto Cauldron" (Mimura *et al.*, 1976), and its outline is traced by the occurrence of dyke rocks. The diameter of the cauldron is about 30 km, and vertical displacement on the outer cauldron fault is about 700 m (Nishikawa *et al.*, 1983). Pyroclastic dykes correlative with the Yuzurio pyroclastic rocks have recently been found at several sites outside the Koto Cauldron. Some of these occur in the Tanakami area, far outside the original outline of the cauldron (CRGGLB, 2000; RGBGLB, 2002). Moreover, porphyry dykes in the Hira, Hiei, and Tanakami plutons have been recognized to represent a much larger ring-like fracture related to the formation of the cauldron (Fig. 6). This much larger cauldron has been renamed "the Biwako Cauldron" (CRGGLB, 2000; RGBGLB, 2002). Plutonism in the Hira, Hiei, Tanakami, Suzuka, and Yasu plutons around the southern part of Lake Biwa formed a huge ring complex. This plutonism is thought to be correlated with the activity of the Koto Rhyolites (Sawada *et al.*, 1994), and therefore to the formation of the

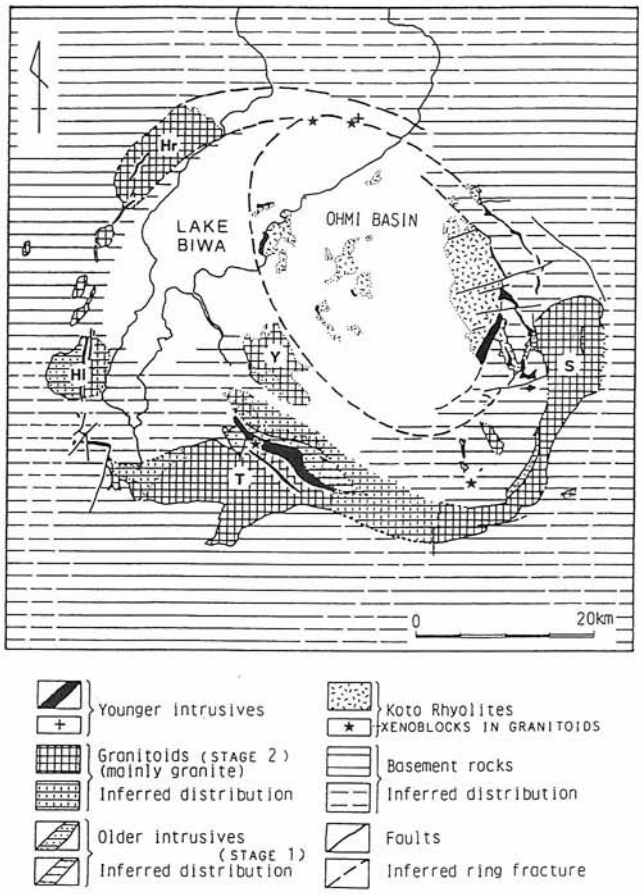

Fig. 6. Geological relations and stratigraphy of the Cretaceous granitoids and the Koto Rhyorites in and around southern Lake Biwa.

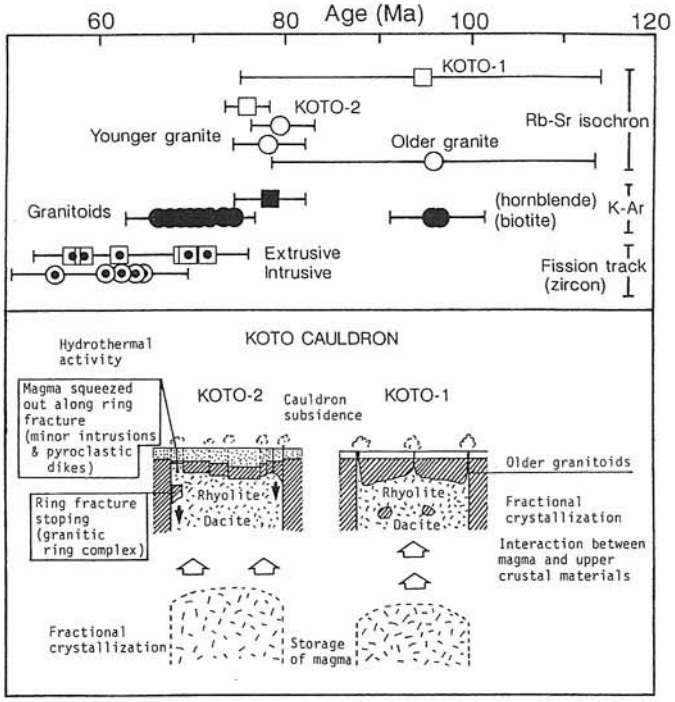

Fig. 7. Schematic diagram showing the episodes of igneous activity in the Biwako Cauldron. Radiometric age data from Seki (1978), Ito (1989), Harayama *et al.* (1989), Sawada and Itaya (1993) and Sawada *et al.* (1994).

Biwako Cauldron (CRGGLB, 2000; RGBGLB, 2002).

Figure 7 shows the episodes of igneous activity forming the Biwako Cauldron, along with radiometric age data. The history of the igneous activity and cooling of granitoids is summarized as follows:

1) Igneous activity started around 95 Ma with the Koto-1 eruptions and synchronous intrusion of the stage-1 granitoids (older Suzuka, Tanakami and Hiei granitoids) as part of the ring dykes. Large scale collapse took place along the ring fracture after the Koto-1 eruptions.

2) A new felsic magma ascended and formed another magma chamber at about 80 Ma. This magma was erupted as Koto-2, ascending by ring fracture stopping, and forming the stage-2 ring complex.

3) The Biwako Cauldron collapsed at least twice, in relation to the Koto-1 and -2 eruptions, with at least 3 or 4 concentric ring fractures. The inner ring fracture zone is estimated to have an area of 35 km by 30 km, and the outer zone is represented by the 60 km by 40 km granitic ring complex (Fig. 6).

4) After solidification of the main part of the granitic ring complex, unsolidified magma remained in the chamber through to *ca.* 66 Ma, when it was squeezed out and intruded along the solidified ring complex during post-collapse magmatism as porphyry and pyroclastic dykes (Yuzurio).

5) Hydrothermal activity continued through to at least 56 Ma, resetting the zircon fission track ages.

Figure 8 shows the cooling history of the granitic ring complexes and Koto Rhyolites in the Biwako Cauldron, compared with the Kaizukiyama granite, which has no relation to the cauldron. The Kaizukiyama granite is exposed over an area of more than 100 km^2. Its Rb-Sr whole rock age is close to its mica K-Ar ages, suggesting that the Kaizukiyama pluton cooled quickly. In contrast, the granitoids forming ring complex have differing radiometric ages. Rb-Sr whole rock ages are 80 Ma, K-Ar ages of biotite are mainly 70 Ma, and up to 66 Ma. The granitic ring complex is considered to have cooled at a rate of 40-80℃/m.y. before it reached the closure temperature (300℃) of the K-Ar system in biotite. This suggests that a huge magma chamber existed beneath the Biwako Cauldron.

7. Excursion

The late-Cretaceous felsic igneous rocks in this area were classified into five groups by Kutsukake *et al.* in RGBGLB (2002): Group-1: The Shigaraki granite and probably Kan'nonji granodiorite as the younger Ryoke granitoids. Group-2: Koto Rhyolites. Group-3: Dyke rocks correlated with activity of the Koto Rhyolites. Group-4: Granites of the San'yo-Naegi belt forming a ring complex. Group-5: Dyke rocks showing a ring outline, which corresponds to the occurrence of the ring complex.

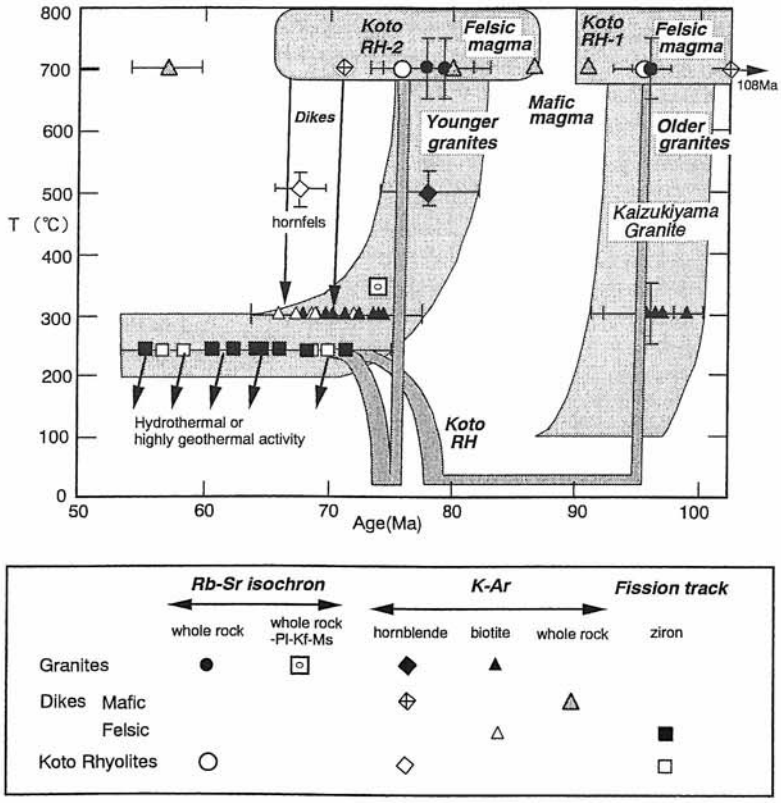

Fig. 8. Igneous activity and cooling history of felsic magmas, granites and Koto Rhyolites around Lake Biwa. Sources of data: Seki (1978), Miyamura *et al.* (1981), Ito (1989), Harayama *et al.* (1989), Sawada and Itaya (1993), Sawada *et al.* (1994), Saito and Sawada (2000).

Stop 1: Tanakami granite and Kan'nonji granodiorite

The geological map of the Tanakami area is shown in Figure 9. This stop provides observation of facies variation in the Tanakami granite (group-4), and the Kan'nonji granodiorite (group-1), and aplitic alteration at the border between the two granites.

The Tanakami granites are classified into the following four facies: medium- to coarse-grained biotite granite, medium- to coarse-grained porphyritic granite, fine- to medium-grained porphyritic granite, and fine-grained granite (CRGGLB, 2000). The second and fourth facies do not occur near this stop, but are found in the western margin of the pluton along with world-famous where pegmatite minerals such topaz and beryl. The medium- to coarse-grained facies is typical of the granites in the San'yo belt. The fine- to medium-grained facies is a roof facies of the magma chamber.

The Kan'nonji granodiorite-tonalite contains hornblende, and has a moderately porphyritic alkali feldspar and foliated texture by biotite, and occurs adjacently to and north of the Tanakami granite. This granodiorite-tonalite, which is intruded by the Tanakami granite, probably belongs to the younger Ryoke granitoids, as does the Shigaraki granite 7 km south of this stop. The morphology of this mass is peculiarly long and narrow,.

Pyroclastic rocks and quartz porphyries occur in both the Tanakami and Kan'nonji granitoids (CRGGLB, 2000; RGBGLB, 2002). They may be correlated to the dyke rocks in the Koto Rhyolites, but all the rocks in this area are thermally metamorphosed.

As well as pegmatite minerals, hydrothermally altered feldspathic ores are well known in the Tanakami pluton, where they have been mined for the use in porcelain manufacture (Sudo, 2001). The most typical ores occur on the western margins of the pluton (Kobayakawa, 1991; Sudo, 2001), but aplitic or altered granite ores are scattered around the margin of the pluton. Aplitic rocks similar to those of this stop were exposed from the Higashiyama Mine, and altered granites were taken from the Hakusui Mine. These two mines are situated on the boundary between the Tanakami granite and Kan'nonji granodiorite.

Stop 2: Yasu granite

The Yasu granite pluton occurs north of the Tanakami pluton over the Yasu River. The main facies of fine- to medium-grained porphyritic texture represent the character of the pluton at shallow depth. A 1500 m drill core shows that a coarse grained hornblende bearing biotite granite occurs (Hosono and Makino, 2002).

The Yasu granite pluton contains many small pegmatites (druses and veins) (Hosono and Makino, 2002), and hydrothermally altered rocks (Nishimura and Nakano, 2002). The alteration is due to greizenization or syenitization with Zn-mineralization. Molybdenite occurs along cracks in a small abandoned quarry (Tsuji and Kitahara, 1978). Deuteric

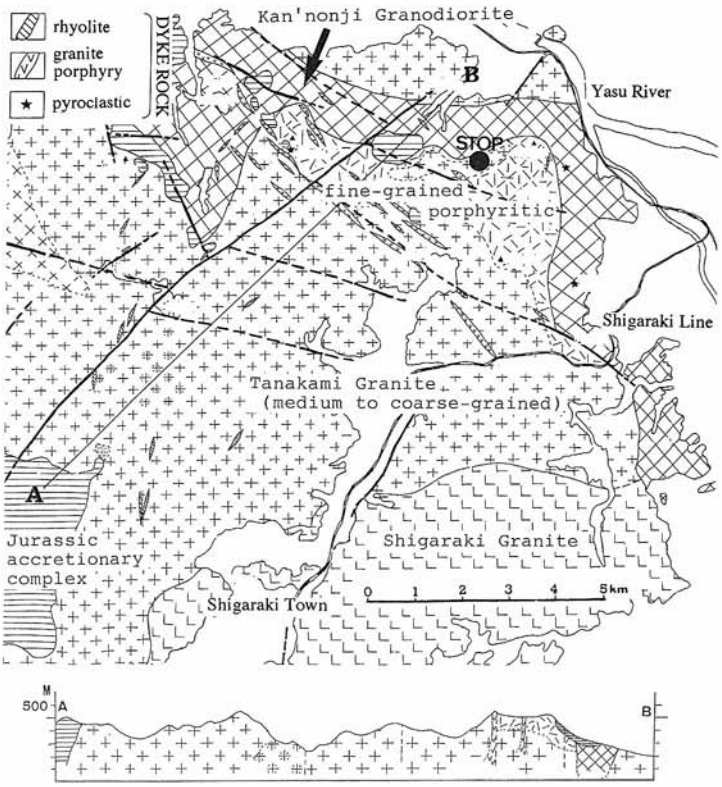

Fig. 9. Geological map around the field stop-1. After CRGGLB (2000).

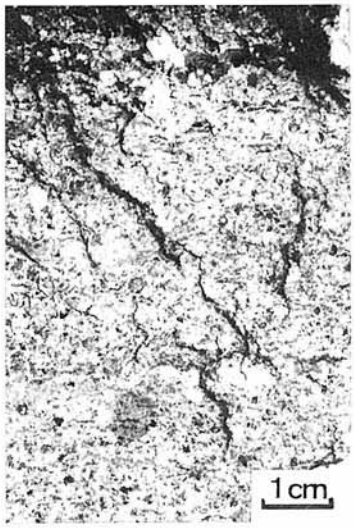

Fig. 10. Close-up photograph of the Kamewariyama welded tuff.

alteration of alkali feldspar from the Hanazono pegmatite zone near the southern margin of the pluton is described by Nakano *et al.* (2001).

Stop 3: Welded tuff of Koto Rhyolites

A typical welded tuff of the Koto Rhyolites is observed in this outcrop (Fig.10). The welded tuff is named "the Kamewariyama tuff" (Nishikawa *et al.*, 1983). Description was also given by Kawasaki and Nakano (1982). This rock is greenish in hue and shows a striking welded texture of essential lens of variable size. Glass shards are strongly welded under the microscope.

Stop 4: A sequence of welded pyroclastic rocks

A sequence of three layers of welded pyroclastic rocks is observed in this outcrop. These are the Azuchi welded tuff (Z layer), the Koshigoe tuff (K layer) and the Azuchi-jyoshi tuff (J layer) in ascending order. (Fig.11). All are more less hydrothermally altered, or prophylitised (Nakano, 1990).

The Azuchi tuff is a peculiar reddish brown, and contains abundant lithic fragments and large essential lens which are not so welded. This rock is rhyolitic or rhyodacitic. The Koshigoe welded tuff consists of three sub layers. The black layer consists of vitric welded tuff with a few small crystal fragments, and greenish layers are coarse-grained crystal tuff, somewhat similar to the upper Azuchi-jyoshi tuff. The third sub-layer is a fine mixture of the above sub-layers showing lamina structures. Nakano *et al.* (1984) suggest that the Koshigoe tuff is a pyroclastic surge, although Nishikawa *et al.* (1978) considered that the layer represented lacustrine deposits. The rock is rhyolitic, green or greenish gray and contains many large flattened essential lenses. The Azuchi-jyoshi tuff may be correlative with the Kamewariyama tuff observed at stop 3.

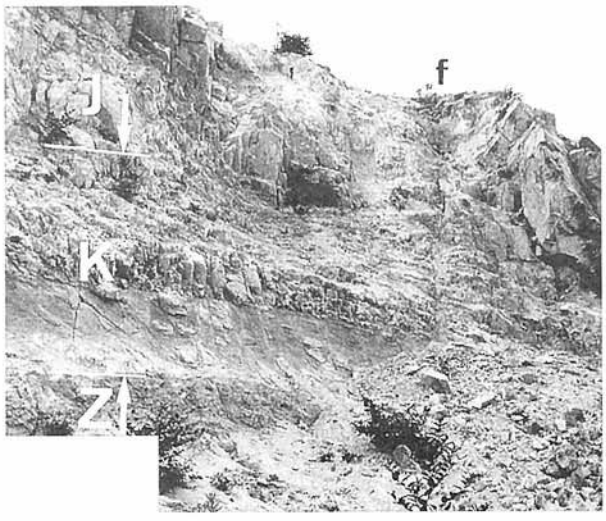

Fig. 11. Photograph of the outcrop of the field stop 4 and close-up of welded tuffs.

Stop 5: Overview from the rope-way terminal of the Hira mountains

We get a bird's eye view of Lake Biwa and the Ohmi basin here. We can imagine the outline of the Biwako Cauldron and the granitic ring complex in the southern area of Lake Biwa.

Lake Biwa has a area of about 670 km^2. Normal water level has an altitude of about 86 m above mean sea level, and maximum depth is 104 m. The name "Biwa" means a Japanese lute, and the lake is called because its shape is similar to a biwa. The length is *ca.* 64 km, whereas width is *ca.* 23 km at the widest point.

The mountains surrounding Lake Biwa consist of a Jurassic accretionary complex and Cretaceous granitic rocks. On the left side to the Seta river, we see the Tanakami mountain range, which consists of granitic rocks. Several islets consisting of Koto Rhyolites and granite porphyry occur within the lake. Beyond the islets, the Koto Plain spreades out to the granitic Suzuka mountain range. Several small hills consisting of the Koto Rhyolites, welded tuffs, associated with granite porphyry are scattered on the plain.

The Hira granite can be seen around the rope-way terminal (altitude: 970 m). The rock around here is medium- to coarse-grained biotite granite consisting of alkali feldspar, plagioclase, quartz, biotite, ilmenite, zircon, apatite and allanite.

Acknowledgements: Most of geological information on this field trip has been obtained by the collaboration work with the CRGGLB, and RGBGLB and with the Research Group for the Koto Rhyolites. The office of the Koka Country Golf Club and the office of Azuchi Town have provided several co-operations for this trip. We thank gratefully for these persons. We would like to thank to Dr. Barry Roser for critical comments on the manuscript.

References

Collaborative Research Group for the Granites around Lake Biwa (1982) Granitic masses around Lake Biwa, southwest Japan — On the granites in the Koka area. *Jour. Geol. Soc. Japan*, **88**, 289-298. *

Collaborative Research Group for the Granites around Lake Biwa (1990) Granitic masses around Lake Biwa, southwest Japan — Part 2 : The Suzuka Granite pluton. *Earth Sci.* (*Chikyu Kagaku*), **44**, 184-195. *

Collaborative Research Group for the Granites around Lake Biwa (1997) Granitic masses around Lake Biwa - Part 4 : Geology and Petrography of the Hira Granite pluton. *Earth Sci.* (*Chikyu Kagaku*), **51**, 188-198. *

Collaborative Research Group for the Granites around Lake Biwa (2000) Granitic masses around Lake Biwa - Part 5 : The Tanakami Granite pluton. *Earth Sci.* (*Chikyu Kagaku*), **54**, 380-392. *

Harayama, S., Miyamura, M., Yoshida, F., Mimura, K. and Kurimoto, C. (1989) *Geology of the Gozaishoyama district*. Quadrangle Series, 1:50,000. Geol. Surv. Japan, 145p. *

Hosono, T. and Makino, K. (2002) Variation of rock facies in Yasu granitic pluton, southern part of Lake Biwa, southwest Japan. *Jour. Geol. Soc. Japan*, **108**, 1-15. *

Ikeda, T., Nishikawa, K., Kobayakawa, T., Tajima, T. and Nishibori, S. (1980) Trace element variations in the Koto Rhyolites and granites around Lake Biwa. *Tsukumo Earth Sci.*, **15**, 38-49. **

Ishida, S., Kawada, K. and Miyamura, M. (1984) *Geology of the Hikone-Seibu district*. Quadrangle Series, 1:50,000, Geol. Surv. Japan, 121p. *

Ito, H. (1989) Fission track ages of the Koto Rhyolites, southeast area of Lake Biwa. *Jour. Geol. Soc. Japan*, **95**, 479-482. **

Kawasaki, F. and Nakano, S. (1982) A note on the Koto Rhyolites in the Mt. Kamewari area. *Mem. Fac. Educ., Shiga Univ.*, **32**, 59-66. *

Kobayakawa, T. (1991) Mineralization of Inoue-Hiratsu Mine. *Land and life of Shiga Pref., Found. Natur. Conserv. Shiga Pref.*, 809-846. **

Koido, Y., Harayama, S., Endo, T., Shimohata, I. (1995) K-Ar ages of igneous rocks in the Ryohaku Mountains, Central Japan. *Bull. Gifu Pref. Mus.*, **16**, 15-20. *

Kurimoto, C., Naito, K., Sugiyama, Y. and Nakae, S. (1999) *Geology of the Tsuruga district*. With Geological Sheet Map at 1:50,000, Geol. Surv. Japan, 73p. *

Mimura, K., Katada, M. and Kanaya, H. (1976) Igneous Activity of the Koto rhyolites in the Yatsuoyama district, southeast of Lake Biwa. *Jour. Japan. Assoc. Mineral. Petrol. Econ. Geol.* 71, 327-338.

Miyamura, M., Yoshida, F., Yamada, N., Sato, T. and Sangawa, A. (1981) *Geology of the Kameyama District*. Quadrangle Series, Scale 1:50,000, Geol. Surv. Japan, 128p. *

Nakano, S. (1990) Behavior of alkali feldspar during hydrothermal alteration of the Koto Rhyolites, southwest Japan. *Earth Sci.* (*Chikyu Kagaku*), **44**, p.61-76.

Nakano, S., Makino, K. and Eriguchi, T. (2001) Microtexture and water content of alkali feldspar by Fourier - transform infrared microspectroscopy. *Mineral. Mag.*, **65**, 675-683.

Nakano, S., Kawasaki, F., Kitamura, A. and Nishimura, S. (1984) Structural features of the Koshigoe welded tuff of Mt. Kinugasa, Koto district, Shiga Prefecture, Japan. *Mem. Fac. Educ., Shiga Univ.*, **34**, 15-27. *

Nishikawa, K., Nishibori, T., Kobayakawa, T., Tajima, T., Tsuji, K. and Sato, Y. (1978) The Koto Rhyolites. *Land and life of Shiga Prefecture, Found. Natur. Conserv. Shiga Pref.*, 225-244. **

Nishikawa, K., Nishibori, T., Kobayakawa, T., Tajima, T., Ueshima, M., Mimura, K. and Katada, M. (1983) Koto Rhyolites and their igneous activities. *Jour. Japan Assoc. Mineral. Petrol. Econ. Geol.*, **78**, 51-64. *

Nishimura, S. and Nakano, S. (2002) Hydrotherrmally altered and mineralized rocks from the Yasu Granite pluton, east of Lake Biwa, southwest Japan. *Mem. Fac. Educ. Shiga Univ.*, **52**, 21-35. *

Research Group for the Basement Geology of Lake Biwa (2002) Studies of the caldera formation around the Lake Biwa area. Geological studies of the late Cretaceous Biwako Cauldron. *Res. Rep. Lake Biwa Mus.*, **15**, 120p. **

Saito, M. and Sawada, Y. (2000) *Geology of the Yokoyama District, IV. Igneous rocks*. Quadrangle Series, 1:50,000. Geol. Surv. Japan, 91p. *

Sawada, Y. and Itaya, T. (1993) K-Ar ages of a Late Cretaceous granitic ring complex around southern Lake Biwa, southwest Japan - Cooling history of a huge cauldron. *Jour. Geol. Soc. Japan,* **99**, 975-990. *

Sawada, Y., Kagami, H., Matsumoto, I., Sugii, K., Nakano, S. and the Collaborative Research Group for the Granites around Lake Biwa. (1994) A Cretaceous granitic ring complex and the Koto Cauldron around the southern part of Lake Biwa. Southwest Japan. *Jour. Geol. Soc. Japan*, **100**, 217-233. *

Seki, T. (1978) Rb-Sr geochronology and petrogenesis of the late Cenozoic igneous rocks in the inner zone of the southwestern part of Japan. *Mem. Fac. Sci. Kyoto Univ., Ser. Geol. Mineral.*, 71-110.

Smith, R. L. and Bailey, R. A. (1968) Resurgent cauldron. *Geol. Soc. Amer. Mem.*, **116**, 613-662.

Sudo, S. (2001) Feldspathic rock resources of Nango-Shigaraki area, Shiga Prefecture, Central Japan - Classification of ore deposite types and its geologic and oregenetic significance. *Chishitsu News*, **559**, 41-49. **

Sugii, K. and Sawada, Y. (2000) Late Creatceous Kaizukiyama granite, northeast of Lake Biwa, southwest Japan. *Geosci. Rep. Shimane Univ.*, **18**, 69-84. *

Yamada, N., Teraoka, Y. and Hata, M. (1982) Geological map of Japan, Scale 1:1,000,000, Geol. Atlas of Japan, *Geol. Surv. Japan*, 3-19 and 22-25.

Tainosho, Y., Kagami, H., Yuhara, M., Nakano, S., Sawada, K. and Morioka, K. (1999) High initial Sr isotopic ratios of Cretaceous to early Paleogene granitic rocks in Kinki district, southwest Japan. *Mem. Geol. Soc. Japan*, **53**, 309-321. *

Tsuji, K. and Kitahara, T. (1978) On minerals and ore deposits in Shiga Prefecture. *Land and Life of Shiga Pref., Found. Natur. Conserv. Shiga Pref.*, 479-541. **

* in Japanese with English abstract.
** in Japanese.

Received May 26, 2003
Accepted July 10, 2003